Purification strategy development for the recombinant vesicular stomatitis virus (rVSV) based HIV vaccine

Thèse

Anahita Bakhshi Zadeh Gashti

Doctorat en génie chimique
Philosophiæ doctor (Ph. D.)

Québec, Canada

Purification strategy development for the recombinant vesicular stomatitis virus (rVSV) based HIV vaccine

Thèse

Anahita Bakhshizadeh Gashti

Sous la direction de :

Alain Garnier, directeur de recherche

Résumé

Malgré le nombre croissant d'individus infectés par le virus de l'immunodéficience humaine (VIH) chaque année, il n'existe toujours pas de vaccin efficace qui prévienne son infection chez l'homme. Seulement en 2020, on peut encore compter 37,6 millions d'infection et 690 000 décès liés au SIDA. Le développement d'un vaccin contre le SIDA, sûr et efficace, serait donc un moyen très pertinent pour combattre les ravages de cette maladie. Le virus de la stomatite vésiculeuse (VSV), membre de la famille des *Rhabdoviridae*, infecte principalement les bovins, mais est relativement bénin pour l'humain, n'étant associé qu'à de légers symptômes pseudo-grippaux. Par ailleurs, le VSV recombinant a déjà été utilisé pour le développement de vaccins humains contre divers virus, notamment Ebola, Marbourg, Lassa, la fièvre hémorragique de Crimée-Congo (CCHFV), Nipah, les coronavirus MERS et SRAS, Zika, Influenza et VIH.

Dans ce travail, effectué dans le cadre plus large du développement de nouveaux candidats vaccins contre le VIH, basé sur les VSV recombinants (rVSV), nous proposons différents schémas de purification pour le traitement de ces candidats. Une série de filtres avec des tailles de pores et des supports de filtration différents ont été testés pour leur efficacité à éliminer les débris cellulaires du surnageant de culture cellulaire tout en permettant aux particules infectieuses de traverser le filtre. Cette microfiltration en série a également été appliquée pour éliminer le besoin de centrifugation à basse vitesse à l'étape de la clarification et améliorer les rendements, la simplicité et l'extrapolabilité des schémas proposés. Afin de réduire le volume de l'échantillon à traiter, l'application de différentes unités d'ultrafiltration (UF), soit des unités d'UF centrifuge ou à flux tangentiel (TFUF), ont été testées. Pour ce faire, les paramètres de fonctionnement de la TFUF ont été maintenus à des valeurs ne générant que de faible taux de cisaillement ($\leq 2000\ s^{-1}$) pour préserver l'intégrité du rVSV.

Pour l'étape de la purification chromatographique proprement dite, plusieurs technologies candidates ont été testées pour leur capacité à séparer les particules infectieuses de l'ADN et des protéines contaminants. Des résines échangeuses

d'anions fortes et faibles, à savoir HiTrap™ DEAE FF, HiTrap™ ANX FF, HiTrap™ Q FF et HiTrap™ XL (Cytiva), ont été testées en colonne. Dans les meilleures conditions, ces colonnes ont permis de récupérer 77 % des particules infectieuses tout en éliminant respectivement 93 % et 92,7 % des protéines totales et de l'ADN. Par la suite, un schéma de purification chromatographique en deux étapes utilisant initialement un adsorbeur échangeur d'ion membranaire (Sartobind® Q, Sartorius), suivi d'une résine multimodale (Captocore™ 700, Cytiva) a également été testé car les adsorbeurs membranaires sont plus pratiques pour les procédés à grande échelle. La purification des rVSV à l'aide de ce protocole a permis de récupérer 51 % de particules infectieuses et a éliminé 95 % et 85 % de l'ADN et des protéines contaminants, respectivement. Cependant, étant donné que les micrographies électroniques de ces préparations virales purifiées présentaient encore une quantité notable de vésicules extracellulaires ou d'exosomes, deux résines à base de céramique d'hydroxyapatite (CHT) ont aussi été testées pour leur capacité à séparer les rVSV de ces contaminants. La colonne CHT II (BioRad) a montré des résultats prometteurs en terme d'élimination des vésicules extracellulaires, comme vérifié par microscopie électronique à transmission (TEM). De plus, une récupération de 78 % de rVSV infectieux ainsi que l'élimination de 98 % de l'ADN résiduel et de 99 % des protéines ont été mesurées dans les éluats de cette colonne.

Abstract

Despite the growing number of Human immune deficiency virus (HIV) infected individuals every year, there is still no effective vaccine that prevents new HIV infection in humans. As of 2020, a total of 37.6 million individuals were found globally to be infected with HIV. With 690,000 AIDS-related death reports in 2020, developing a safe and effective HIV vaccine is of utmost importance. Vesicular stomatitis virus (VSV), a member of the *Rhabdoviridae* family, mainly infects cattle, but its infection in human is mainly benign and can only be associated with mild flu-like symptoms. In addition, the VSV platform has already been used to develop vaccines against a variety of virus infections, including Ebola, Marburg, Lassa, Crimean-Congo hemorrhagic fever (CCHFV), Nipah, MERS- and SARS- coronaviruses, Zika, Influenza, and HIV.

In the current work, carried out within the broader framework of developing new vaccine candidates against HIV based on recombinant VSVs (rVSVs), we propose different purification schemes for the DSP of the candidate vaccine. A series of filters with different pore sizes and filtration media were tested for their effectiveness in removing cellular debris from the cell culture supernatant while allowing the infectious particles to pass through the filter. Serial microfiltration was also applied to eliminate the need for low-speed centrifugation at the clarification step and improve the proposed schemes' yield, simplicity, and scalability. In order to reduce the volume of the sample to be processed, the application of different ultrafiltration (UF) units, either centrifugal based UF units or tangential flow UF (TFUF) systems, were tested. The TFF operation parameters were maintained at values generating low shear (≤2000 s^{-1} shear rate) for preserving the integrity of the rVSV as an enveloped virus.

For the actual chromatographic purification step, multiple candidate technologies were tested for their ability to separate infectious particles and to remove the contaminant DNA and proteins. Strong and weak anion exchanger resins, namely, HiTrap™ DEAE FF, HiTrap™ ANX FF, HiTrap™ Q FF, and HiTrap™ XL (Cytiva), were put into test in the column mode. In best condition, these columns resulted in

the recovery of 77 % infectious particles while eliminating 86.6 % and 92.7 % of the total proteins and DNA, respectively. Subsequently, a two-step chromatographic purification scheme initially used a membrane adsorber (Sartobind® Q, Sartorius), followed by a multimodal resin (Captocore™ 700, Cytiva) was tested since membrane adsorbers are more applicable for large-scale processes. Purification of rVSVs using this protocol resulted in the recovery of 51 % infectious particles but removed 95 % of the contaminant DNA contents and 85 % of total proteins. However, since the electron micrographs of these purified virus preparations still showed a noticeable amount of extracellular vesicles or exosomes (visually through TEM), two resins based on ceramic hydroxyapatite (CHT) were screened for their ability in separating the rVSVs from these contaminants. The CHT II (BioRad) column showed promising results in removing extracellular vesicles from the virus preparations as verified by transmission electron microscopy (TEM). Moreover, a recovery of 69.2 % infective rVSVs alongside the removal of 88 % residual DNA and 87 % of protein contents was measured in this column's eluates.

Table of contents

List of figures

List of tables

List of abbreviations and symbols

AEX: anion exchange chromatography

CA: cellulose acetate

CsCl: cesium chloride

DBC: dynamic binding capacity

DLS: dynamic light scattering

DMEM: Dulbecco's modified Eagle's medium

DNA: deoxyribonucleic acid

DSP: Down-stream processing

EDTA: ethylenediamine tetraacetic acid

ELISA: enzyme-linked immunosorbent assay

FBS: fetal bovin serum

FDA: food and drug administration

FT: flow-through

HEK293: human embryonic kidney cells

HIV: human immunodeficiency virus

HRP: horseradish peroxidase

kDa: kilo Dalton

MEM: minimal essential medium

MWCO: molecular weight cut-off

NaCl: sodium chloride

$NaPO_4$: sodium phosphate

PAGE: polyacrylamide gel electrophoresis

PBS: phosphate buffered saline

PES: polyethersulfone

PP: polypropylene

PVDF: polyvinylidene fluoride

RC: regenerated cellulose

RNA: ribonucleic acid

rVSV: recombinant vesicular stomatitis virus

SD: standard deviation

SEC: size exclusion chromatography

SFCA: surfactant-free cellulose acetate

SN: supernatant

TCID50: median Tissue Culture Infectious Dose

TEM: transmission electron microscope

TFF: tangential flow ultrafiltration

UF: ultrafiltration

Vero: African green monkey kidney epithelial cells

VSV: vesicular stomatitis virus

Acknowledgements

First and foremost, I wish to express my sincere appreciation to my supervisor, Dr. Alain Garnier. I am fully indebted to him for inspiring me and providing an environment where I could perform my research independently. Without his persistent support and encouragement, the objectives of this project would not have been achieved. I have been very fortunate to have such a supportive and positive supervisor, whose insights, valuable comments and criticism helped the project progress.

I am also thankful to Dr. Bruno Gaillet, head of the chemical engineering department, Laval University, for his constant support during my research and to allow me to use the facilities of his laboratories for the continuation of my work.

The completion of this project could not have been possible without the help of Dr. Parminder Chahal at the NRC-CNRC (BRI, Montreal). I would like to thank him for the training on tangential flow ultrafiltration process and for all the valuable discussions on my research project. I would also like to thank Dr. Renald Gilbert, the leader of viral vector production at NRC (BRI, Montreal) for providing me with the opportunity to visit NRC.

I would also like to acknowledge Dr. Gary Kobinger and the former post-doctoral researcher in his lab, Dr. Hiva Azizi, for providing the virus production stocks and Dr. Amine Kamen (McGill University) for generously sharing the Vero CCL-81.5 cell line.

I like to thank Julie-Christine Levesque, coordinator of the Bio-imaging platform at CHUL, for performing the transmission electron microscopy. Special thanks goes to Jean-Nicolas Ouellet, technician of the Department of chemical engineering, Laval University, for his constant technical supports throughout my studies.

I would like to acknowledge my colleague, Dr. Mathias Mangion, who familiarized me with the lab and for his constant support throughout my studies. Special thanks to my colleagues and friends Juliette Champeil, Dr. Thiery Vincent, and Barbara Valeria Mejia Bohorquez who made this journey more enjoyable.

I would like to express my gratitude to my family, particularly my father for his constant encouragement and advice. Finally yet importantly, I want to thank my husband, Vahid, for all the support and motivation he gave me during this period and for always believing in me.

Foreword

The current thesis is composed of a general introduction, followed by five chapters and a general conclusion. The five chapters cover the literature review, the materials and methods, and three results chapters. The three result chapters, written in the form of manuscripts, are either submitted or to be submitted for publication at the time of the thesis submission.

The first chapter includes a literature review covering several aspects, including the need for virus purification, the possible contaminants of cell culture produced viral vaccines, the steps involved in the purification of cell culture produced viruses, the approaches involved in clarification of cell culture supernatant, the concentration of viruses using ultrafiltration, tangential flow ultrafiltration, and ultracentrifugation, and purification using either ultracentrifugation for laboratory-scale and chromatography for large-scale processing of viruses. In chromatographic purification, the commonly used principles for downstream processing of viruses are discussed. I was the principal writer of this chapter.

The second chapter describes the materials and methods used to perform the experiments used in this thesis. I was the principal writer of this chapter.

The third chapter includes the article entitled “Purification of recombinant vesicular stomatitis virus-based HIV vaccine candidate”. This chapter consists of the primary and initial assessments performed for the clarification step of the rVSVs, including the testing of different microfiltration units with various filtration media and pore sizes. Moreover, two approaches for the concentration of viruses were assessed for laboratory (less than 250 mL of supernatant) and large-scale (1 to 2 L of supernatant). These included pelleting by ultracentrifugation for small volumes against tangential flow ultrafiltration for higher volumes. For the purification step, density gradient ultrafiltration was performed at small-scale, while, for larger volumes of supernatant, two strong and two weak anion exchanger columns were tested. In the end, the purification scheme at a small-scale was set side by side with a large-scale purification scheme, comparing their capacity in the removal of proteins, DNA, and recovery of infectious particles. I was the principal investigator and writer of this

chapter. The co-authors of this chapter include Bruno Gaillet, Parminder S. Chahal and Alain Garnier. This article is to be submitted to the journal *Vaccine*.

The fourth chapter includes the article entitled “Two-step chromatographic purification of an rVSV based HIV vaccine candidate expressing HIV and Ebola glycoproteins” that describes a two-step chromatographic process for purification of rVSVs produced in serum-free media using a membrane adsorber. The proposed purification process includes a clarification and nuclease treatment before chromatographic purification. The purification step was performed in a bind and elute mode using Sartobind® Q strong anion exchanger membrane followed by a flow-through mode chromatographic approach using Captocore™ 700 column for further elimination of contaminant DNA contents. I was the principal investigator and writer of this chapter. The co-authors of this chapter include Bruno Gaillet, Parminder S. Chahal and Alain Garnier. This article is to be submitted to the *Biotechnology Journal*.

The fifth chapter includes the article entitled “Purification of recombinant vesicular stomatitis virus based HIV vaccine candidate using ceramic hydroxyapatite”. Here, we propose a chromatographic purification protocol for a better separation of rVSVs from extracellular vesicles. For this purpose, we tested two multimodal resins, namely, ceramic hydroxyapatite type I and II. Their effectiveness in the purification of rVSVs from the cell culture contaminants, including contaminant DNA, proteins, and extracellular vesicles was confirmed by quality control assays. I was the principal investigator and writer of this chapter. The co-authors of this chapter include Bruno Gaillet, Parminder S. Chahal and Alain Garnier. This article is to be submitted to the journal *Biotechnology and Bioengineering*.

The results obtained during this project were also presented in the following scientific conferences:

A Bakhshizadeh G, B Gaillet, A Garnier, “Downstream process development for the purification of recombinant vesicular stomatitis virus (rVSV) based HIV vaccines”, 15th Vaccine congress, 3-6 Oct 2021, Online. (The main intellectual and technical contributor)

A Bakhshizadeh G, M. Mangion, B Gaillet, A Garnier, “Laboratory- and large-scale purification schemes for candidate HIV vaccines based on vesicular stomatitis virus”, PROTEO annual symposium, 10th May 2019, Quebec City, Quebec, Canada. (The main intellectual and technical contributor)

A Bakhshizadeh G, M. Mangion, B Gaillet, A Garnier, “Purification of candidate HIV vaccines at laboratory and pilot-scale”, CNPN 2018 Annual Symposium, 29th April to 9th May, Quebec City, Quebec, Canada. (The main intellectual and technical contributor)

A Bakhshizadeh G, M. Mangion, B Gaillet, A Garnier, “Laboratory and pilot-scale purification of recombinant vesicular stomatitis virus (rVSV) based HIV vaccine candidates”, Chemical engineering research day (Polytechnique Montréal, McGill, Laval), 19-20th March, 2018, Montreal, Canada. (The main intellectual and technical contributor)

A Bakhshizadeh G, M. Mangion, B Gaillet, A Garnier, “Development of a purification strategy for recombinant vesicular stomatitis virus (rVSV) based HIV vaccine candidates”, Journée annuelle ThéCell, 21st November 2018, CRCHUM, Montréal, Canada. (The main intellectual and technical contributer)

A Bakhshizadeh G, T Vincent, M Mangion, B Gaillet, A Garnier, “Development of a purification strategy for recombinant Vesicular stomatitis virus (rVSV) based HIV vaccine candidates’’, PROTEO Annual Symposium, 18th May 2018, Quebec City. (The main intellectual and technical contributor)

Introduction

To date, the global pandemic of AIDS has killed 36.3 million people, and 37.7 million individuals are currently living with it [1]. Despite the high number of new cases every year, there are still no vaccines that can protect healthy individuals from HIV infections. Therefore, the development of an effective and safe vaccine is of the utmost importance for ending this epidemic. The main hurdles in the HIV vaccine development have been the high divergence of the HIV envelope glycoprotein and rapid generation of mutants that are resistant to the neutralizing antibodies [2].

Vesicular stomatitis virus (VSV), as a member of the *Rhabdoviridae* family, has been used in several research fields as a gene therapy vector, an oncolytic virus, and a viral vaccine vector. In general, VSV targets livestock, and its infection in cattle can appear as lesions in the oral cavity, hoofs, and teats. VSV infection is not common in humans, but its occurrence has been reported in individuals in contact with the virus in laboratories or with infected farm animals [3]. VSV infection in humans is mainly controlled by interferons (INF) response, and therefore, it has mainly been associated with only mild flu-like symptoms [4,5]. The two serotypes of VSV, namely, Indiana and New Jersey, are enzootic in southern Mexico and northern South America but are not widespread in the United States and only occur sporadically, with the latest two outbreaks happening in 1982 and 1966 [6–8].

The VSV genome consists of a single-stranded negative-sense RNA of about 11 kb, encoding five structural proteins, namely; the nucleocapsid (N), the matrix (M), the large RNA-dependent RNA polymerase (L), the phosphoprotein (P), and the VSV glycoprotein (G) [8–11]. Several characteristics make VSV a suitable platform for a recombinant, replication-competent viral vaccine. These features include low chances of viral RNA integration into the genome, promising titers when grown *in vitro* and the ability to grow in a variety of mammalian cell lines, very low prevalence of VSV pre-existing immunity in humans, the ability to elicit robust cellular and humoral immunity *in vivo,* and mild flu-like symptoms upon infection in humans [12–14]. Also, the VSV platform, as a replication-competent vaccine, has been shown to

induce strong immune responses against antigens from different pathogens, including Influenza [15], measles [16], Zika virus [17], AIDS [18], Lassa, and Ebola Virus [19], Marburg [13], Crimean-Congo hemorrhagic fever (CCHFV), and Nipah [20].

The recombinant VSV base has been used for the FDA-approved Ebola vaccine (rVSVΔG-ZEBOV-GP/rVSV-ZEBOV) used in the Democratic Republic of the Congo during the 2018 outbreak. The rVSV-ZEBOV vaccine was marketed under the name Ervebo, and it showed an efficacy of 97.5 % in clinical trials [21,22]. The rVSV-ZEBOV vaccine had been produced through reverse genetics and designed in such a way that the gene encoding for Ebola glycoprotein (EBOV-gp) would replace the gene responsible for VSV glycoprotein (VSV-gp). These observations highlight the use of VSV backbone for replication-competent viral vaccines, including HIV. The rVSV backbone has been employed in phase I clinical trials of three HIV vaccines (ClinicalTrials.gov, NCT01438606, NCT01578889, and NCT01859325).

Following these successes, the CIHR funded a project entitled "Development of a safe, effective and clinically acceptable VSV-based HIV vaccine", proposed by Dr. Kobinger and his colleagues, that aims at developing an HIV vaccine based on the rVSV-ZEBOV backbone. The rVSV used in this project expresses both the EBOV-gp and modified HIV glycoprotein (HIV-gp) on its surface. The HIV surface proteins are expected to trigger the immune response against HIV infection and result in robust protection against HIV, while the presence of EBOV-gp improves the cell tropism and helps the vaccine production process by enabling the virus production in CD4- and CCR5- cell lines.

The design and modifications of the rVSV-based HIV vaccine and optimization of the upstream production process by the production of rVSVs in serum-free Vero cells were carried out by other parties involved in the project. In contrast, the development of the downstream purification process (DSP) of the vaccine was carried out in the current Ph.D. project under the supervision of Dr. Garnier. Therefore, the main aim of this thesis includes the study and the selection of purification schemes for laboratory- and large-scale processes. The laboratory-scale protocols could

eventually be applied for VSV characterization studies or for preparation of purified virus doses for the trial of VSV-based vaccines in mice or rodents that require small quantities of virus material. The large-scale methods could be implemented for non-human primate and human trials that require higher concentrations of rVSV or for pilot-scale production of rVSV as a viral vaccine or a gene therapy vector.

One of the main challenges associated with the purification of enveloped viruses is the sensitivity of the viruses to changes in environmental conditions, such as pH, salt concentration, temperature, and storage media [23–25]. Therefore, special care must be taken to avoid or minimize the exposure of viruses to these extreme conditions. Downstream processing of cell culture produced viruses comprises a series of steps that intend to concentrate the virus preparation and bring the concentration of contaminants to the lowest possible and safe level. These contaminants can be introduced from different sources, including the cell culture medium or through the purification process [26–28]. The presence of these contaminants, that could be nucleic acids or proteins that can be found in undefined culture medium additives such as blood serum, have been shown to influence the transduction efficiency of viruses *in vitro* and cause inflammation and systemic immune responses when used *in vivo* [29,30]. As a result, their removal is mandatory, and it can improve the efficacy and safety of the vaccines.

A DSP scheme for cell culture produced viral vaccine often includes a nuclease treatment to reduce the amount of contaminant DNA or RNA that can increase the sample's viscosity and affect the performance of the membrane-based approaches used in the process. It also consists of; 1) a clarification step that aims to remove the larger contaminants, including cellular debris, 2) a concentration step to reduce the volume of the sample for the next DSP steps and also to partially eliminate the contaminants, and 3) a purification step that separates the viruses from the contaminants, based on distinctive physical or chemical characteristics, such as size, polarity, and hydrophobicity, often time by the use of chromatography. Finally, an ideal purification scheme for pilot-scale processing should be scalable, with the capacity to be employed at large-scale purification of viruses, take the least

processing time to prevent the loss of viral infectivity, and yet be economical to meet the market demand [31,32].

In order to obtain an efficient process for the purification of rVSVs produced in Vero-SF cells, a series of microfiltration filters of different media with low protein binding capacity will be tested for clarification. For this purpose, filters based on Polyethersulfone (PES), Polyvinylidene Fluoride (PVDF), Regenerated Cellulose (RC), and Cellulose Acetate (CA) with low protein binding characteristics will mainly be tested for their ability to recover infective particles and eliminate large contaminants at both small-scale and large-scale. Eventually, the two-step clarification step (comprised of low-speed centrifugation and microfiltration) will be replaced by serial microfiltration using a series of microfiltration filters of decreasing pore sizes to eliminate the need for low-speed centrifugation and improve the scalability of the scheme. To reduce the volume of the sample and process time, different tangential flow ultrafiltration and centrifugal-based ultrafiltration units will be tested for pilot-scale and laboratory-scale, respectively. Moreover, the use of ultracentrifugation for purification of the smaller quantities of supernatant and its efficiency in removing contaminant proteins and DNA will be assessed. The virus preparations obtained from this step will serve as a standard for comparing the efficacy of the laboratory-scale process to the large-scale protocols. As one of the most commonly used approaches for purifying enveloped viruses, anion exchange chromatography will be studied for the large-scale purification scheme. For this purpose, two different chromatography media, including resin and membrane, will be tested to recover infective particles while eliminating the possible contaminants. Mixed-mode chromatography will also be evaluated for separation of virus particles from microvesicles, one of the main cell culture derived contaminants in enveloped virus production.

Chapter 1: Review of literature

The use of mammalian cell cultures to produce vaccines is well established in the biopharmaceutical industries (e.g., a vaccine against influenza, rabies, polio, and smallpox) [33]. However, developing an upstream and DSP for every new cell culture-based vaccine is challenging and requires additional optimizations [34,35]. In general, DSP comprises multiple steps, aiming for vector concentration, contaminant removal, and buffer exchange [36]. The possible impurities present in the vaccine suspension harvested from cell culture can arise from different sources. The impurities can be introduced by cell culture media and its supplements, including the plasmid DNA used for transfection, the animal sera used to enhance the cell growth, the cellular components including the cellular enzymes, the cellular genomic DNA, the extracellular matrix materials, released by disrupted host cells, and also the materials added during the purification process such as the endonucleases used for nucleic acid removal [35,37]. These contaminants have been shown to interfere with virus transduction efficiency and result in inflammation and systemic immune responses when used *in vivo*. As a result, their removal improves viral vaccines' safety and efficiency [35,38–40].

Developing a purification scheme for DSP of viruses requires a combination of multiple steps and optimization of several parameters for the highest recovery of the viruses. An optimal purification strategy must be designed based on several factors, including the type of the vaccine (inactivated or active viral vaccine, subunit, or whole virus preparation), the physical and chemical characteristics of the virus, including the virus morphology, isoelectric point, stability, its tolerance to pH and temperature, and the stringent quality standards defined by regulatory agencies in terms of the level of contaminants such as the genomic DNA, host cell proteins and endotoxin for *in vivo* experiments [33,41,42]. In addition to these factors, the proposed purification schemes should also be scalable with the capacity to be employed at large-scale purification of viruses, take the least processing time to prevent the loss of viral activity, and yet be economical to meet the market demand [36,43,44].

The use of viruses has attracted pharmaceutical industries due to their broad spectrum of medical applications, such as vaccines and gene therapy [33]. Several successful viral vaccines against viral diseases are already on the market, including influenza, chickenpox, rubella, mumps, measles, and Ebola [33,35,44,45]. However, with 1.5 million new Human Immunodeficiency Virus (HIV) infections per year and over 37.7 million infected people worldwide, there are still no vaccines that could prevent the occurrence of HIV [1].

The NSERC-funded project "Optimizing the VSV vector towards an HIV vaccine" aims to develop a vaccine for HIV based on recombinant vesicular stomatitis virus (rVSV). The VSVs used in this project are formed on the same backbone as the rVSVΔG-ZEBOV-GP vaccine for Ebola approved by the FDA in the 2018 Ebola outbreak and marketed under the name Ervebo [14]. In this project, the viral vector carries the modified HIV surface protein that trigger the immune response and protect the host against HIV infection. The design and modifications of the rVSV-based HIV vaccine and its production in serum-free Vero cells are carried out by other parties involved in the project. However, the development of purification schemes for downstream processing of these cell culture-produced rVSV based vaccines before their test in rodents and non-human primate trials will be carried out through the work done in this Ph.D. project. For this purpose, a review of the physical characteristics of VSV, its stability, the construction of the vaccine used in this project, different steps involved in DSP of viral vaccines, including clarification by low-speed centrifugation and microfiltration, concentration by ultracentrifugation and ultrafiltration, and purification by different chromatography principles including ion-exchange, affinity, size-exclusion, and mixed-mode chromatography, are provided in this chapter.

1.1. Structure, physical and chemical characteristics of VSV

The development of a successful purification scheme requires the knowledge of the virus's physical, chemical, and biological characteristics. Vesicular stomatitis virus is a rod-shaped, negative-strand RNA virus belonging to the *Rhabdoviridae* family. The virus measures about 70 × 200 nm (Fig. 1. A) [46]. VSV infection can cause oral

diseases in animals, including cattle, horses, and swine; however, due to the interferon response, its infection in humans only causes flu-like symptoms [43,47]. The genome of VSV is around 11 kb and is made up of five core genes that encode five structural proteins, including the nucleocapsid protein (N), the phosphoprotein (P), a cofactor of the RNA-dependent RNA polymerase (L), the matrix protein (M) and the attachment glycoprotein (G) [48] (Fig. 1. B & C).

The possibility of replacing the VSV-G envelop protein with antigens of human pathogens makes VSV an excellent platform in recombinant technology for gene therapy and replication-competent vaccines [47,49,50]. As a result, its applications in experimental vaccines have been featured in vaccines against Ebola, Marburg, Lassa, Crimean-Congo hemorrhagic fever (CCHFV), Nipah, MERS- and SARS-coronaviruses, Zika, Influenza and Human immune deficiency virus (HIV) [51].

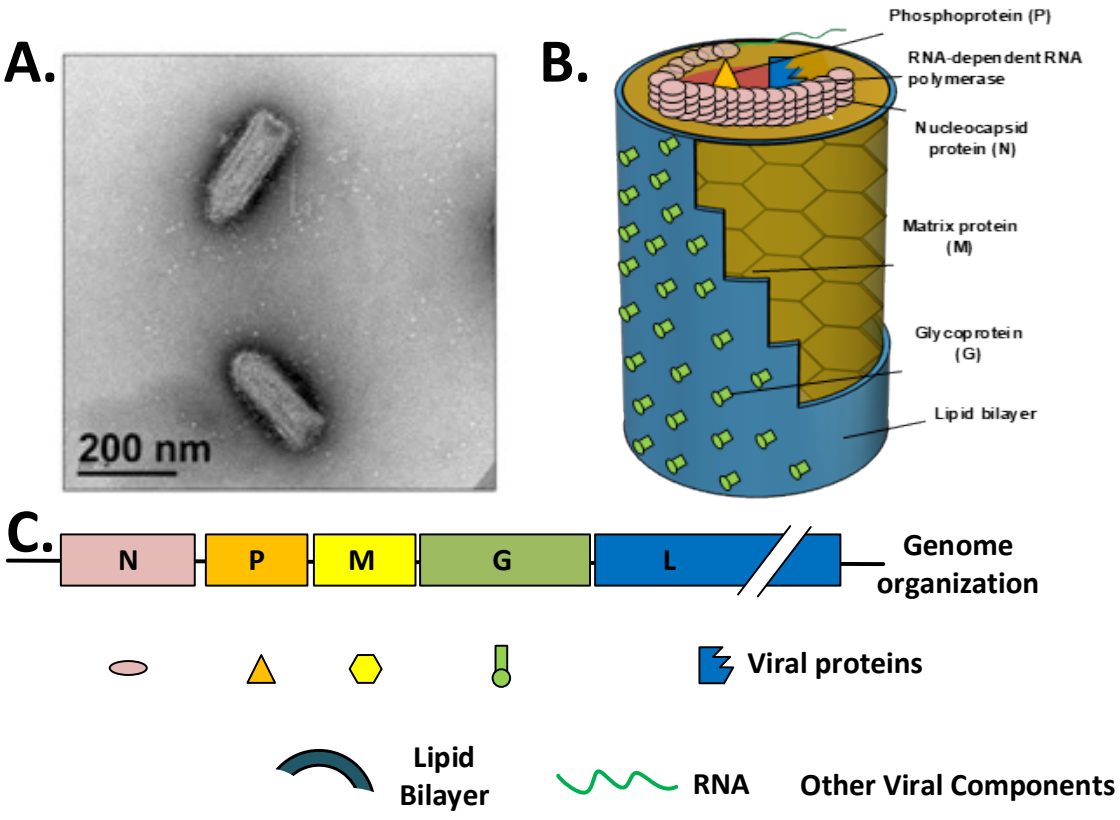

Fig 1. A) TEM image of rVSV [46], B) Cutaway diagram of a VSV particle, C) Genome organization of vesicular stomatitis virus (VSV). Adapted from Strauss & Strauss [48].

1.2. Stability of VSV

The enveloped viruses such as human coronaviruses and H1N1 are more labile than non-enveloped viruses and survive for a shorter time on surfaces and show more sensitivity to environmental variants including pH, temperature, and the preservation media [23,24,52]. Zimmer *et al.* [53] assessed the stability of VSV serotype *Indiana* expressing enhanced GFP in MEM media supplemented with 5% FBS at different temperatures and incubation times. As shown in Fig. 2. A, in the presence of serum, VSV showed high stability when stored at 4 °C for up to 28 days. However, incubation of VSV at 22 °C resulted in continuous loss of infective particles and 90 % ($t_{90\%}$) of the viral titer was lost after 7.8 days of incubation. On the other hand, incubation of VSV at 37 °C had a severe effect on its infectivity with the loss of 90 % of infective particles after 2.8 days, which indicates the negative effect of high temperature on storage of VSV.

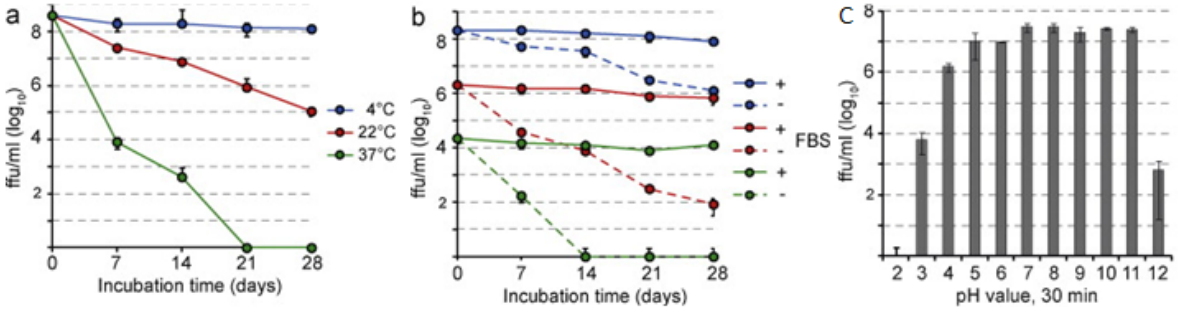

Fig 2. The impact of a) temperature, b) presence or absence of FBS in the preservation media, and c) pH on the infectivity of GFP expressing VSV Indiana. Adapted from Zimmer et al. [53].

However, addition of FBS was shown to reduce the infectivity loss considerably, for instance, when VSV was incubated at 4 °C without FBS, the $t_{90\%}$ was 12.2 days, whereas the addition of FBS to the media improved the viral titers and resulted in a $t_{90\%}$ of >28 days (Fig. 2. b). These results indeed confirm the importance of FBS addition on the long-term stability and storage of VSV. However, the addition of FBS to the final vaccine preparation is often not compatible with GMP practices. The viral titer in live viral vaccines could be improved by the addition of other components, including sugars and sugar alcohols (trehalose, sorbitol, sucrose, lactose), amino

acids (glycine, arginine complexes, monosodium salt of glutamic acid, histidine), salts (sodium chloride, magnesium chloride), and polymers (sodium hyaluronate, dextran 40, gelatin, carboxymethyl cellulose) [54–56].

Moreover, the effect of environmental pH on VSV infectivity was tested by incubating VSV at pH varying from 2 to 12 for 30 min at room temperature, as is shown in Fig. 2. C, VSV exhibits higher stability in an alkaline environment in pH ranging from 7 to 11. Even though fewer infective particles were found at pH 5 and 6, it is still stable in these two conditions, but below 5 or above 11, its stability decreased considerably. The loss of virus infectivity at lower pH has been previously shown to be associated with the pH sensitivity of virus surface glycoproteins [57].

The short-term and long-term stability of recombinant VSV-based Ebola vaccine (rVSV-ZEBOV) was also reported by Arnemo *et al.* [58]. As presented in Fig. 3. A, the rVSV-ZEBOV vaccine was stable when stored at 4 °C and 25 °C for one day. However, similar to the results of Zimmer *et al*. [53], the virus stability was significantly lower at 40 °C. The thawed rVSV-ZEBOV was stable at 4 °C for a week, but infective particle count was significantly reduced after two weeks, and infectivity kept decreasing for several weeks (Fig. 3. B).

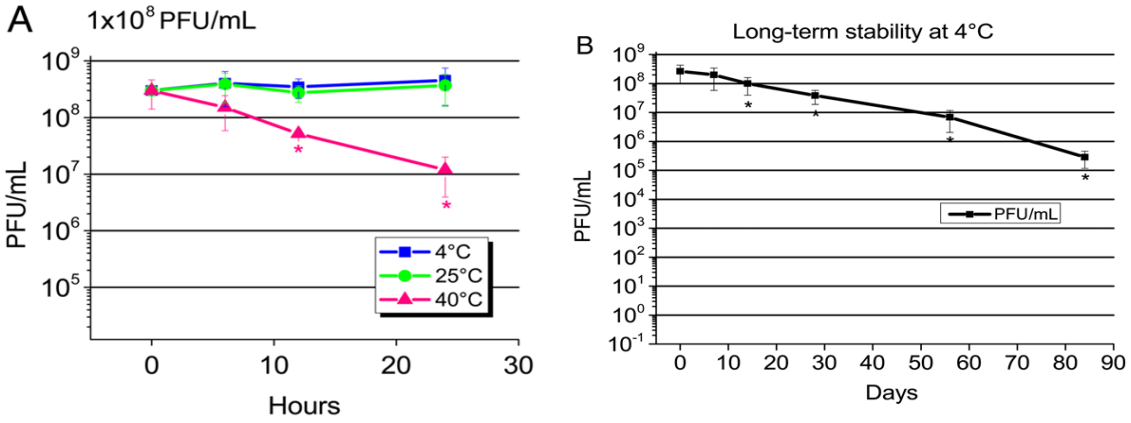

Fig 3. The A) short-term and B) long-term stability of rVSV-ZEBOV stored at different temperatures. Adapted from Arnemo et al. [58].

1.3. Construction of the vaccine

The viral vaccine used in this project is a recombinant live attenuated Vesicular Stomatitis Virus strain Indiana (VSV) with the Zaire Ebolavirus glycoprotein gene (ZEBOVGP) and the HIV envelope gene (HIVenv) replacing the VSV glycoprotein (VSV-gp) gene. This combination of genes results in a virus structure with a VSV backbone, but expressing the Ebola-gp and HIV-gps (HIVenv gene encodes for gp160 which is later cleaved into gp120 and gp41) of its surface (Fig. 4. A & B). Replacement of the VSV-gp gene with both Ebola and HIV GPs forms a non-pathogenic and attenuated recombinant VSV (rVSVΔG/ZEBOVGP.HIVenv) with narrower cell tropism compared to wild type VSV that replicates more slowly and results in lower yields but workable viral titers. It has been shown that the virus still keeps its bullet-shaped structure despite these genetic manipulations [47] (Fig 1. A).

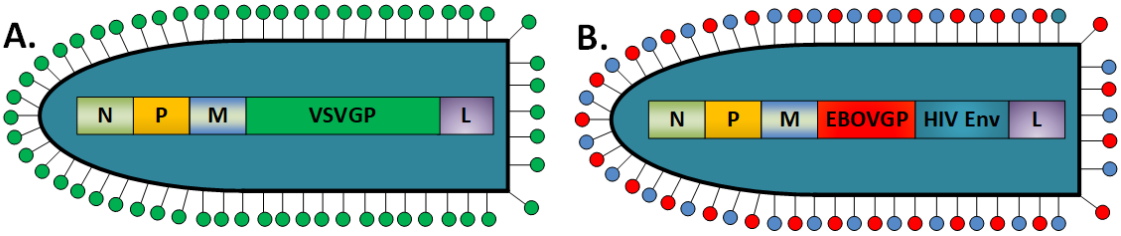

Fig 4. A) The graphical representation of the five main genes of VSV in the wild-type virus and B) replacement of the VSV-GP gene with EBOV-GP and HIV-GP genes in the recombinant rVSV. Adapted from Racine *et al*. [59].

The rVSVs are produced through the process of reverse genetics. Therefore, to obtain the rVSVΔG/ZEBOVGP.HIVenv viruses, tissue culture cells (Vero-E6 or HEK293) are transfected with five plasmids (Fig. 5);

- VSV-ZEBOVGP.HIVenv plasmid contains the entire VSV genome with the ZEBOV GP gene and HIVenv gene replacing the VSV GP gene, which constitutes the rVSVΔG/ZEBOVGP.HIVenv viral genome.
- The other 4 viral plasmids are simply helper plasmids required in the reverse genetics system.
  - pCAGGS-T7 (helper plasmid containing the T7 promoter)
  - pBS-N (helper plasmid containing VSV N protein gene)

- pBS-L (helper plasmid containing VSV L protein gene)
- pBS-P (helper plasmid containing VSV P protein gene)

Therefore, the transfection of cells with the plasmids mentioned above results in the production of VSV proteins required for viral replication, followed by virus assembly and budding from the host cell of the VSVs expressing Ebola and HIV glycoproteins on their surface (Fig. 5).

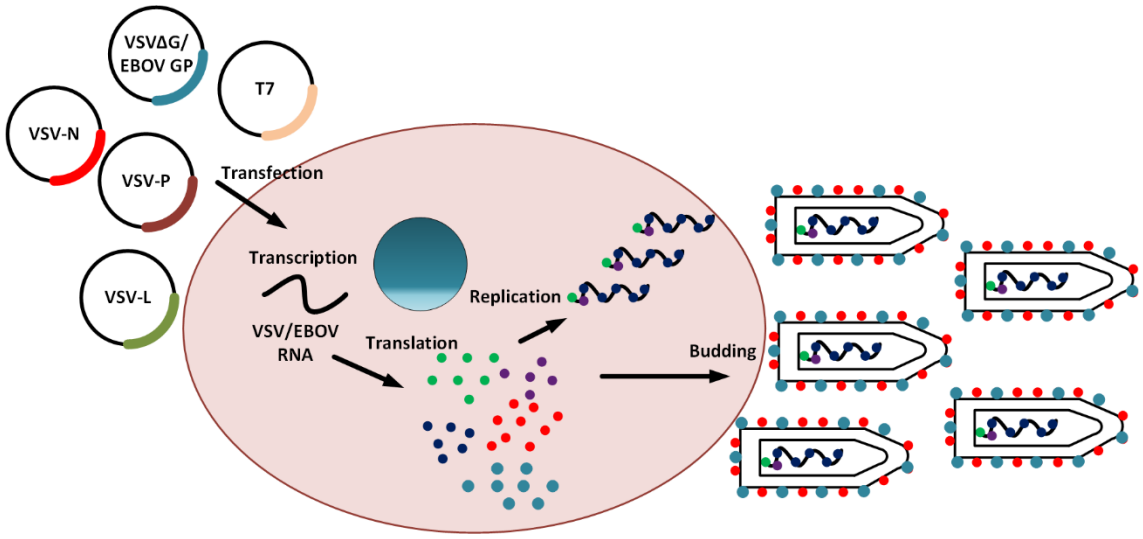

Fig 5. The synthesis of rVSV vaccine through the reverse genetic system.

1.4. Purification of enveloped viruses

The virus preparations obtained from mammalian cell culture aimed for clinical use should go through stringent purification schemes to meet the regulatory authorities' requirements, such as FDA. Downstream processing of viral vectors of vaccines is intended to eliminate the contaminants originating from either the culture medium, the producer cell, or even through the process of purification itself in order to obtain pure, concentrated, and highly efficient virus preparations [42,43]. Different steps of purification protocol must be deliberately designed and chosen to obtain the maximum purity with the most negligible loss of infectivity of virus in the final preparation [60].

Multiple purification steps are needed to deliver the final product with the desired purity and concentration [60]. The purification steps are based on the vector's different properties, such as the virus charge, hydrophobicity, size, or other surface

features [41], where each step can be chosen in order to purify the virus according to one of these properties, in an orthogonal fashion [60].

Table 1. Steps involved in the DSP of viruses. Adapted from Segura et al. [35].

Process	Separation principle	Laboratory-scale	Large-scale
Clarification	Size, density	Centrifugation Microfiltration	Microfiltration
Concentration	Size, density	Pelleting	Ultrafiltration
Purification	Charge, Size, density	Ultracentrifugation	Chromatography

Downstream processing of viruses broadly consists of sequential clarification steps (Table 1), concentration, and purification. The purified viruses also need to be concentrated and re-suspended in the formulation buffer at the polishing step for their long-term storage [35,41]. The primary step (clarification) is mainly involved in removing the host cells and cellular debris by microfiltration and/or centrifugation, after which the supernatant is concentrated mainly by ultrafiltration or ultracentrifugation. Even though these primary stages remove some contaminants, they are undoubtedly insufficient to prepare the vaccine for *in vivo* applications.

When setting a purification protocol, one must consider many criteria such as scalability, maximal productivity, purity, robustness, manufacturing cost, and broad applicability of the selected candidate process to various vectors [41,42]. Although all approaches could be possible for large-scale schemes, some are more compliant to scale up and usability by industry [36]. Therefore, we will review the potential methods used at each purification step, their scalability, advantages, and possible drawbacks.

1.4.1. Nucleic acid removal

The presence of nucleic acids as RNA, plasmid-derived DNA or the DNA released from the lysed producer cells or free viral RNA should be minimized to an acceptable level (10 ng/dose) before being used in animal studies or humans trials [44].

Practically, any large sequences of nucleic acid contamination need to be digested early in the process, before any clarification or concentration steps, since these can increase the sample's viscosity and result in membrane fouling. Moreover, since they carry negative charges, they can interfere both at the purification stage (especially when ion exchange is involved) and impede virus potency and transduction [60,61]. The most commonly used endonuclease is Benzonase®, which requires $MgCl_2$ and incubation at 37 °C for optimal activity [41]. In addition to the digestion of large DNA into smaller fragments, Benzonase® has also been shown to facilitate the exclusion of these fragments during the purification process [44]. However, the addition of Benzonase® introduces the additional source of protein contamination to the supernatant, and incubation at 37 °C for its optimal activity could also affect the stability of viruses.

1.4.2. Clarification

The first step after the harvest of virus-containing cell culture supernatant is clarification. This step's primary goal is to efficiently remove the crude supernatant's contaminants, including cells and cell debris, and prepare it for further purification steps such as ultrafiltration and chromatography [35]. Low-speed centrifugation and membrane microfiltration are the two methods that are used predominantly for this purpose. Low-speed centrifugation is generally considered a centrifugation speed within the 3,000 ×g to 10,000 ×g range [62]. At a laboratory-scale, low-speed centrifugation has been used as a primary clarification step for many viral vectors, including VSV-G pseudotyped lentiviruses and wild-type VSV in a range of 6,000 ×g to 10,000 ×g (Table 2). The application of centrifugation before membrane filtration could significantly increase the operation time of these membranes before clogging occurs by removing the larger contaminants that can otherwise foul the membrane.

When choosing a membrane for the DSP of viruses, different criteria such as filter material (PES, CA, and PVDF), pore size, and working conditions (pH, flow rate, and ionic strength) must be considered carefully to minimize the risk of clogging and loss of viruses [64,65]. The filtration membranes used to clarify supernatants usually have pore sizes varying from 0.1 to 10 µm, and they are found either as depth or

membrane filters [64]. A typical membrane filter traps particles larger than its pore size on its surface. However, in a depth filter consisting of either a single or multiple layers of filtration media, the retention of solids occurs within the membrane depth. Microfiltration has been used for various viruses, including lentiviruses, retroviruses, and rhabdoviruses, resulting in high virus recoveries ranging from 82% to 96% (Table 2).

Table 2. Methods used for clarification of virus-containing cell culture supernatant.

Mode of clarification	Virus	Specification	RCV (%)	Ref
Centrifugation	Lentivirus pseudotyped with VSV-G	10,000 × g,15 min, 4 °C	-	[44]
	Rhabdovirus (VSV)	6,238 × g, 30 min, room temperature	55-77	[62]
Microfiltration	Lentivruses	Sartopore capsule (0.8+0.45 µm)	91	[63]
	Rhabdovirus (VSV)	Whatman PolyCap™ HD75 (0.2 µm)	82	[62]
	Rhabdovirus (VSV)	Pall Acrodic ™ Supor ™ (0.2 µm)	96	[62]
	Rhabdovirus (VSV)	Sartorius Sartorbran ™ (0.2 µm)	94	[62]
	Rhabdovirus (VSV)	Sartorius Sartopore ™ 2 (0.2 µm)	82	[62]
	Rhabdovirus (VSV)	Millipore Millex (0.2 µm)	87	[62]

Ref: Reference, RCV: recovery.

Clarifying virus-containing cell culture supernatant in a single step could result in membrane fouling and subsequently loss of viruses on the membrane due to the membrane obstruction by the larger cell culture contaminants, including cellular debris and genomic DNA [44]. Low recoveries of viruses after clarification by

membrane filtration had been linked to the virus's stability, its affinity to the membrane or clogging of the membrane pores by cellular debris [43,66]. Sequential microfiltration of the crude supernatants is one of the approaches that help avoid membrane clogging. In sequential microfiltration, the viral suspension is passed through a series of membranes with decreasing pore sizes [37,67]. Also, the effect of flow rate on membrane filtration should not be neglected. Higher titer recoveries were reported by Segura et al. [35] and Schweizer and Merten [37] using increased flow rates for the crude supernatant's filtration that decreased entrapment of viruses in the membrane pores.

1.4.3. Concentration

Introducing a concentration step in the purification process can facilitate the performance of later purification steps, including chromatography, by lowering the viral stock volume to be processed and removing a part of cell culture contaminants. The concentration of viruses by pelleting can be achieved through both low-speed centrifugation and ultracentrifugation. However, longer centrifugations are required to efficiently pellet viruses by low-speed centrifugation. Concentrations of about 100 fold or higher have been reported after low-speed centrifugation of retroviruses when the pellet was re-suspended in a small quantity of buffer (Retroviruses) (Table 3) [35].

1.4.3.1. Ultracentrifugation

Ultracentrifugation is the most commonly used conventional method for the concentration of virus particles at a laboratory-scale. The use of ultracentrifugation for the concentration of viral supernatant has been reported for many enveloped viruses, including lentiviruses, retroviruses, and rhabdoviruses (Table 3) [68–71]. More importantly, high concentrations of 50 to 300 fold with more than 60 percent recovery of infective particles have been observed using ultracentrifugation [40,69]. As mentioned earlier, one of the main challenges in the purification of viruses is separation of the infective particles from the defective vectors such as empty capsids and vesicles that share a high level of property similarities with viruses. However,

ultracentrifugation is among those methods that can separate functional viruses from other contaminants that can interfere with virus potency and dose [41].

The two types of ultracentrifugation used for the concentration of crude supernatant are differential and density gradient ultracentrifugation. The differential centrifugation principle is based on the separation of elements by their sedimentation rate. When exposing a mixture of components with a different size and density to an increasing gravitational force, the particles sediment based on their sedimentation rate with the largest particle pelleting at the earliest, followed by the next smaller particle with decreasing sedimentation rates [72,73].

On the other hand, the density gradient centrifugation is mainly performed under two principles: the isopycnic ultracentrifugation that separates elements based on their buoyant density and rate zonal sedimentation that relies on the mass and size of the particles [33,67]. In rate zonal centrifugation, the elements are centrifuged through a gradient of a hyperosmotic medium with increasing density towards the bottom of the tube. However, the highest density in the gradient is lower than the density of the particles to be separated, resulting in pelleting upon longer centrifugation times. On the other side, in the isopycnic centrifugation, the highest density in the gradient that is located at the bottom of the tube goes beyond the density of the particles to be separated. Therefore, this type of centrifugation results in the formation of bands holding the particles with the same density, and in this approach, longer centrifugation time does not result in pellet formation [73].

One of the commonly used density gradient methods is the use of a cushion of a hyperosmotic medium with a density lower than the particles of interest at the bottom of the tube and filling the top of the tube (60 to 70 % of the tube capacity) with the virus-containing supernatant. This method allows any particle with a higher density to pass through and pellet while the lower density elements remain on the top of the cushion. Density gradient ultracentrifugation has been used for the purification of several enveloped viruses, including influenza virus [33], murine leukemia virus [74], Japanese encephalitis virus [75], mumps virus [76], and rabies virus [77] (Table 3). Additionally, the use of the rate zonal sedimentation principle for concentration has

been shown to bring higher grades of purification for retroviruses than isopycnic or density gradient ultracentrifugation at laboratory-scale [67].

There are three media used traditionally for density gradient centrifugation: CsCl, sucrose, and iodixanol [42]. Sucrose and cesium chloride are the most commonly used hyperosmotic media for the purification of viruses. However, both of the mentioned media are highly viscous and usually take a long time for sedimentation and banding of viruses at the proper density (24 h for CsCl) [35,41]. In addition to the centrifugation duration, sucrose's high viscosity has been shown to adversely affect the surface structure of viruses and their activity [78,79]. These drawbacks indicate that iodixanol is a better alternative for purifying virus particles by ultracentrifugation.

Compared to other media, the lower viscosity of iodixanol has been reported to reduce the centrifugation time for adenoviruses from 24 h (using CsCl) to 2 h [41]. Therefore, low viscosity, less processing time, and safety of iodixanol (non-toxic to cells) highlight this medium's potential to be used in DSP of viruses both at laboratories and in biopharmaceutical industries.

Despite ultracentrifugation being a powerful method for obtaining highly purified virus particles, there are a few practical issues for its application at both laboratory- and large-scales. Firstly, preparation for this method is time-consuming and labor-intensive [36,37,60]. Moreover, the scalability of ultracentrifugation is very difficult, and its usage is limited by the total volume of the supernatant to be processed, and it requires high facility investments at the industry level. The drawbacks of ultracentrifugation are not limited to scalability as there is a possibility of co-concentration of the impurities and viruses if the virus band is not picked correctly. These contaminants could include vesicles, empty capsids, or DNA interfering with virus transduction efficiency [35]. These disadvantages have made ultracentrifugation a less frequent method of choice for large-scale virus purification, while its advantages at a small-scale are appreciated.

1.4.3.2. Ultrafiltration

Ultrafiltration is the method of choice for a fast but gentle approach for volume reduction of the virus-containing supernatant at the large-scale. Unlike ultracentrifugation, membrane-based methods can easily be scaled up. Ultrafiltration can be used at two steps; before chromatography for concentration and buffer exchange and after chromatography for polishing purposes, such as removing salts and balancing the pH. The membranes used in ultrafiltration units consist of polymeric materials such as polysulfone (PS), regenerated cellulose (RC), cellulose acetate (CA), Polyvinylidene fluoride (PVDF), modified polyethersulfone (mPES), and modified RC. Among these membranes, RC membranes and RC modified membranes exhibit an interesting combination of high mechanical strength, low protein binding capacity, and high resistance to detergents [80,81]. However, the lowest protein binding capacity has been observed in PES and CA membranes [62].

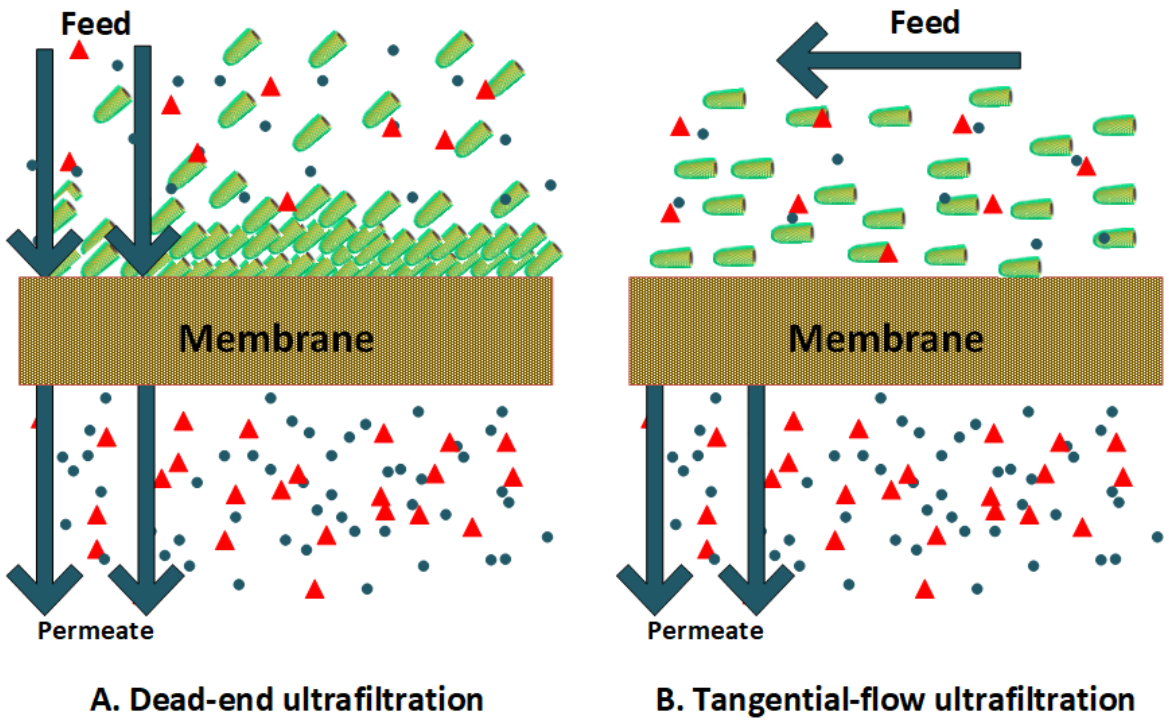

Fig 6. Graphical comparison of virus flow over a membrane in A) Dead-end ultrafiltration and B) Tangential flow ultrafiltration concentration methods.

Table 3. The concentration of viruses using ultracentrifugation and different ultrafiltration approaches, including centrifugal-based ultrafiltration and tangential flow ultrafiltration.

Mode of conc.	Virus	Membrane	Conc. factor	RCV (%)	Ref.
Tangential flow UF	Retrovirus (MoMLV)	Polysulfone, hollow fiber, 500 kDa	-	101	[88]
	Retrovirus	Regenerated cellulose, flat sheet, 300kDa	-	91-96	[89]
	Orthomyxovirus (Influenza A)	Polysulfone, hollow fiber, 750 kDa	-	106	[90]
	Orthomyxovirus (Influenza A)	Polyethersulfone, flat sheet, 100 kDa	-	95	[91]
	Orthomyxovirus (Influenza A)	Polyethersulfone, flat sheet, 100 kDa	-	100	[92]
	VSV-G pseudotyped Lentivirus	flat sheet 100kDa and 300kDa	66	100	[71]
	Oncoretrovirus	Sartocon ultrafiltration module, 100 kDa	122 to 160	65	[93]
Centrifugal UF	Lentivirus pseudotyped with VSV-G	Centricon plus-20, 100 kDa	-	243	[71]
UC	Lentivirus pseudotyped with VSV-G	28,000 rpm in a SW-28 rotor at 4 °C for 90 min	-	61	[71]
	HIV-1 pseudotyped with MoMLV Env	-	-	> 80	[69]
	HIV-1 pseudotyped with rabies GP	-	-	> 80	[69]
	Lentivirus pseudotyped with VSV-G	26,000 g 5h 60,000 g 2h	-	69 70	[71]
UC with sucrose cushion	VSV-G pseudotyped oncoretrovirus	100,000 ×g for 2 h at 4 °C	25 to 100	45 to 89	[94]
Pelleting by LSP	Oncoretrovirus	6000 ×g for 16 h at 4 °C	10 to100	90 to 97	[95]

Conc: Concentration, UF: ultrafiltration, UC: ultracentrifugation, LSP: Low-speed centrifugation, Ref: Reference, RCV: recovery.

During ultrafiltration, contaminants with sizes smaller than the membrane pores pass through the membrane and are removed as permeate while the virus particles are retained on the membrane's upstream side as retentate [35]. Based on the experiment's scale, ultrafiltration and diafiltration can be performed using different types of filtration units [69]. For processing lower volumes of supernatant (up to 2 L), centrifugal filter units and stirred cell tanks (dead-end filtration units) are more convenient (Fig. 6. A) [82,83]. However, for larger volumes, tangential flow ultrafiltration (TFUF) systems using tubular units, flat membrane, or hollow fibers can be employed that allow concentration and diafiltration of samples at the same time (Fig. 6 B and Table 3) [84–86].

The use of TFUF has been successfully employed to purify retroviruses, influenza A virus, and lentiviruses resulting in high recoveries (> 90%, Table 3) using different types of units such as flat membrane and hollow fibers. When using flat membranes, the high turbulence inside the membrane channels causes a high flux of permeate within these channels. However, hollow fibers use milder handling of the particles due to the important feed flow across their membrane makes them well suited for purifying enveloped viruses [43,87].

During the process of TFUF, the clarified cell culture supernatant is tangentially circulated along the membrane (pore size between 0.001 µm to 0.1 µm) using a peristaltic pump (Fig. 6. B). Usually, the membrane used for ultrafiltration has cut-offs between 100 kDa to 50 kDa; however, 750 kDa (50 nm) pore sizes are also used, especially for separating large viruses [35,96].

During the flow of a solution in a TFUF unit, the pressure difference across the membrane leads to the exclusion of contaminants with molecular weights lower than the membrane pore size (small proteins, e.g., BSA, or residual DNA) through the membrane pores as permeate while the virus particles will be retained and concentrate upstream of the filter surface [36,43]. One of the main advantages of TFUF is that the constant flow of the solution along the membrane surface delays the membrane clogging and fouling, which in turn allows higher titer recovery per cycle compared to dead-end filters [43]. If ultrafiltration is optimized to reduce

membrane fouling and shear effect, it can result in high overall yields at both laboratory- and large-scales (Table 3).

1.4.4. Chromatography

Chromatography is the most commonly used mode of virus purification at a large-scale since it provides a fast and efficient separation of virus particles from the crude supernatant that can be adapted to GMP-compliant operations [97]. The samples used in chromatographic separation are usually clarified and concentrated at the initial steps of purification to minimize the contaminants and the volume to be processed at this stage. A typical chromatography column consists of a stationary phase packed in the column and can comprise beads, membrane, or monolith and a mobile phase that runs through the stationary phase and carries the analytes. During the chromatographic separation process, the supernatant is passed along a column containing beads with functional groups responsible for capturing and separating viruses from the rest of the supernatant. Washing steps are also included to remove the contaminants as much as possible. Desorption agents then elute the particles that are captured by the beads in fractions [35,37].

Chromatography principally functions based on the specific interaction between the target molecule (virus particles) and the functional groups grafted on the surface (internal or external) of chromatography beads, membranes, or monoliths. These interactions are based on the characteristics of the particles, including surface charge (ion-exchange chromatography), size (size exclusion chromatography), and affinity (affinity chromatography) toward a specific molecule (e.g., metals). The stationary phase's physical structure in chromatography can be made up of packed beds, membrane adsorbers, and monoliths [33,64].

In the case of a packed bed, a column is first filled with polymeric or inorganic beads (resins) before it can be used for separation. Chromatography beads can be found as porous, non-porous, and solid core in various sizes [33,98]. Polymeric resins are supplied either as natural polymers including agarose, cellulose, dextran, or agarose-dextran beads, or they can be found as polyacrylamide, polystyrene divinylbenzene, polyacrylamides, or polymethacrylates as synthetic polymers

[33,99]. The matrixes used in packed beds can also consist of inorganic beads such as hydroxyapatite [100], glass [101], and silica [102]. The large size of viruses prevents them from diffusing into the pores of any chromatography resins (except for adeno- and polio-associate viruses)[103].

The other chromatography types, including monoliths and membranes, are considered connective chromatography media [64]. Monoliths are made up of solid matrixes with interconnected macroporous channels that allow the mobile phase's flow into the entire matrix [33,104]. Monoliths are available in different polymers, namely polymethacrylate copolymers, polyacrylamide, polystyrene-divinylbenzene, polystyrene, silica, and modified cellulose [33] that are available in different sizes varying from 13 nm to 6 μm [64]. They have been successfully used for the separation of viruses, including influenza [105], rubella [106], lentiviruses [44], and hepatitis A [107]. However, monoliths' main disadvantage is their susceptibility to clogging, especially with high DNA concentration in the sample, which is expected to occur lesser by using monolith of 6 μm wide channels [64,108].

Membrane adsorbers are another simple, affordable mode of chromatography for the large-scale separation of viruses. These membranes are available in various materials such as cellulose, polysulfone and its derivatives, and hydrazine [109] supplied in different physical structures, namely flat sheets, hollow fiber, and radial flow adsorbers devices [110]. Hollow fibers provide a larger surface area and the possibility of having the charged affluent flowing tangentially to the membrane, thus minimizing the membrane clogging rate. The same can be said about radial flow devices with spirally coiled flat sheet membranes that also have the volume to membrane surface ratio comparable to hollow fibers. However, for both tools, the purified samples are heavily diluted and require further concentration steps. The commercially available beads are mostly reusable and require a cleaning step after purification, which might be laborious and include the costs for cleaning and sanitization; however, most of the monoliths and membrane adsorbers are made for single use [33].

1.4.4.1. Ion exchange chromatography

Ion exchange chromatography functions based on the different charges of the molecules to be separated. The stationary phase polarity is fixed to be opposite to the molecules that are aimed at being retained longer in the column/cartridge. The molecules with polarity similar to the stationary phase's, or neutral, will flow through, and the molecule with a charge opposite to the stationary phase will separate according to their charge strength, with retention time inversely proportional to their charge. The bound molecules can be desorbed from the chromatography medium when the forces between the charged molecule and the medium are weakened. This can be achieved either by lowering the pH or increasing the ionic strength.

The ion exchanger resins are categorized into anion exchangers (AEX) and cation exchangers (CEX) based on the resin's charge. The AEX resins carry a positive charge on their surface hence suitable for separating negatively-charged molecules, whereas CEX resins are negatively charged on the surface and proper for binding to positively charged analytes. Since most of the enveloped viruses have isoelectric points lower than 7 and are thus negatively charged, AEX is a more suitable option for their purification at neutral pH [111].

1.4.4.2. Anion exchange chromatography

AEX is based on a positively charged stationary phase that separates the molecules in the mobile phase based on the strength of their negative charge [93]. Desorption of the particles bound to the AEX matrix is usually accomplished by a high salt concentration solution that competes with the particles in binding to the charged stationary phase [11, 26]. Recovery yields ranging from 17% to 86% have been reported to purify enveloped viruses using AEX (Table 4). However, the high concentration of salt used for elution has been shown to have adverse effects on particles' infectivity and result in lower virus yield [57]. An immediate diafiltration can be employed after AEX chromatography to dilute and remove the salts from the purified samples [26] to minimize the adverse effects of salinity of the elution buffer. Many resins are available with anionic exchange properties, as shown in Table 4, with the diethylamino-ethyl (DEAE) and quaternary ammonium (Q) being the most

commonly used ones [64]. The strong anion exchangers are positively charged over the entire pH range, while the weak anion exchangers are only charged in specific pH conditions. Recovery yields of above 65 % have been reported for influenza A and B virus and VSV-G pseudotypes viruses using Sartobind® Q and Mustang Q robust anion exchanger membranes, respectively.

Moreover, lower recoveries of 51 % to 57 % have also been published for retroviruses using DEAE FF HiTrap™ and Q XL HiTrap™ resins and 45 % for VSV using Matrex™ Cellufine® (Table 4). The use of AEX chromatography has also been reported for wild-type inactivated HIV-1 virus [12, 77]. Taken together, these results show that AEX chromatography can be a suitable candidate for the purification of intact enveloped viruses carrying negative charges on their surface.

1.4.4.3. Hydrophobic interaction chromatography

Hydrophobic interaction chromatography (HIC) separates molecules or particles based on the differences in their hydrophobicity. The working principle of HIC is parallel to that of salt precipitation. However, at high salt concentration, if the aqueous media's salt concentration is below the precipitation point of the protein, the particles bind to the column instead of precipitating. This occurs through binding the hydrophobic chemical groups on the resin to the protein's hydrophobic patches. Elution of the bound proteins from the HIC column occurs upon decreasing the salt concentration either through a gradient or a step elution [113,114].

This type of chromatographic separation is controlled by the solvation of hydrophobic patches of proteins in polar solvents. At higher salt concentrations and ionic strengths, the molecules are repelled from the water shield and directed to interact with the resin's hydrophobic groups. The unique separation principle of HIC remark this method of separation as an orthogonal approach to other types of chromatography. HIC has been used for the purification of viruses, including the foot and mouth disease virus [115], modified vaccinia Ankara virus [116], influenza A and B virus [117], mumps virus, and measles virus [118] with virus recoveries of 89 %, 55 %, 92 %, and 60 %, respectively (Table 4). However, the high salt concentration used during the process, mainly in the binding step, can have detrimental effects on

the stability of enveloped viruses that are sensitive to salt concentration. Therefore, assessing virus stability in the high salt concentration used for HIC before the chromatography purification could determine if this method could be applied to the process.

1.4.4.4. Mixed-mode chromatography

Mixed-mode chromatography (MMC) or multi-modal chromatography is a separation approach where the interaction between the stationary phase and the molecules or particles to be separated occurs through more than one form of interaction principle, including ionic, hydrophilic, and hydrophobic interactions. For example, IEX and SEC or IEX and reverse phase chromatography (RP) can be combined. A few commercially available MMC resins are Capto^{TM}core 700 and Capto^{TM} MMC from Cytiva, ceramic hydroxyapatite/CHT, ceramic fluoroapatite/CFT, Nuvia cPrime from BioRad, and PPA Hypercel^{TM} and MEP hypercel^{TM} from Pall industries. For instance, Capto^{TM}core 700 resin with nominal pore sizes of 700 kDa contains a functionalized core from the ligands that are both positively charged and hydrophobic while non-functionalized on the outer shell. The charged core allows retaining smaller contaminants such as small cellular proteins or DNA fragments, while larger particles such as viruses or VLPs are collected in the flow-through [119], therefore, combining the size-exclusion and binding properties for separation.

Hydroxyapatite, used as an MMC resin, is believed to interact with molecules either by metal affinity through the calcium ions, electrostatic interactions through negatively charged phosphate groups, and less likely due to the hydrogen bonding with hydroxyl groups or a combination of these bindings [120,121]. Ceramic hydroxyapatite (CHT), formed by the hardening of the HA crystals at high temperature to a ceramic, has been used to separate enveloped viruses, including the Dengue virus, with a recovery of 53 % [122]. Moreover, CHT resins have also been employed to purify oncoretroviruses with variable results, from yields between 18% to 31% [59] to a yield of 46% [123].

1.4.4.5. Affinity chromatography

Affinity chromatography (AC) is based on specific interactions between the immobilized ligand and the biomolecule of interest. This method's selectivity results in samples with fewer contaminants, higher purity, and concentration, reducing the number of steps required for purification [124].

The most commonly used approaches in this type of chromatography are immune interaction (IAC), metal ions (IMAC), lectin, heparin, mucin, and avidin affinity chromatography [124]. Moreover, purification of recombinant proteins tagged with certain peptide sequences can be done using affinity chromatography. For instance, human influenza hemagglutinin (HA) tagged protein, or a biotinylated peptide can be purified using an antibody or a streptavidin column, respectively.

Affinity chromatography application has been evaluated for different enveloped viruses, including VSV-G pseudotyped oncoviruses, retroviruses, influenza A and B, and rhabdoviruses (VSV) (Table 4). Multiple AC techniques have been implicated in the purification of retroviruses, including heparin affinity [67], streptavidin-biotin [125–127], and metal affinity [128]. Successful purification of many viruses, including hepatitis A [129], measles [130], porcine reproductive and respiratory syndrome [131], and polio viruses [132], has been reported using immune affinity chromatography.

Heparin, sulfated cellulose, and streptavidin-biotin affinities are amongst the most commonly used principles. Heparin, as a stable and cost-effective ligand, has gained attention for purification purposes. Virus and heparin affinity is based on the interaction of cell surface proteoglycans (heparin sulfate) that is an attachment molecule for many viruses, including herpes simplex (HSV- 1 and HSV-2) [67,136], dengue 2, and [137] human immunodeficiency viruses (HIV-1) [67,138]. The elution of viruses in heparin affinity chromatography occurs at neutral pH and low salt concentration (ca. 0.35 M NaCl), considered more gentle conditions than those required for AEX elution.

Table 4. Overview of different chromatography types used to separate enveloped viruses with a few examples of their application in virus purification.

Type		Virus	Matrix	RCV (%)	Ref.
Ion-exchange	Anion exchange	Orthomyxovirus (Influenza A and B)	Sartobind® Q	86	[133]
		Retrovirus pseudotyped with VSV-G	Mustang Q	65	[86]
		Retrovirus (MoMLV)	DEAE FF HiTrap™	53-57	[100]
		Rhabdovirus (VSV)	MatrexTM CellufineR	45	[62]
		Retrovirus (MoMLV)	Q XL HiTrap™	51-53	[100]
		Lentivirus pseudotyped with VSV-G	HiTrap™ Q HP	17-33	[38]
		Lentivirus pseudotyped with VSV-G	Fractogel TMAE	45	[40]
	Mixed-mode	Amphotropic Onco-retrovirus	Macro- Prep® ceramic hydroxyapatite	46	[93]
		Dengue virus	Ceramic Hydroxyapatite	53	[122]
		Oncoretrovirus	Ceramic Hydroxyapatite	18-31	[93]
Hydrophobic interaction		foot and mouth disease virus		89	[115]
		vaccinia Ankara virus		55	[116]
		influenza A and B virus		92	[117]
		mumps virus and measles virus		60	[118]
Affinity	Heparin	Retrovirus (MoMLV)	Fractogel EMD heparin	43	[34]
		Rhabdovirus (VSV)	Heparin Sepharose®	N/A	[62]
		Orthomyxovirus (Influenza A and B)	Sulfated cellulose MA	73-94	[134]
	Sulfated cellulose	Retrovirus (MoMLV)	Sepharose CL-4B	85	[135]
Size-exclusion		Oncoretrovirus pseudotyped with VSV-G	Sepharose CL-4B	70	[94]
		Lentivirus pseudotyped with VSV-G	Sephacryl S-500	80	[86]
		Orthomyxovirus (Influenza A and B)	Sepharose CL 2B	38	[91]
		Rhabdovirus (rabies virus)	Sepharose 4FF	35–40	[33]
		Retrovirus pseudotyped with VSV-G	Sepharose CL-4B	70	[94]

Chr: Chromatography, Ref: References, RCV: recovery.

The mild elution conditions used for heparin affinity chromatography can potentially minimize the infectivity loss during the chromatography step and highlight the interest of its application for the separation of VSVs in our project. However, the use of metal affinity for bioprocessing of vaccines introduces the risk of metal leakage from matrixes and the adverse effects of histidine tags required for the process [43]. Moreover, to induce affinity towards specific metal ions or even non-metal resins, certain modifications such as the addition of molecules with a high affinity toward these resins must be done, limiting the application of affinity chromatography, especially if these modifications are not possible.

1.4.4.6. Size exclusion chromatography

Size exclusion chromatography (SEC) or gel permeation is a non-adsorptive method that separates particles based on their size differences [60]. The beads used in SEC are porous and can have high porosities of up to 95 %, and their bead can vary between 4 to 700 µm. The beads must be selected properly based on their nominal pore sizes since the use of beads with pore sizes close to the particles can capture them instead [139]. As a result, upon injection of the feed into the column, the larger particles cannot diffuse into the pores of the medium and hence appear later in the column effluent [43].

SEC has been reported to be used as a final polishing step for the large-scale purification of retroviruses, VSV-G pseudotyped lentiviruses, influenza A and B viruses with recoveries between 70 and 85 %, as presented in Table 4 [35,86]. Conditions used in this type of chromatography are gentler than for other chromatography approaches since the viruses are not bound to the matrix, so no elution is needed [140]. SEC is a non-adsorptive method and is not based on the binding of the viruses to a matrix which remarks it as a gentle method for purification viruses. However, SEC might not be appropriate for large-scale applications as it often requires operation at low flow rates, resulting in a long process time which negatively affects virus stability. Other limitations of the SEC could be its limited loading capacity (≤ 10 % column volume) which demands very large SEC columns if used at a large-scale [60,141] and it's requirement for significant dilution of the

product. Therefore, considering the challenges associated with the scalability of SEC, this chromatographic approach is only convenient for the final polishing step rather than the primary purification steps.

1.5. Conclusion

Downstream processing of viral vaccines produced through mammalian cell culture is necessary for concentration and purification purposes. This consists of multiple steps that need to be designed by selecting the approaches that result in the highest purity while keeping the viruses' functionality, thus also allowing high recoveries. Additionally, the scalability of the methods used for purification and their cost is critical for industrial applications. Therefore, to find a suitable protocol for both the laboratory and the industrial scales, the best candidates need to be tested for their functionality in terms of overall yield and removal of contaminants by considering each method's pros and cons.

Based on the reports on the VSV-EBOV vaccine's stability [24], incubation at 40 °C significantly affects VSV-based viral vaccines' infectivity. This result denotes the importance of harvest time, which, if too long, can have a negative effect on viral titer and end in loss of viral infectivity if delayed since the production of these viruses in mammalian cell culture occurs at 37 °C. Moreover, the known susceptibility of VSV to acidic environment dictates the use of neutral pH during the whole DSP to avoid affecting the virus surface glycoproteins and loss of infectivity [142]. As mentioned earlier, although techniques such as ultracentrifugation can give highly concentrated and pure virus stocks, their scalability is considered a limiting factor for their use on a large-scale. Moreover, the concentration of viruses by pelleting can also result in viral aggregation and co-pelleting of these viruses with those contaminants that share similar density with viruses. Therefore, ultracentrifugation can be a good strategy for small-scale purification of VSVs, but it needs to be replaced with other alternative technologies at the industrial scale. Removal of contaminating nucleic acids that are released into the supernatant from different sources should also be carried out at a proper step (preferably in the early stages) since their presence can

result in clogging of membranes used during the process and lower the virus yield in addition to their interference with viral transduction.

To find the best chromatography resins for the separation of rVSV used in our project, we tend to assess the best candidates' functionality in terms of yield and contaminant removal. Anion exchangers, both membrane and resin, are amongst the most commonly used approach for purifying enveloped viruses, could be the best candidate for the purification of rVSVs, but also, it would be interesting to test other types of approaches, such as mix-mode chromatography. With these data, we expect to develop optimized purification schemes for rVSV based HIV vaccine candidates at both laboratory- and large-scales that could easily be adapted to GMP compliant manufacturing.

Chapter 2: Materials and methods

The summary of methods used to obtain the results of each chapter will be described in every corresponding chapter. However, this chapter consists of the detailed protocols that were used for rVSV production, purification, and quality control assays.

Important note:
All the live VSV containing samples must be handled by an authorized individual in a biological safety cabinet at a Biosafety Level 2 (BSL-2) laboratory.

2.1. Benzonase® treatment

Objective:

The following procedure describes the Benzonase® treatment for eliminating contaminant nucleic acids in the rVSV containing cell culture supernatant.

Materials:

Benzonase® endonuclease (> 90% pure)
$MgCl_2$ solution
EDTA solution
37 °C water bath

Procedure:

1. Add the required amount of $MgCl_2$ to the harvested cell culture supernatant to maintain the 2 mM concentration.
2. Add 10 unit of Benzonase® to the supernatant and shake the bottle/tube gently to distribute the enzyme uniformly.
3. Incubate the mixture in a water bath maintained at 37 °C for 2 h.
4. Add 1 mM EDTA to stop the endonuclease activity of the enzyme.

2.2. Microfiltration

Objective:

The following procedure describes the clarification of the rVSV containing cell culture supernatant using Miniprofile™ filter (Pall corporation, Canada), 1.2 µm, and Sartopure PP3 filters. This protocol applies to the microfiltration of rVSVs containing supernatant produced using Vero-sf cells maintained in serum-free VP-SFM medium that has been partially clarified using low-speed centrifugation at 3500 ×g for 20 min.

Materials:

- Peristaltic pump system (Masterflex L/S variable-speed precision 6-600 rpm, 115V)
- Pump Tubing L/S 18 (Masterflex® L/S® Precision)
- Pressure gauge
- Miniprofile™ filter 1.2 µm (Pall Corporation, Canada)
- PBS
- VP-SFM culture media
- 1 M NaOH
- Autoclaved water
- pH indicator stripes

Procedure:

1. Centrifuge the cell culture supernatant at 3500 ×g for 20 min to eliminate the cells and cellular debris. Collect the supernatant and transfer it to another sterile tube.
2. Store the partially clarified supernatant at 4 °C if the microfiltration is performed on the same day, otherwise aliquot the material and store it at -80 °C until further use.
3. Assemble the filtration system, including the pump, the tubings, and the pressure gauge inside a biological safety cabinet.
4. Sanitize the tubings by passing 1 M NaOH solution through the tubings for 5 to 10 min followed by leaving the tubings in NaOH solution for at least 2 h.

5. Empty the tubes by pumping air and follow with autoclaved water until the pH reaches 7 measured by pH stripes.
6. Attach the Miniprofile™ filter to the tubings, pass approximately 50-100 mL of water, and set the flow rate at 75 mL/min to maintain the flux at 500 Liter/m2/h (filter surface area = 90 cm^2).
7. Condition the filter by passing 25 mL PBS and 25 mL of VP-SFM media before the sample.
8. Filter the sample while maintaining the back pressure below 1.5 psi.
9. The filtrate can be stored at 4 °C during the next purification steps or stored at -80 °C for later use.

2.3. Ultrafiltration

Objective:

The following procedure describes the concentration of rVSV containing clarified, and Benzonase® treated supernatant by tangential flow ultrafiltration using Spectrum® Midikros 750 kDa hollow fiber TFF system.

Materials:

- Midikros 750 kDa hollow fiber TFF system (Spectrum Laboratories, USA)
- PBS
- Autoclaved water
- pH indicator stripes
- Peristaltic pump system (Masterflex L/S variable-speed precision 6-600 rpm, 115V)
- Pump Tubing L/S 16 (Masterflex® L/S® Precision)
- Pressure gauge
- VP-SFM culture media
- Autoclaved 0.5 M NaOH
- Scissor clamp

Procedure:

1. Assemble the system, including the pump, the tubings, and the pressure gauge inside a biological safety cabinet.
2. Sanitize the tubings by passing 0.5 M NaOH solution through the tubings for 5 to 10 min followed by leaving the tubings in NaOH solution for at least 2 h or overnight.
3. Rinse the tubings with water to bring the pH back to neutral as measured by pH stripes. Measure the capacity of the tubings by passing water through them and measuring the quantity of water passed using a 50 mL tube.
4. Attach the Midikros cartridge to the tubings following Fig. 7.

Fig 7. Tangential flow ultrafiltration setup, including the peristaltic pump, feed, pressure gauge, and the TFF cartridge.

5. Pass approximately 100 mL of 0.5 M NaOH through the system.

*The membrane should always be kept wet and avoid the introduction of air bubbles into the cartridge.

6. Allow 300 to 400 mL of water to flow through the membrane to wash the membrane's glycerin contents while maintaining the back pressure below 1 psi.
7. Change the reservoir to 0.5 M NaOH and allow the system to be filled with it. The pH at the permeate will be between 13 and 14 (13.69).
8. Sanitize the cartridge by leaving it with 0.5 M NaOH for at least 1 h.
9. Rinse the system with water and set the flow rate at 53 mL/min, a flux rate of 25 LMH to maintain a shear rate of 2000 s-1 throughout the process, and transmembrane pressure (TMP) of 0.1 bar. Lower the flow rate at the permeate by pinching the tubing.

*Continue the rinsing until the pH comes back to 7.

10. Condition the membrane by passing 100 mL PBS and 100 mL of VP-SFM media before the sample.
11. Initiate the concentration process of the sample by placing the sample as the feed. Maintain the TMP at 1 psi throughout the experiment.
12. Depending on the concentration needed and considering the volume occupied by the tubings, lower the flow rate by $1/4^{th}$ and close the permeate.
13. Allow the sample to recirculate in the cartridge.
14. Lower the flow rate by $1/3^{rd}$ of the initial flow rate and empty the system by pumping air into the system and collecting the sample.
15. If the TFUF unit is reusable, rinse the system with 500 mL of water immediately by allowing the retentate to empty to a waste bottle. The permeate should be closed at this step.
16. Reconnect the retentate tubing into the system, open the permeate end, and pass about 100 mL of PBS through the whole system, followed by 0.5 M NaOH.
17. Leave the system in 0.5 M NaOH for 1 h, then disconnect it from the tubings and store it at room temperature.
18. Aliquot the concentrated sample and store it at -80 °C for later use.

2.4. Density gradient ultracentrifugation

Objective:

The following procedure describes the concentration of rVSVs by pelleting using a cushion of sucrose and their purification using a discontinuous gradient of iodixanol.

Materials:

- Iodixanol
- Sucrose
- 10 mM Tris, pH 7.4
- 10 mL syringe with needle
- Pipette controller
- 36 mL polyethylene terephthalate (PET) tube
- Sorvall legend XFR ultracentrifuge
- SureSpin™ 630 (36 mL) swinging bucket rotor
- Biological safety cabinet
- Paraffin film
- 0.2 µm filter
- Analytical balance

Pelleting rVSV using sucrose cushion:

Procedure:

1. Prepare 20% (w/v) sucrose solution in 10 mM Tris, pH 7.4, and filter using a 0.2 µm filter.
2. Place the rotor inside the ultracentrifuge and start the cooling process (4 °C) 1 hour before the process.
3. Keep the virus-containing sample at 4 °C until use.
4. Pipette 30 mL of sample into the ultracentrifugation tube. If the amount of sample is lower than 30 mL, the difference can be compensated by 10 mM Tris, pH 7.4.

5. Pipette 5 mL of 20 % sucrose solution and pass the pipette through the sample, touching the bottom of the tube with a slanted position, slowly releasing the sucrose solution without disturbing the top later.
6. Place the tube inside the tube holder and balance all the tubes using 10 mM Tris, pH 7.4 as measured by an analytical balance before loading them into the ultracentrifuge.
7. Run the samples at 156,359 g for 3 hours at 4 °C.
8. Remove the supernatant carefully and gently add the desired amount of 10 mM Tris, pH 7.4 to the pellet through the tube walls.
9. Store the tube at 4 °C overnight to loosen the pellet.
10. Resuspend the pellet in the buffer by pipetting and store at -80 °C for future use.

Purification of rVSV using density gradient ultracentrifugation:

Procedure:

1. Prepare 40, 37, 31, 27, 23, 19, and 14 % of iodixanol in 10 mM Tris, pH 7.4, and store at 4 °C a few hours before the experiment.
2. Place the rotor inside the ultracentrifuge and start the cooling process (4 °C) 1 hour before the process.
3. Keep the virus-containing sample at 4 °C until use.
4. Pipette 13 mL of the sample into the 36 mL ultracentrifuge tube.
5. Pipette the iodixanol layer from the lowest concentration (14 %) to the highest concentration (40 %) by passing the pipette through the latest layer, touching the bottom of the tube in a slanted position, and slowly releasing the solution without disturbing the top layers.

*Use 5 mL of 40 % solution and 3 mL of the rest of the solutions.

6. Place the tube inside the tube holder and balance all the tubes using 10 mM Tris, pH 7.4 as measured by an analytical balance before loading them into the ultracentrifuge.
7. Run the samples at 156,359 g for 3 hours at 4 °C.

8. Collect the virus-containing band by pricking a hole using a syringe on the side of the tube and pulling approximately 5 mL.
9. Store the purified rVSVs at -80 °C for further analysis.

2.4. Anion exchange chromatography using HiTrap™ IEX columns

Objective:

The following procedure describes the purification of rVSVs concentrated by TFF using HiTrap™ DEAE FF and HiTrap™ XL, weak and strong anion exchanger columns, included in the HiTrap® IEX selection kit.

Materials:

- ÄKTA start chromatography system (GE Healthcare, Canada)
- UNICORN start 1.0 software
- Buffer A (A): 20 mM Tris, 4% sucrose, pH 7.4
- Buffer B (B): 2 M NaCl, 20 mM Tris, 4% sucrose, pH 7.4
- Storage buffer: 20 % ethanol
- 1.5 mL, 15 mL/50 mL centrifuge tubes
- rVSV containing eluate from Sartobind® Q membrane
- HiTrap® IEX selection kit (Cytiva, Canada)
- Concentrated rVSV containing supernatant

Procedure:

1. Run a rinse cycle through the A, B, sample injection, and fractionation lines using Milli Q H_2O followed by 1 M NaOH with a pause of 30 minutes.
2. Connect the column to the system. For the first usage of the column, equilibrate the column with 20 CV of Milli Q H_2O to wash off the storage buffer at 1 mL/min.
3. Equilibrate the column with 10 CV of A until the Uv baseline and the conductivity is stable.

4. Equilibrate the column with 20 CV of 100 % B (1 M) followed by 10 CV of 3% A at 2 mL/min.
5. Mix the rVSV containing TFF retentate (approximately 15 fold) with A (1:1). Based on the sample volume, either inject them through the injection loop or use the sample valve at 1 mL/min. Collect the flow-through for further analysis of the column binding capacity.
6. When designing a purification program, set 5 to 2000 mAU for sample collection.
7. Start a wash step using 5 % B for HiTrap™ DEAE FF and 10 % B for HiTrap™ XL to remove the unbound materials from the column.
8. Elute the viruses from the column using 30 CV of 20 % B (400 mM) for HiTrap™ DEAE FF and 40 % B (800 mM) for HiTrap™ XL at 1 mL/min.
9. Regenerate the column using 20 CV of 100 % B at 2 mL/min.
10. Equilibrate the column with 20 CV of A at 2 mL/min, followed by 10 CV of MilliQ H_2O.
11. Store the column in a storage buffer at room temperature.

2.5. Anion exchange membrane chromatography

Objective:

The following procedure describes the purification of rVSV carrying HIV and Ebola glycoproteins using Sartobind® Q membrane chromatography.

Materials:

- ÄKTA start chromatography system (GE Healthcare, Canada)
- UNICORN start 1.0 software
- Buffer A (A): 20 mM Tris, 4% sucrose, pH 7.4
- Buffer B (B): 2 M NaCl, 20 mM Tris, 4% sucrose, pH 7.4
- Storage buffer: 20 % ethanol in A
- 1 M NaOH
- Sartobind® Q nano 3 mL membrane (Sartorius, Germany)
- 1.5 mL, 15 mL/50 mL centrifuge tubes

- Clarified and Benzonase® treated rVSV containing supernatant

Procedure:

1. Run a rinse cycle through the A, B, sample injection, and fractionation lines using Milli Q H_2O followed by 1 M NaOH with a pause of 30 minutes.
2. For the first usage of the membrane, fill it with a 10 to 20 mL Luer syringe filled with A, while holding it vertically with the outlet facing upward.
3. Connect the membrane to the system. Clean the membrane with 10 membrane volumes (MV) of 1 N NaOH at 3 mL/min with a hold time of 30 min.
4. Wash the membrane with 15 MV of A at 5 mL/min.
5. Equilibrate the membrane with 10 MV of 50 % B (1 M), 10 MV of A, and 10 MV of VP-SFM media diluted in A (1:1) at 5 mL/min.
6. Mix the supernatant with A (1:1), and based on the volume of the sample, either inject it through the injection loop or using the sample valve at 3-5 mL/min, depending on the back pressure. Collect the flow-through for further analysis of the membrane-binding capacity.
7. When designing a purification program, set 5 to 2000 mAU for sample collection.
8. Start a wash step using 15 MV of 2 % B to remove the unbound materials at 5 mL/min.
9. Initiate the elution phase using 25-30 MV of 10 % B (100 mM) followed by 10 MV of 50 % B for virus elution at 3 mL/min. Collect the virus-containing fractions for further processing.
10. Regenerate the membrane with 15 MV of 100 % B (2 M) at 1.5 mL/min. If needed, 70 % ethanol for 1 h at room temperature.
11. Equilibrate the membrane with 20 MV of A at 5 mL/min.
12. Store the membrane in a storage buffer at room temperature.

2.6. Polishing purification using mixed-mode chromatography

Objective:

The following procedure describes the polishing of rVSV containing elates of Sartobind® Q membrane elates using Capto™ Core 700 mixed-mode chromatography.

Materials:

- ÄKTA start chromatography system (GE Healthcare, Canada)
- UNICORN start 1.0 software
- Buffer A (A): 20 mM Tris, 4% sucrose, pH 7.4
- Buffer B (B): 2 M NaCl, 20 mM Tris, 4% sucrose, pH 7.4
- Storage buffer: 20 % ethanol
- 1 M NaOH in 30 % isopropanol
- Capto™ Core 700 (Cytiva, Canada)
- 1.5 mL, 15 mL/50 mL centrifuge tubes
- rVSV containing eluate from Sartobind® Q membrane

Procedure:

1. Run a rinse cycle through the A, B, sample injection, and fractionation lines using Milli Q H_2O followed by 1 M NaOH with a pause of 30 minutes.
2. Connect the column to the system. For the first usage of the column, equilibrate the column with 20 CV of Milli Q H_2O to wash off the storage buffer at 1 mL/min.
3. Equilibrate the column with 10 CV of A until the UV baseline, and the conductivity is stable.
4. Re-equilibrate the column with 50 % B (1 M) at 1 mL/min.
5. Inject the samples into the column at 0.7 mL/min and collect the rVSV containing flow-through.
6. When designing a purification program, set 2 to 2000 mAU for sample collection.

7. Start a wash step using 20 CV of A.
8. Regenerate the column using 1M NaOH, 30 % isopropanol at 0.5-0.7 mL/ min with a hold time of 30 mn.
9. Wash the column with 30 CVs of Milli Q H_2O.
10. Store the column in a storage buffer at room temperature.

2.7. Ceramic hydroxyapatite mixed-mode chromatography

Objective:

The following procedure describes the purification of rVSVs expressing HIV and Ebola glycoproteins on their surface using a ceramic hydroxyapatite type II (CHTII) 5 mL column.

Materials:

- ÄKTA start chromatography system (GE Healthcare, Canada)
- UNICORN start 1.0 software
- Buffer A (A): 20 mM Tris with 5 mM $NaPO_4$, 4% sucrose, pH 7.5
- Buffer B (B): 1 M $NaPO_4$, 4% sucrose, pH 7.5
- Storage buffer: 0.1 N NaOH
- 1 M NaOH
- MilliQ H_2O
- Bio-scale^{TM} mini CHT type II cartridge (BioRad, Canada)
- 1.5 mL, 15 mL/50 mL centrifuge tubes
- Concentrated rVSV containing supernatant

Procedure:

12. Run a rinse cycle through the A, B, sample injection, and fractionation lines using Milli Q H_2O followed by 1 M NaOH with a pause of 30 minutes.
13. For the first usage of the column, while holding it vertically with the outlet facing downward, tap the column against the top of the bench for about 10 times.

14. Connect the column to the system. Fill and equilibrate the column with 5 CV of 1 N NaOH at 2 mL/min.
15. Equilibrate the column with 10 CV of 100 % B (1 M) followed by 10 CV of A at 2 mL/min.
16. Mix the rVSV containing TFF retentate (approximately 15 fold) with A (1:1). Based on the sample volume, either inject them through the injection loop or use the sample valve at 1 mL/min. Collect the flow-through for further analysis of the column binding capacity.
17. When designing a purification program, set 5 to 2000 mAU for sample collection.
18. Start a wash step using 0.5 % B to remove the unbound materials in the column.
19. Initiate the elution phase using 10 CV of 10 % B (100 mM) followed by 10 CV of 50% B for virus elution at 2 mL/min. Collect the virus-containing fractions for further processing.
20. Equilibrate the column with 20 CV of A at 2 mL/min, followed by 10 CV of MilliQ H_2O.
21. Store the column in a storage buffer at room temperature.

2.8. Virus titration assay

Objective:

The following procedure describes the TCID50 assay protocol adapted from Gélinas et al. [143] to determine plaque-forming units (PFU) present in the samples.

Materials:

- Round bottom 96 well cell culture plate
- Flat bottom 96 well cell culture plate
- HEK293-A cells
- FBS
- PBS
- Glutamine

- DMEM media
- Multichannel pipettors
- Filter tips
- Sterile Multichannel Disposable Solutions Basin

Procedure:

1. Seed 100 µL/well of HEK293-A cells (maintained in DMEM, 2 mM glutamine, 5 % FBS) in a flat bottom 96 well plate at the density of 5E04 cells/mL, incubate at 37 °C and 5 % CO_2 in a humidified incubator until the cells reach 80 % confluence.

*Each sample requires a complete 96 well plate for the assay.

2. Pre-warm the culture media at 37 °C.
3. Add 200 µL of media per well of a round bottom 96 well plate.
4. Add 50 µL of the sample to the first column and mix well.
5. From this mixture, pipette 50 µL and empty into the next column, mix and repeat the same process for the following columns of the round bottom plate.
6. Using a multichannel pipette, transfer 20 µL of each row into a row in a row of the flat bottom plate containing HEK293-A cells.

*It is recommended to titrate the samples of every experiment on the same day.

7. Calculate the virus titer following the Spearman & Kärber algorithm [144] using the excel sheet provided by the University of Heidelberg [145].

2.9. Quantification of total proteins

Objective:

The following procedure describes the determination of total protein contents by Bradford assay.

Materials:

- Flat bottom 96 well plate

- Synergy HTX multi-mode reader (BioTek, USA)
- Plate shaker
- PBS
- Pipettors
- Quick Start Bradford Protein Assay Kit 2 (BioRad)
- bovine serum albumin standard set (set of 7 standards, 0.125–2.0 mg/ml) (BioRad)

Procedure:

1. Remove the1X dye reagent from the 4 °C and let it sit at room temperature for 30 minutes. Invert the dye prior to use.
2. Prepare 3 different dilutions of sample including non-diluted, 1:2, and 1:5, and 1:10 in PBS 1X and 8 different BSA concentrations of BSA standards following Table 5.

Table 5. Guide for the preparation of different BSA concentrations for Bradford assay standard curve.

BSA concentration (µg/mL)	PBS (1X) (µL)	Source of standard	Standard volume (µL)
25	790	2 mg/mL	10
20	495	2 mg/mL	5
15	495	1.5 mg/mL	5
10	495	1 mg/mL	5
5	495	0.5 mg/mL	5
2.5	495	0.25 mg/mL	5
1.25	495	0.125 mg/mL	5
0	500	-	0

3. Pipet 5 ul of each standard and sample in the microplate wells (3x).

4. Add 250 ul of 1x dye reagent with a multichannel pipette and mix by doing ups and downs.
5. Incubate the plate at room temperature for 30 minutes. (up to 1 hour)
6. Set the microplate reader to 595 nm and measure the absorbance.

2.10. Quantification of dsDNA

Objective:

The following procedure describes the quantification of dsDNA contents in the sample using the Quant-iTTM Picogreen™ assay kit.

Materials:

- Quant-iTTM Picogreen™ ds DNA assay kit with standards (Life Technologies)
- Flat bottom 96 well plate
- Synergy HTX multi-mode reader (BioTek, USA)
- Plate shaker
- Pipettors
- Milli-Q water
- Multichannel pipettor

Procedure:

- Dilute the TE buffer (20X) supplied in the kit using Milli Q water.
- Prepare 1:10, and 1:20 dilutions of each sample in 20mM DNase-free Tris buffer. It is recommended to prepare the samples in triplicates.
- Dilute the standard Lambda DNA solution in TE buffer by 50 fold.
- Prepare different concentrations (40, 100, 200, 300, 400, and 500 ng/mL) of Lambda DNA standard in TE buffer.
- Dilute the PicoGreen™ stock solution in TE buffer by 200 fold and cover the tube with aluminum foil. A total volume of 10 mL of PicoGreen working solution is needed for a complete 96 well plate.

- In a flat bottom 96 well plate, add 100 µL of samples and dsDNA standards.
- Using a multichannel pipettor, add 100 µL of the Picogreen™ reagent and mix.
- Incubate the mixture in the dark at room temperature for 5 min.
- Read the fluorescence using a microplate reader with an excitation wavelength of 480 nm and an emission wavelength of 520 nm.

2.11. Quantification of host cell protein (HCP)

Objective:

The following procedure describes the Vero cell HCP quantification assay using the Vero Cell HCP ELISA kit following the manufacturer's instructions.

Materials:

- Vero Cell HCP ELISA kit (Cygnus Technologies, USA)
- Round bottom 96 well plate
- Synergy HTX multi-mode reader (BioTek, USA)
- Plate shaker
- PBS
- Pipettors

Procedure:

1. Dilute the samples 1:250 in PBS in a round bottom 96 well plate.
2. Add 50 µL of diluted samples and standards (supplied in the kit) into the microtiter strips coated with goat anti-Vero polyclonal antibodies supplied by the company.
3. To this mixture, add an amount of 100 µL of the HRP conjugated affinity-purified goat anti-Vero antibody.
4. Incubate for 2 h at 580 rpm, 25 °C.
5. Rinse the wells with the wash buffer 4 X supplied in the kit.
6. Add 100 µL of the tetramethylbenzidine (TMB) solution to the wells and incubate for 30 min at 25 °C.
7. Stop the reaction by adding 100 mL of stop solution.

8. Measure the absorbance at 450/650 nm using Synergy HTX multi-mode reader.

2.12. SDS-PAGE and immunoblot

Objective:

The following procedure describes the analysis of protein profile using SDS-PAGE and visual confirmation of VSV-M/VSV-N proteins using either spot blot or western blot.

Materials:

- Power Supply
- NuPAGE™ 4 to 12%, Tris-glycine, 1 mm thickness (Invitrogen™, Canada)
- Mini Gel Tank and Blot
- 10x Tris/Glycine Buffer
- Ethanol/methanol
- Filter papers
- Amersham Protran 0.45 NC nitrocellulose Western blotting membranes
- Mini Trans-Blot® Cell
- Skimmed milk powder
- Tween® 20
- PBS 10x
- Ince packs
- Ultrapure water
- Pierce™ ECL western blotting substrate (Thermo Scientific, Canada)
- rabbit anti-mouse, HRP (Abcam, Canada)
- VSV-N/VSV-M antibody (Kerafast, USA)
- Thermo Scientific™ Pierce™ Color Silver Stain Kit (Thermo Scientific, Canada)
- ImageQuant LAS 4000 imager (Cytiva, Canada)
- 2-mercaptoethanol (ACROS Organics™, Canada
- 2x Laemmli buffer (BioRad, Canada)
- PageRuler™ Prestained Protein Ladder

- PageRuler™ unstained Protein Ladder
- Shaker

Procedure:

SDS-PAGE:

1. Denature the samples 2x Laemmli buffer and 5% 2-mercaptoethanol followed by 5 min of heating at 95 °C.
2. Take the comb and the tapes out of the Novex™ 4-12% Tris-Glycine Mini Gel, place it in the Mini Trans-Blot® Cell, and fill the unit with 1x Tris/Glycine Buffer up to the marking on the unit.
3. Load 15 µL of each sample and 5 µL of PageRuler™ unstained Protein Ladder into the Tris-Glycine Gel and run at 120 volts until the front dye reaches the end of the gel.

Silver staining:

1. Take the gel out by breaking the holding cassettes and fixing it using 50% Ethanol + 5% Acetic Acid for 4 hours with frequent buffer changes or overnight.
2. Wash gel (4x) for 40 min with ultrapure water.
3. Prepare the working solutions following the instructions provided in Table 6.

Table 6. Preparation of silver staining working solutions

Stock	Preparation
Silver WS	20 mL of silver WS + 280 mL water
Reducer aldehyde WS	20 mL of reducer aldehyde WS +130 mL water
Reducer base WS	20 mL of reducer base WS +130 mL water
Stabilizer base WS	20 mL of stabilizer base WS +880 mL water

4. Incubate the gel in the silver staining WS for 30 min with shaking.
5. Rinse the gel with water for 20 sec.
6. Mix an equal amount of reducer base WS and reducer aldehyde solutions and incubate the gel with the mixture for 5 min.
7. Rinse the gel with water for5 sec.

8. Incubate the gel in the stabilizer solution for 40 min.

Western blot:

1. Prepare the transfer buffer (1x Tris-glycine buffer, 20 % ethanol) and cool it a few hours before the experiment.
2. Run the sample in a Novex™ 4-12% Tris-Glycine following the abovementioned protocol but replace the ladder with PageRuler™ prestained protein ladder.
3. Prepare the precut membrane, the filter papers, and the sponges by soaking them in the transfer buffer.
4. Remove the gel from the electrophoresis cassettes and prepare the western blot sandwich following Fig. 8. Make sure to avoid the introduction of air bubbles in the sandwich.
1. Place the sandwich in the transfer cassette and then into the transfer unit filled with transfer buffer and holding an ice pack.
2. Run the transfer at 300 mAu for 1 h at 4 °C.
3. Take the membrane out and block it using PBS+0.1 % Tween+5% milk (PBST+milk) at room temperature for 1 h with shaking.
4. Wash the membrane with PBST (3x, each for 5 min).

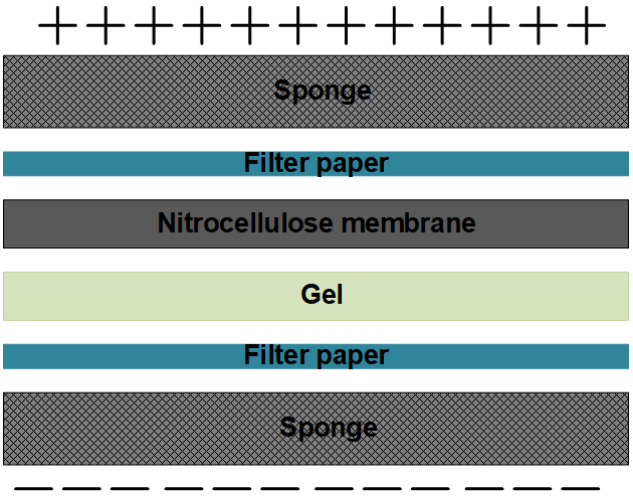

Fig 8. Western blot sandwich.

5. Dilute the primary antibody (anti-VSV-M/N) in PBST+milk (1:1000) and incubate the membrane in the antibody for 2 h with shaking.

6. Wash the membrane with PBST (3x, each for 5 min).
7. Dilute the secondary antibody (rabbit anti-mouse) in PBST (1:10000) and incubate the membrane in it for 1 h.
8. Wash the membrane with PBST (3x, each for 5 min).
9. Mix equal amounts of reagent 1 and 2 from the Pierce™ ECL western blotting substrate kit.
10. Remove excess buffer from the membrane and add Pierce™ ECL western blotting substrate, incubate for 1 min.
11. Expose the membrane to X-ray film using ImageQuant LAS 4000 imager.

Dot blot:

1. Place 2 µL of the denatured sample on a pre-cut nitrocellulose membrane
2. Allow the membrane to air dry for 30 min.
3. Block the membrane with PBST+milk for 1 h.
4. Follow steps 5 to 12 from western blot analysis.

Chapter 3: Purification of recombinant vesicular stomatitis virus-based HIV vaccine candidate

Anahita Bakhshizadeh Gashti [a], Parminder S. Chahal [b], Bruno Gaillet [a], Alain Garnier [a*]

[a] Department of Chemical engineering, Faculty of Sciences and Engineering, Université Laval, Quebec, QC, Canada

[b] Human Health Therapeutics, National Research Council Canada, Montreal, QC, Canada

*Corresponding author: alain.garnier@gch.ulaval.ca

Manuscript

Résumé

Dans ce travail, différentes méthodes de purification d'un candidat vaccin contre le virus de l'immunodéficience humaine (VIH) basé sur le virus recombinant de la stomatite vésiculeuse (rVSV) ont été testées, aussi bien aux échelles laboratoire que pilote. La première étape de la purification, la clarification des rVSV produits en culture cellulaire dans des milieux sans sérum, a été initiée par la centrifugation à basse vitesse ainsi que la microfiltration en utilisant différents médias de filtration et tailles de pores, ces derniers allant de 0,45 µm à 20 µm. Pour réduire le volume de surnageant et le temps de traitement, l'échantillon clarifié a ensuite été concentré et partiellement purifié par ultrafiltration (UF) soit en utilisant une filtration directe ou à flux tangentiel (TFUF), selon l'échelle du processus. L'étape de purification finale a été réalisée, à l'échelle du laboratoire, par ultracentrifugation en gradient de densité (DGUC), qui a ensuite servi de référence pour comparer des méthodes chromatographiques. Les préparations de virus ont été analysées en utilisant la diffusion dynamique de la lumière (DLS) pour vérifier la taille du virus et la microscopie à transmission électronique (MET) pour examiner le degré de contamination par des exosomes et la morphologie du virus. Le DGUC a permis la récupération d'au moins 81 % de particules infectieuses et a réduit le contenu des vésicules extracellulaires contaminantes par rapport à une approche d'ultracentrifugation sur coussin (UC) standard. À plus grande échelle, plusieurs échangeurs d'anions forts et faibles ont été testés et comparés. Les meilleures colonnes ont permis des récupérations de virus infectieux pouvant atteindre 77 % et l'élimination de 92 % des protéines de la cellule hôte. La concentration de l'ADN résiduel de l'hôte dans les préparations de rVSV purifié était conforme aux restrictions de l'OMS.

Abstract

In this work, different laboratory- and large-scale methods were tested for purification of a Human Immunodeficiency Virus (HIV) vaccine candidate, based on recombinant vesicular stomatitis virus (rVSV). The first step of purification, the clarification of the rVSVs produced in serum-free cell culture medium, were initiated by low-speed centrifugation and microfiltration using different filtration media and pore sizes, the latter ranging from 0.45 µm to 20 µm. To reduce the supernatant volume and process time, the clarified sample was concentrated and partially purified by ultrafiltration (UF) either using tangential flow (TFUF) or dead-end units, depending on the process scale. The final purification step at laboratory-scale, was carried out by density gradient ultracentrifugation (DGUC), which was thereafter used as a reference to compare with chromatographic purification. The virus preparations were analyzed using dynamic light scattering (DLS) to verify virus size and transmission electron microscopy (TEM) for exosome contamination and virus morphology. DGUC allowed the recovery of ≥ 81% infectious particles and reduced the contaminant extracellular vesicle content relatively compared to standard ultracentrifugation pelleting using a sucrose cushion (UC). At the larger scale, multiple strong and weak anion exchangers were tested and compared. The best columns allowed infectious virus recoveries as high as 77 % and eliminated 92 % of the host cell proteins. The concentration of the host residual DNA in the purified rVSV preparations complied with WHO requirements.

Keywords: HIV vaccine, recombinant vesicular stomatitis virus (rVSV), viral vaccine, vaccine purification, chromatography, anion exchange

3.1. Introduction

Vesicular stomatitis virus (VSV), a member of the *Rhabdoviridae* family, is a natural livestock pathogen. In affected animals, the VSV infection results in loss of milk production followed by the appearance of vesicular lesions in the oral cavity, hoofs, and teats [146–148]. However, VSV infection in humans is very rare and have only been observed in individuals either in contact with the virus in laboratories or infected animals in rural areas. Despite the VSV pathogenicity in animals, its occurrence in humans is usually controlled by Type I interferon (IFN) response resulting in no or mild flu-like symptoms in worst cases [149,150].

VSV is a bullet-shaped, enveloped virus. A typical VSV particle measures 65 X 180 nm [146,151]. The viral genome is 11,161 nucleotides long, consisting of a single negative-stranded RNA. The VSV genome encodes five structural viral proteins, namely, the nucleocapsid (N), the matrix (M), the large RNA polymerase (L), the phosphoprotein (P), and the VSV glycoprotein (G) [152–154].

The substitution of VSV-G envelop protein with antigens of different human pathogens makes VSV a suitable platform for preventing and treating diseases. In addition, the biology of VSV offers several characteristics that make it an ideal vector for human vaccines. Amongst them, low prevalence of pre-existing immunity in humans, fast *in vitro* propagation and high titer yields in many mammalian cells, low probability of viral RNA integration into the host DNA, the ability to elicit humoral and cellular immunity *in vivo* can be regarded [154–156]. As a result, the rVSV vaccine platform has been applied against several viruses including, Ebola, Marburg, Lassa, Crimean-Congo hemorrhagic fever (CCHFV), Nipah, MERS- and SARS-coronaviruses, Zika, Influenza, and Human immune deficiency virus (HIV) [157]. To date, the rVSV backbone has been employed in phase I clinical trials of three HIV vaccine candidates (ClinicalTrials.gov, NCT01438606, NCT01578889, and NCT01859325).

With 1.5 million newly infected individuals with HIV in 2020 and a total of 36.3 million deaths worldwide (UNAIDS) [1], HIV is still considered as a critical global health threat as no effective vaccine has been developed against it to this day. The rVSV

based HIV candidate vaccine used in this work is constructed based on the FDA-approved, rVSV based Ebola virus vaccine backbone (rVSV-ZEBOV) that expresses both Ebola (EBOV-gp) and HIV glycoproteins (HIV-gp) on its surface. The presence of EBOV-gp in the present rVSV based HIV vaccine improves the cell tropism and enables the virus production in CD4- and CCR5- cell lines. The rVSV-ZEBOV vaccine, marketed under the name Ervebo, has established efficacy of 97.5% during the devastating 2018 outbreak [158].

This work describes the potential purification schemes for laboratory- and pilot-scale purification of candidate HIV vaccine based on the rVSV-ZEBOV platform. The rVSVs used here were produced in Vero cells adapted to serum-free media following recently published work [159]. Two different purification schemes were proposed based on the volume of the sample to be processed. A series of microfiltration filters of different filtration media and pore sizes were tested for removal of the cellular debris and recovery of infectious particles. The impact of nuclease treatment on overall recovery of viruses in a small-scale purification scheme was assessed by introducing the treatment and different steps of the purification scheme. For concentration of supernatant prior to purification step, at small-scale, pelleting by ultracentrifugation and at large-scale, tangential flow ultrafiltration were studied. Purification of cell culture-derived supernatant at laboratory-scale (volume up to 200 mL) was performed by ultracentrifugation using a discontinuous gradient of iodixanol solution. For larger scale (Volume higher than 200 mL) purification, four resin-based anion exchange chromatography columns were tested for their ability to remove contaminants and recover infective particles. The quality of the final rVSV preparations from both methods was then compared in terms of their total protein content, host residual DNA contents, presence of microvesicles, and the recovery of infectious particles.

3.2. Material and methods

3.2.1. Chemicals and cell lines

All chemicals were of analytical grade, if not otherwise stated: sodium chloride (NaCl) (ACROS Organics, Canada), Tris buffer powder (Invitrogen, Canada),

Tween-20 (Fisher Bioreagents, Canada), sodium hydroxide (NaOH) (Millipore Sigma, Canada), 1 M $MgCl_2$ (ThermoFisher Scientific, Canada), sucrose (Bioshop, Canada).

VP-SFM medium (ThermoFisher Scientific, Canada), 200 mM L-glutamine (Wisent Bio Products, Canada), Dulbecco′s Modified Eagle′s Medium (DMEM, Corning, Canada), 1X TrypLE™ Select enzyme (Thermo Fisher Scientific, Canada), Fetal Bovine Serum (FBS, Wisent, St-Bruno, QC, Canada), Benzonase® (Millipore Sigma, Canada), Serum-free adherent Vero cell line (CCL-81.5) was a generous gift from Dr. A. Kamen laboratory (McGill, Montreal), and HEK 293A cells were obtained from Dr. R. Gilbert laboratory (NRC-Montréal).

3.2.2. Cell culture, virus production, and harvest

Vero cells used for virus production were maintained in serum-free VP-SFM medium, supplemented with 4mM L-glutamine, without antibiotics at 37 °C and 5 % CO_2 in a humidified incubator, and passaged twice weekly. Cells were detached using 1X TrypLE™ Select enzyme, centrifuged at 400 g, 5 min, resuspended in fresh medium, and seeded at 1.5 × 10^5 cells/mL in 100 mm cell culture dish holding 12 mL of medium.

HEK 293A cells used for virus titration were maintained in Dulbecco′s Modified Eagle′s Media supplemented with 2 mM L-glutamine and 5 % FBS, without antibiotics at 5 % CO_2 and 37 °C in a humidified incubator. The cells were passaged twice a week using the 1X TrypLE™ Select enzyme. They were pelleted at 400 g, 5 min, resuspended in fresh medium, and seeded at 1.5 × 10^5 cells/mL in a 100 mm cell culture dish holding 12 mL of medium.

Recombinant VSVs were produced following the protocol described previously [159]. Briefly, to produce 1 L of virus-containing supernatant, the cells were seeded in 175 cm^2 culture plates (35 plates) at the initial density of 3 × 10^6 cells per plate in 25 ml of medium, incubated at 37 °C, and 5 % CO_2. When 80 % confluent, the cells were infected with the rVSV stock at a multiplicity of infection (MOI) of 0.001, and incubated at 34 °C, 5 % CO_2 for 72 h.

The cell culture supernatant was harvested 72 hours post-infection (hpi) and low-speed centrifuged 20 min at 3500 g, 4 °C to remove the cellular debris. As a second clarification step, a series of microfiltration filters with varying filtration media and pore sizes were tested independently. These include Miniprofile™ filter (Pall corporation, Canada), rapid-Flow™ filter (Nalgene, Canada), bottle-Top vacuum filter (Corning, Canada), Stericup® filter unit (Millipore, Canada), Supracap™ depth filter capsule (Pall Laboratory, Canada), Sartopure PP3 filter (Sartorius, Canada), Whatman GD/X Syringe Filter (Cytiva, Canada). The filtration was ran at ≃500 Liter/m^2/h (LMH) except for the vacuum-driven filters. The filter that resulted in the highest virus recovery was selected for the next step of the purification scheme.

3.2.3. Nucleic acid removal

The filtrate of the clarification step was treated with Benzonase® (Millipore Sigma, Canada) at a concentration of 10 units per mL for 2 h at 37 °C in the presence of 2 mM $MgCl_2$ with a few seconds of gentle shaking every 30 min. In order to find the best step to incorporate the Benzonase® treatment, it was introduced between different steps of the purification process, and the step that resulted in higher recovery of infectious particles was selected for further experiments. The different moments where it was tested were 1) right after harvest, 2) between low-speed centrifugation and microfiltration, 3) between microfiltration and ultrafiltration, and lastly, 4) after ultrafiltration. The purification protocol used to test Benzonase® in addition consisted of low-speed centrifugation for 20 min at 3500 g, 4 °C, microfiltration using a GD/X 25 mm Whatman filter, and ultrafiltration with a Centricon® Plus-70. A total volume of 25-30 mL supernatant was used.

3.2.4. Concentration

The concentration method was selected based on the scale of the experiment where ultracentrifugation was employed for laboratory-scale experiments, and ultrafiltration was chosen for a large-scale purification scheme. Both approaches' effectiveness was compared side by side in terms of protein removal, DNA elimination, and infective virus recovery.

3.2.4.1. Ultrafiltration

The virus suspension was concentrated by ultrafiltration, either using centrifugation with 100 kDa Centricon® Plus-70 (Millipore, Canada) or tangential flow (TFF) using Midikros® 750kDa hollow fiber TFUF system (Spectrum Laboratories, Rancho Domingez, CA, USA) or 500 kDa Xampler™ hollow fiber cartridges (GE Healthcare, Canada) and diafiltrated against the equilibration buffer used in chromatography. The flow rate in TFUF units was selected so that a shear rate of 2000 s^{-1} was maintained throughout the experiment. The resulting virus retentate, identified as 'virus material' hereafter, was stored at - 80 °C before chromatography experiments.

3.2.4.2. Pelleting by ultracentrifugation

The supernatant was concentrated by ultracentrifugation using a 20% sucrose, prepared in 10 mM Tris, pH 7.4. A total volume of 5 mL of 20% sucrose solution was placed in a 36 mL polyethylene terephthalate (PET) tube (Thermo Scientific, Canada), and the rest of the tube was filled by layering 30 mL of clarified, and endonuclease treated supernatant. The tube was centrifuged at 156,359 g for 3 hours at 4 °C in a Sorvall legend XFR ultracentrifuge (Fisher Scientific, Canada) using SureSpin™ 630 swinging bucket rotor (Thermo Fisher Scientific, Canada), after which a virus pellet was formed at the bottom of the tube. The supernatant was carefully removed, and 1-2 mL of 10 mM Tris buffer, pH 7.4, was added to the pellet and stored overnight at 4 °C. The loosened pellet was then resuspended by pipetting and either used for further purification using density gradient centrifugation or stored at -80 °C for future use.

3.2.5. Purification

The purification of concentrated and partially purified virus preparations was performed using density gradient ultracentrifugation for laboratory-scale purification scheme or anion exchange chromatography for large-scale protocol. The approaches were then compared for their ability to recover infective particles, remove contaminant DNA, and reduce protein contents.

3.2.5.1. Density gradient centrifugation

The virus concentrated by pelleting was further purified using a discontinuous iodixanol gradient (OptiPrep™ density gradient medium, Millipore Sigma, Canada), prepared in 10 mM Tris buffer, 150 mM NaCl, pH 7.4. The gradient consisted of 18 x 2 mL layers of iodixanol with concentrations varying from 50 % (at the bottom of the tube) to 16 % (at the top), in 2 % increments. A total volume of 1 mL of the concentrated rVSVs was layered on the top of the gradient. The tubes were centrifuged for 5 hours at 156,359 g, at 4 °C. The fractions (1 mL) were collected by pricking a hole in the bottom of the tube. The fractions were stored at -80 °C for further analysis.

Once the proper concentration of iodixanol for separation of rVSVs was found, in the 36 mL ultracentrifuge tubes, the concentrated samples from sucrose cushion were loaded on a discontinuous gradient consisting of, from bottom to top, 45, 37, 31, 27, 23, 19, and 14 % of iodixanol, 5 ml for 40 % and 3 mL for all the other concentrations, on top of which was layered up to 17 mL of concentrated rVSVs. The samples were centrifuged at 156,359 g for 3.5 h. The virus band (4 to 5 mL) was then pricked using a syringe from the side of the tube. The collected virus-containing fraction was stored at -80°C.

3.2.5.2. Chromatography system and buffers

The chromatographic experiments were performed using an ÄKTA Start chromatography system (Cytiva, Canada) operating with UNICORN start 1.0 software that monitored the conductivity and UV absorbance at 280 nm. The fractions were collected in 1 mL aliquots, and the flow rate was maintained at 1 mL/min. Equilibration buffer (buffer A) consisted of 20 mM Tris, 4% sucrose, pH 7.4, and elution buffer (buffer B) was made up of 2 M NaCl, 20 mM Tris, 4% sucrose, pH 7.4.

3.2.5.3. Anion exchange chromatography

For the virus capture step, four prepacked weak and strong anion-exchange chromatography columns (HiTrap™ IEX selection kit, Cytiva, Canada) were tested. The 1 ml column was equilibrated with 10 column volumes (CV) of 50 % and 10 CV

of 5 % B. The sample was equilibrated with buffer A (1:1) and injected into the column at 1 mL/min. The column was washed first with 5 CV of 0.5 % B followed by 5 CV of 5 % B. Elution was achieved by a step gradient of buffer B with successively 5 CV of each 15%, 20%, 25%, 30%, 35%, 40%, 45%, 50% and 100% for strong anion exchangers and 15%, 20%, 25%, 30%, 35%, 40%, 45% and 50% B for weak anion exchanger resins to find the proper salt concentration required for virus elution. The virus-containing fractions were collected based on the peak of 280 nm UV absorbance monitored online and later confirmed by immunoblot analysis of fractions using the VSV-N/VSV-M antibody (Kerafast, USA). The column was regenerated with 2M NaCl, equilibrated with buffer A and stored in 20% ethanol at 4 °C.

3.2.6. Determination of dynamic binding capacity

A volume of 40 mL and 50 mL of the pre-conditioned sample (1:1, sample: buffer A) were fed to the equilibrated HiTrap™ XL and HiTrap™ DEAE columns, respectively. The flow-through was collected in 5 mL fractions. The presence of VSV-N protein in these fractions was verified using immunoblot staining.

3.2.7. Particle size distribution

The size distribution of particles was examined using a Zetasizer Nano ZS, Malvern. Prior, the samples were diluted at 1:2 or 1:4 using 20 mM Tris, 4% sucrose.

3.2.8. Infectious virus titer

Quantification of infectious particles was measured following the method reported in Gélinas et al., using the TCID50 assay [160] with HEK 293A cells. Briefly, 100 µL/well of HEK293 A cells were seeded in 96 well plates at 5E04 cells/mL density. Once the cells were 80% confluent, a serial dilution of virus samples was performed in another 96 well plate (round/U bottom). For this purpose, the plate was first filled with DMEM medium (200 µL/well), then, 50 µL/well of the sample were added to the first column of the plate and mixed with the medium. From this mixture, 50 µL was pipetted and emptied in the next column, mixed, and the process was repeated for all the following columns of the plate. A total volume of 20 µL of each row, using a multichannel pipette, was transferred to the HEK293A containing plate. Samples of

every experiment were titrated the same day, having undergone the same number of freeze-thaw cycles (N = 8). The virus titer, expressed in FFU/mL (FFU: Focus-forming units), was calculated following the Spearman & Kärber algorithm using the excel sheet provided by the University of Heidelberg.

3.2.9. Total protein quantification

The total protein concentration was determined using the Bradford method with the BioRad protein assay kit II (BioRad, Canada). The assay was performed following the manual's instructions in a 96 well plate. Briefly, a standard curve was generated using the BSA standards supplied in the kit. A volume of 150 µL of each sample was added to the plate (N=3). To the sample, 150 µL of the dye reagent was added. The mixture was incubated for 30 min at room temperature. The absorbance was measured at 595 nm.

3.2.10. Host cell protein (HCP) detection

HCP quantification in the samples was carried out using the Vero Cell HCP ELISA kit (Cygnus Technologies, Southport, NC, USA), following the manufacturer's instructions. To the microtiter strips coated with goat anti-Vero polyclonal antibodies, supplied by the company, 50 µL of diluted samples (1:250) was added. An amount of 100 µL of the HRP conjugated affinity-purified goat anti-Vero antibody was added to the existing mixture in the wells. The mixture was incubated 2 h at 580 rpm, 25 °C. The wells were rinsed with wash buffer 4 X. The tetramethylbenzidine (TMB) solution (100 µL) was added to the wells and incubated 30 min, 25 °C. To stop the reaction, 100 mL of stop solution was added and the absorbance was measured at 450/650 nm using Synergy HTX multi-mode reader (BioTek, Winooski, VT, USA). The Vero cell lysates were used as the positive control.

3.2.11. DNA content quantification

The residual double-stranded DNA was quantified using Quant-iT™ Picogreen™ ds DNA assay kit (Life Technologies, Canada) following the manual's instructions. Briefly, the samples were diluted at 1:2, 1:10, and 1:20 in 20mM DNase-free Tris buffer (N=3). A volume of 100 µL of the Quant-iT™ Picogreen™ reagent was added to the samples. The mixture was incubated for 5 min. The fluorescence was

measured at 520 nm. The calibration curve was obtained using Lambda DNA (supplemented in the kit) in concentrations ranging from 1 to 1000 ng/mL.

3.2.12. Electrophoresis and immunoblot

The samples were denatured using 2x Laemmli buffer (BioRad, Canada) and 5% 2-mercaptoethanol (ACROS Organics™, Canada), followed by heating, 95 °C, 5 min.

The protein profile of the sample was assessed by SDS-PAGE. For this purpose, 15 µL/lane of each sample was loaded into a Novex™ 4-12% Tris-Glycine Mini Gel (Invitrogen™, Canada) and ran at 120 volts in 1x Tris/Glycine/SDS buffer for approximately 1 h. PageRuler™ unstained protein ladder (Thermofisher Scientific, Canada) was used as the molecular weight marker. The gel was stained using Thermo Scientific™ Pierce™ Color Silver Stain Kit (Thermo Scientific, Canada) following the manufacturer's instructions and imaged with ImageQuant LAS 4000 imager (Cytiva, Canada).

Western blot analysis was performed following the same protocol as the SDS-PAGE. The protein bands were transferred to Amersham™ Protran® Western blotting membranes (Cytiva, Canada) using a wet blotting system (BioRad, Canada) at 300 mA for 1 h at 4 °C. The membrane was blocked using 5 % milk, PBS, 0.1 % Tween (PBST) for 1 h at room temperature. The membrane was incubated with the VSV-M/VSV-N (Kerafast, USA) antibody diluted with the blocking buffer (1:1000) overnight at 4 °C. The next day, the membrane was washed 3 times for 5 min with PBST on a shaker. The horse radish peroxidase (HRP) bound rabbit anti-mouse (Abcam) in PBST (1:10000) was added to the membrane and incubated for 1 h at room temperature. The membrane was washed 3 times for 5 min with blocking buffer with shaking. The membrane was semi-dried and covered with 2 mL of Pierce™ ECL western blotting substrate (Thermo Scientific, Canada) and incubated for 1 min and revealed using ImageQuant™ LAS 4000 unit.

Spot blot analysis was performed using 2 µL of the sample placed on a nitrocellulose membrane. The membrane was air-dried for 30 min, blocked with PBST containing 5% milk for 1 h, hybridized with VSV-N/VSV-M antibody, incubated 1 h with rabbit anti-mouse HRP bound antibody in the blocking buffer, and incubated with Pierce™

ECL western blotting substrate for 1 min. Gels were observed using an ImageQuant™ LAS 4000 imager.

3.2.13. Electron microscopy

The virus-containing suspension was fixed with 4% paraformaldehyde for 1 h at room temperature. They were adsorbed on 400 mesh nickel grids coated with formvar and carbon for 20 minutes. The grids were blotted with bibulous paper and stained with 2% PTA (phosphotungstic acid) for 30 seconds, blotted, and let dry for at least 2 hours. They were then observed with a Tecnai Spirit G2 (FEI, Netherlands) at 80 kV. 10-20 images were taken per sample. Before TEM pretreatment and analysis, the samples were desalted using Amicon 15 (Millipore, Canada).

3.3. Results and discussion

In this work, we aimed to test, compare and select different methods to purify rVSVs produced in a serum-free culture medium. The overall final process can be applied either at the laboratory- or large-scale, or both. A screening step was performed before every stage of purification to select the best possible candidates. Methods that resulted in the highest recovery of infectious particles were selected for purification in the final overall process. An overview of the proposed purification schemes is represented in Fig. 9.

The overall purification protocol for both laboratory- and larger-scale begins with a Benzonase® treatment immediately after harvest to eliminate the residual host DNA, low-speed centrifugation for clarification of the virus-containing supernatant, and the removal of large contaminants such as cellular debris. The scheme then splits into two streams at the microfiltration step depending on the volume of preparations where a maximum of 200 mL and 2000 mL were tested at the lab- and large-scale, respectively. As presented in Fig. 9, the laboratory-scale purification of rVSVs was carried out using density gradient ultracentrifugation (DGUC).

For larger volumes, the concentration step was performed using tangential flow ultrafiltration (TFUF) to reduce the working volume and further remove the contaminant DNA and proteins with molecular sizes smaller than the membrane MWCO. Moreover, the introduction of TFUF before chromatographic purification can

reduce the competition of contaminant proteins or DNA with rVSVs in column binding and improve the column's dynamic binding capacity (DBC). At this step, the viruses are retained in the TFUF cartridge (retentate), whereas the smaller molecules pass through the pores and are collected in the permeate. The final large-scale purification step is performed using anion exchange chromatography to purify the rVSVs from their contaminants based on their surface charge.

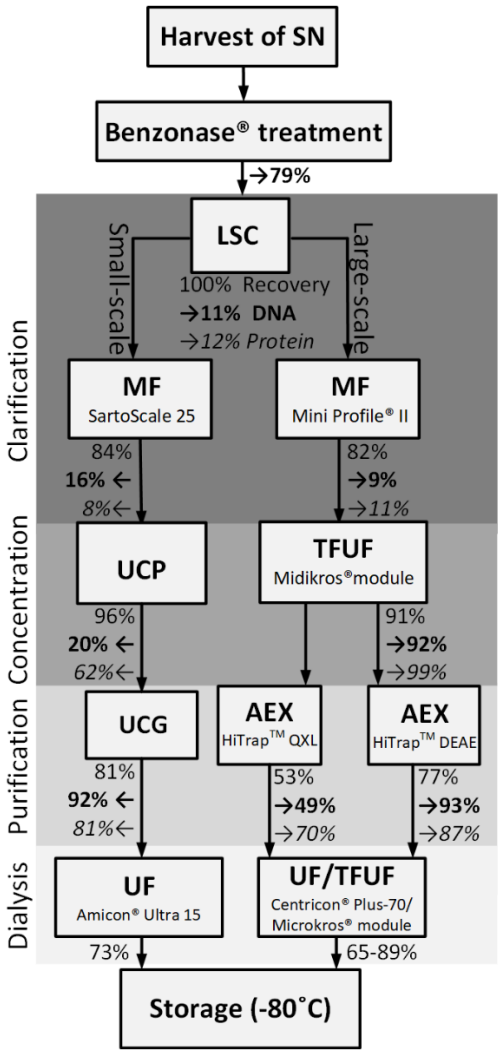

Fig 9. The overall scheme of the proposed purification processes at the laboratory- and large-scale. Recovery: ratio of recovered infectious particles from the previous step measured by TCID50 assay. DNA: Reduction ratio of host residual DNA from the previous step measured using Quant-itTM PicogreenTM assay. Protein: Removal ratio of total protein content from the previous step using Bradford assay, SN: cell culture supernatant, LSC: Low-Speed centrifugation, MF: Microfiltration, UCP: Ultracentrifugation pelleting using a 20% sucrose cushion, UF: Ultrafiltration. TFUF: Tangential flow ultrafiltration, UCG: Ultracentrifugation using an iodixanol gradient, UF: Ultrafiltration, AEX: anion-exchange chromatography.

3.3.1. Elimination of host cell DNA

To determine the proper step for Benzonase® treatment, the supernatant was treated with the final concentration of 10 U/mL of 99% pure Benzonase® enzyme, 2 mM $MgCl_2$ at 37 °C for 2 h at four different purification stages including 1) right after harvest, 2) low-speed centrifugation, 3) microfiltration, and 4) ultrafiltration. Even though the addition of Benzonase® after the concentration step would reduce the quantity required for its use, and therefore the cost of the process, its addition in the early stages of purification could positively impact the recovery of rVSVs. As shown in Table 7, treatment of supernatant with Benzonase® right after harvest (Table 7. Last column) provided a higher step recovery compared to when it was not used (Table 7. First column) or even when used at later steps (Table 7. middle column). Results from the early introduction of Benzonase® treatment can be observed more specifically on the effectiveness of membrane-based technologies (MF and UF, Table 7).

Table 7. Introduction of Benzonase® treatment at different stages of purification step and its effect on rVSV recovery.

Step of purification	Global recovery (%)		Step recovery (%)
	Without Benzonase®	With Benzonase® after each step	With Benzonase® after harvest
After harvest	100	107.3 ± 6	107.3 ± 6
After LSP	82 ± 6	89 ± 5.3	100
After MF	36.4 ± 4.9	52.4 ± 4	65.7 ± 4.2
After UF	24.7 ± 5.1	-	89.4 ± 5.7

LSP: low-speed centrifugation, MF: microfiltration.

Moreover, digestion of dsDNA fragments in initial steps has also been found to help DNA elimination during the purification process [161], as shown in the virus recovery overview (Table 7). The presence of nucleic acids before the concentration step has been reported to increase the sample's viscosity and result in membrane fouling and obstruction [162]. Therefore, the nucleic acid digestion step was placed immediately after the virus harvest in the final overall process. As shown in Fig. 9, the host DNA

content was reduced by 79 % from 226 ng/mL to 48 ng/mL after 2 h of Benzonase® treatment. In some instances, virus recovery values obtained were higher than 100 % after the Benzonase® treatment. This can be explained by the release of DNA and virus aggregates after DNA digestion.

3.3.2. Clarification by centrifugation and microfiltration

Adherent Vero cells maintained in serum-free media (VP-SFM) were used for the production of rVSVs. The cells were infected with a virus seed stock at a MOI of 0.001 and incubated at 34 °C and 5% CO_2. The rVSV containing cell culture supernatant was harvested 72 hpi. It was then clarified with low-speed centrifugation at 3500 g for 20 min at 4 °C. The centrifugation supernatant was collected and further clarified through microfiltration. In order to find the best filter for clarification, a series of filters with pore sizes varying from 0.45 µm to 30 µm and different filter medium including cellulose acetate (CA), surfactant-free cellulose acetate (SFCA), regenerated cellulose (RC), polyvinylidene fluoride (PVDF), polyethersulfone (PES), and polypropylene (PP) were tested for their efficiency in recovering rVSVs. Table 8 shows the recovery of infectious particles after clarification using the filters mentioned above.

The volume of the supernatant passed through the filters was maintained at less than 10 mL/cm^2 for membranes with a pore size of 0.45 µm and at 40 mL/cm^2 for all other membranes. Among the tested candidates, PES and PP filters were the most efficient ones, with recoveries of up to 86.3 ± 7.4 % using Mini Profile® II filters. The PVDF-based bottle-top filter showed low virus recoveries of 24 ± 6.6 % that could partially be due to its pore size. Although the VSV dimension has been reported as 120 × 70 nm [163], we had previously observed a substantial loss of rVSVs when using membranes with pore sizes ≤ 0.45 µm. In addition, cellulose-based membranes including RC, CA, and SFCA did not show high virus recoveries. This observation is on par with the report of Kang *et al*. [62] on titer recoveries lower than 20% when using cellulose-based membrane for clarification of VSV regardless of the membrane pore size.

Table 8. Different filter types were used to clarify (microfiltration) of the Benzonase® treated and centrifuged culture supernatant.

Filter name	Filtration Media	Type of filter	Pore size (µm)	Volume processed (mL)	Surface area (cm^2)	RCV ± SD (%)
Nalgene™ Rapid-Flow™ Filter	SFCA	Bottle-top	0.45	≃200	74.66	38.3 ± 7.1**
Corning® Bottle-Top Vacuum Filter	CA	Bottle-top	0.45	≃150	13.6	26 ± 8.5**
Millipore Stericup® filter unit	PVDF	Bottle-top	0.45	≃450	40	24 ± 6.6
Mini Profile® II	PP	depth filter capsule	1	400-1200	46	68 ± 7
Mini Profile® II	PP	depth filter capsule	1.5	1000-2000	46	86.3 ± 7.4
GD/X 25 mm Whatman filter	PES	Syringe filter	0.45	40	4.6	65.7 ± 5.7
SartoScale 25	PES	Capsule/ syringe filter	1.2	200 50	4.5	17.3 ± 3.5 84 ± 6
SartoScale size S	PES	Capsule filter	1.2	800-1200	17.3	58.7 ± 10.7
Supracap™ 50	RC	depth filter capsule	6 to 30	≃500	22	18*
Supracap™ 50	RC	depth filter capsule	1 to 3	≃150	22	<5*

RCV: recovery, SD: Standard deviation, SFCA: Surfactant-free cellulose acetate, CA: Cellulose acetate, PVDF: Polyvinylidene fluoride, PP: Polypropylene, PES: Polyethersulfone, RC: Regenerated cellulose. *The unit was only tested once. **The unit was only tested twice.

The massive loss of viruses when using RC-based filters despite their large pore size (30 to 6 µm) indicates that the loss of viruses was not due to the membrane fouling. Since Miniprofile™ polypropylene depth filter with pore size 1.5 µm was able to provide the highest quantity of infectious particles, it was used at 200 LMH for the filtration step throughout all purifications for volumes higher than 200 mL.

The Miniprofile™ filter (1.5 µm) resulted in removing 64 % of the host proteins and 8.9 % of the residual DNA (Table 12). Additionally, GD/X 25 mm Whatman and SartoScale 25 filters with the recovery of 65.7 ± 5.7 % and 84 ± 6 % were used (Table 8). However, the weaker performance of the SartoScale 25 filter in terms of virus recovery (17.3 ± 3.5) was only observed when used for processing higher than 50 mL of sample. Overall, SartoScale 25, when employed for filtration of 50 mL of supernatant, eliminated 58 % of the host cell proteins and 16.3 % of the contaminant DNA (Table 12).

3.3.3. Concentration

3.3.3.1. Ultracentrifugation

At laboratory-scale, ultracentrifugation was used to concentrate the supernatant before the final purification step. A volume of 32 mL of the clarified supernatant was loaded on the top of a 5 mL, 20% sucrose solution in 10 mM Tris, pH 7.4, and centrifuged at 156,359 g for 3 hours at 4 °C. The supernatant was carefully discarded at this step, and 2 to 3 mL of 10 mM Tris, pH 7.4 was added to the pellet. The tube was stored at 4 °C overnight to allow the pellet to loosen from the tube. The pellet was resuspended the next day, used immediately for purification or aliquoted and stored at -80 °C until further use. The virus pelleting using sucrose cushion resulted in 16 X concentrations of rVSVs while recovering 96% of the infective particles. This approach helped reduce the DNA contents by 20 % by bringing the contents to 192 ng/mL and eliminating 88 % of the host cell proteins from the virus preparations (Table 12).

3.3.3.2. Ultrafiltration

Ultrafiltration can advantageously replace ultracentrifugation at a large-scale as it is less costly and, in the right conditions, does not generate mechanical stress that

could disrupt the viral particle. It can be used both before and after chromatography for volume reduction and polishing purposes. At laboratory-scale purification, ultrafiltration can be employed to purify and concentrate the supernatant before ultracentrifugation partially. However, at larger volumes, ultrafiltration before chromatography purification can reduce the concentration of contaminant proteins and, therefore, increase the resin's dynamic binding capacity. Use of TFUF has been successfully employed for the purification of viruses, including retroviruses [164], influenza A virus [90], and lentiviruses [165] resulting in < 90 % virus recoveries.

Table 9. Ultrafiltration units tested.

Unit name	Filtration media	Type of unit	Pore size (kDa)	Volume (mL)	Surface area (cm^2)	Conc factor (x)	RCV of infectious units (%)
Amicon® Ultra 15	Ultracel RC	CFU	100	14	7.6	≃10	49±14.3
						-	73±9.2
Centricon® Plus-70	RC	CFU	100	60	19	≃15	89.4±5.7
MidGee ultrafiltration	PS	HFC	100	200	26	≃5.5-6	37±4.2
Xampler ultrafiltration	PS	HFC	500	300 to500	230	≃6	59±7
Microkros® TFUF module	mPES	HFC	750	200	13	≃6	22.3±6.4
						≃3-4	65.1±4.3
Midikros® TFUF module	mPES	HFC	750	500 to 2500	235	20	94.6±1.5

Conc: Concentration, HFC: Hollow fiber cartridge, CFU: Centrifugal filter unit, RCV: recovery.

The rVSV-containing clarified supernatant was concentrated through TFUF or dead-end UF using hollow fiber cartridges or centrifugal ultrafiltration units. Two centrifugal-based UF units with regenerated cellulose (RC) membranes with MWCO of 100 kDa were tested for laboratory-scale concentration and partial purification (Table 9). Centricon® Plus-70 and Amicon® Ultra 15 units showed 89.4 ± 5.7 % and 49 ± 11.1 % virus recoveries, respectively. The Amicon® Ultra 15 unit, when

employed for buffer exchange (not for concentration), resulted in higher virus recoveries of 73 ± 9.2 %, compared to when it was used for concentration that resulted in the recovery of 49 ± 14.3 % of infectious particles (Table 9). The centrifugal-based UF units can only be used for laboratory-scale experiments since they can uphold 15 to 60 mL of supernatant. It is noteworthy that despite being effective in infectious unit recovery, these UF systems did not help in the successful removal of DNA fragments (data not shown) as the retentate still had high levels of residual DNA.

To concentrate larger sample volumes, four different hollow fiber TFUF products were used to process 200 to 2500 mL of clarified supernatant. Higher sample volumes were processed using Midikros® or Xampler ultrafiltration modules (Table 9) with a similar surface area of 230 to 235 cm^2 and MWCO of 750 and 500 kDa, respectively. The flow rate was selected so that a maximum shear rate of 2000 s^{-1} would be maintained throughout the process. The Midikros® and Xampler TFUF modules resulted in the recovery of 94.6 ± 1.5 % and 59.0 ± 7.0 % of infectious particles measured by TCID50 assay. The use of the Midikros® unit resulted in the elimination of 95 % of host proteins and 92.1 % of the residual DNA contents (Table 12) concerning the previous purification step. Considering these observations and given the scalability of Midikros® hollow fiber cartridge, it was decided to use it for the concentration step in all subsequent purification experiments.

As presented in Table 9, MidGee and Microkros® modules were tested for final diafiltration and buffer exchange of sample volumes smaller than 200 mL. These two units with MWCO of 100 and 750 kDa and low protein binding membrane materials resulted in the recovery of 37 ± 4.2 % and 22.3 ± 6.4 % rVSVs (Table 9). The effect of the concentration factor on recovery was tested with the Microkros® TFUF unit. It was found that a lower concentration factor (3 to 4 X) had a positive effect on the recovery (recovery = 65.1 ± 4.3%) compared to a concentration factor of 6X (recovery = 22.3 ± 6.4%).

In addition, the processing time for both the large-scale and small-scale methods was relatively similar (≈ 5 h). When performing TFUF, the processing time includes preparation of solutions (rinse buffer, water, and sanitization solution), sanitization of the unit, the equilibration of the membrane for the experiment (≈ 2 h), the experiment run, unit clean up, and final sanitization before storage. The virus concentration process by UC also consists of preparing the sucrose solution, sanitization of the tubes, loading of the samples, UC run (≈ 3 h), collection of pellet, and resuspension of the pellet the next day.

3.4. Purification

3.4.1. Ultracentrifugation

Ultracentrifugation over a discontinuous iodixanol gradient was chosen to purify the clarified rVSV-containing supernatant at a laboratory-scale. In order to determine the right concentration of iodixanol to use for purification, a discontinuous gradient of iodixanol consisting of 2 mL layers ranging from 50 % to 16% iodixanol, in 2 % decrements (Table 10) was prepared in 10 mM Tris at a pH of 7.2. A total volume of 1 mL of concentrated virus from UCP (as described in section 3.3.3.1) was added on top of the gradient and centrifuged for 5 h at 156,359 g, 4 °C. The resulting band after UCG was collected by pricking the ultracentrifugation tube and collecting 1 mL fractions for further analysis using the spot blot method.

Fig. 10 panel A shows that the virus bands appeared in the gradient between 18 % and 28% iodixanol. The refractive index of these virus-containing fractions was measured, 1.3632 to 1.3788, corresponding to fluid densities between 1.100 and 1.153 g/mL, respectively. Densities ranging from 1.16 to 1.22 g/mL have been reported for wild-type VSV recovery based on cesium chloride or potassium tartrate gradient separation [68]. The purity of the virus-containing fractions (pulled together) compared to clarified supernatant is shown in Fig 10. panel B.

Table 10. Iodixanol layer composition in the originally proposed gradient for purification of rVSV consisting of 18 layers of 2 mL.

Layer No	Volume (mL)	Accumulative volume (mL)	Iodixanol (%)
1	2	2	50
2	2	4	48
3	2	6	46
4	2	8	44
5	2	10	42
6	2	12	40
7	2	14	38
8	2	16	36
9	2	18	34
10	2	20	32
11	2	22	30
12	2	24	28
13	2	26	26
14	2	28	24
15	2	30	22
16	2	32	20
17	2	34	18
18	2	36	16

A simpler iodixanol gradient has been devised for the final overall process, passing from 18 layers (Table 10) to 6 layers (Table 11), and tested for rVSV purification and concentration. The virus band collected at the end of this step resulted in 81 % recovery of infectious particles while removing 81 % of total protein, 80 % of host cell proteins, and 92 % of DNA contamination concerning the previous purification step. In comparison to pelleting, using iodixanol gradient for purification of rVSVs resulted in the elimination of approximately 4 times more DNA and 3.5 times more contaminant proteins. Another advantage of purification using step gradient over concentration with sucrose cushion could be regarded as its capacity to remove a higher number of extracellular vesicles (EVs).

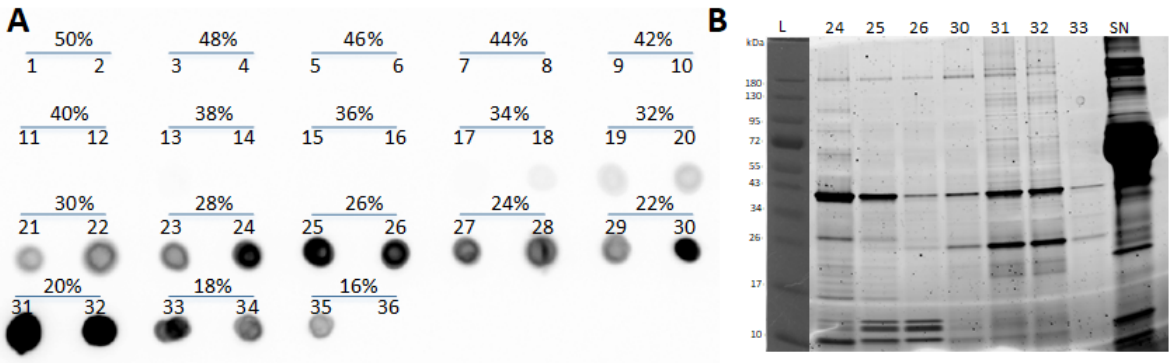

Fig 10. A) Spot blot analysis of fractions obtained from the purification of purified supernatant by ultracentrifugation using a discontinuous gradient of iodixanol. The % iodixanol and the fraction number are shown. B) SDS-PAGE analysis of purified virus-containing fractions from iodixanol gradient comparing the purity of the purified fractions to the Benzonase® treated and clarified supernatant. L: Molecular weight marker, SN: Clarified supernatant.

The separation of these extracellular components from rVSVs is challenging due to morphological similarities [166]. Electron micrographs of viruses prepared using these two approaches show a distinct difference in the number of EVs and outline the advantage of purification with a discontinuous gradient of iodixanol (Fig. 11). This approach (UCG) resulted in highly concentrated VSV preps with titers of 2E09 TCID50/mL and higher. The high titer of these purified viruses subsequently requires further dilution prior to vaccination that will eventually result in less final DNA content than what is presented in Table 12, making these doses compliant with regulatory agency regulations (10 ng/dose) [167].

Table 11. Simplified iodixanol gradient composition for UC purification of rVSV.

Layer No	Volume (mL)	Accumulative volume (mL)	Iodixanol (%)
1	5	5	40
2	3	8	33
3	3	11	28
4	3	14	23
5	3	17	18
6	3	20	13

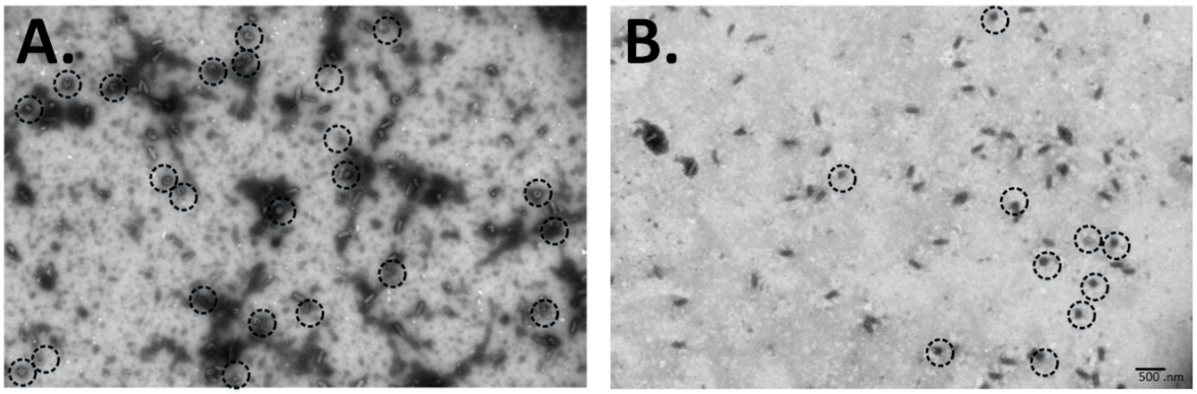

Fig 11. Electron micrographs of rVSVs purified by ultracentrifugation through either A) pelleting using a sucrose cushion, B) density iodixanol gradient, showing the number of extracellular vesicles/exosomes in the purified rVSV preparations. The images are taken at 6800 x magnification. The encircled structures are suspected to be extracellular vesicles/exosomes.

3.4.2. Chromatography

Different anion exchanger resins were compared using Benzonase® treated, clarified, concentrated, and pre-equilibrated (20 mM Tris) virus supernatant as the starting material. These resins were first tested for their recovery of infectious particles. The candidate with the highest recovery was analyzed for its dynamic binding capacity (DBC) and its ability to remove contaminants such as cellular proteins and DNA. In addition, the optimum salt concentration to use for virus particle elution was identified. In order to find the most suitable column for purification of rVSVs, four 1 mL anion exchange columns, namely, HiTrap™ DEAE FF, HiTrap™ ANX FF, HiTrap™ Q FF, and HiTrap™ XL, were tested for the highest percentage of infectious particle recovery.

For this purpose, a total volume of 20 mL feed was passed through the weak anion exchanger columns (HiTrap DEAE FF and ANX FF) at a flow rate of 1 mL/min. The elution was carried out using a multiple-step gradient of the composition of the mobile phases A and B (described in the method section), culminating at 2 M NaCl in 20 mM Tris (100% Buffer B). The fractions with absorbance higher than 5 mAU were collected. The peaks obtained from each elution step were collected in 1 mL fractions and analyzed by spot blot and TCID50 assays to confirm the presence of the VSV-N protein and infectious particles, respectively (Fig. 12).

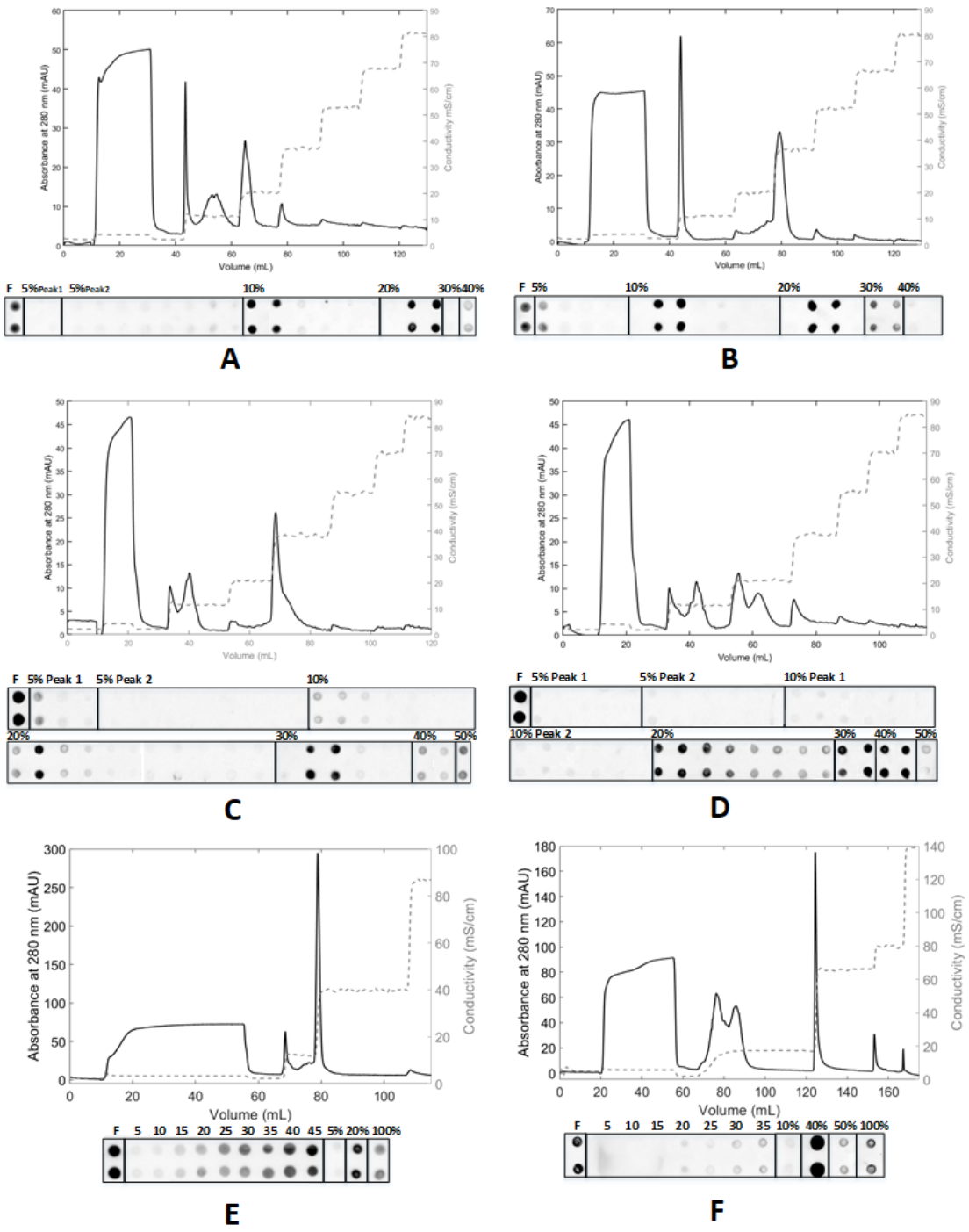

Fig 12. Chromatograms and spot blot analysis of ion-exchange chromatography columns. A) HiTrap™ DEAE FF, B) HiTrap™ ANX FF, C) HiTrap™ Q FF, D) HiTrap™ XL. Spot blot analysis of each experiment is presented at the bottom of each chromatogram. The rVSV was detected using an anti-VSV-N antibody. Determination of the binding capacity of the E) HiTrap™ DEAE FF and F) HiTrap™ XL for the clarified and concentrated rVSVs. The flow-through was collected in 5 mL fractions. F: clarified and concentrated load from TFUF (Feed), 5%-100%: Percentage of 2M NaCl in 20 mM Tris, 4% sucrose as elution buffer (buffer B).

The elution of viruses from weak anion exchangers (Fig.12 A and B) started at a lower salt concentration than strong anion exchanger columns (Fig. 12 C and D). When using HiTrap™ DEAE FF and HiTrap™ ANX FF for purification, the VSVs elution from the column started at 10 % and extended to 20 % buffer B, and in HiTrap™ ANX FF it lasted until 30 % buffer B, corresponding to 200 mM, 400 mM and 600 mM of NaCl, respectively. The combined virus-containing fractions from HiTrap™ DEAE FF and HiTrap™ ANX FF columns accounted for 77 % and 18 % recoveries of infectious particles, respectively (Table 12).

The two strong anion exchanger (HiTrap™ Q FF and XL) columns were loaded with 10 ml of the feed. As shown in Fig 12. C and D, the rVSVs started eluting from the strong anion exchanger columns at 20% buffer B (400 mM NaCl) and continued up to 50% buffer B (1M NaCl). The titer recovery from the combined virus-containing fractions of HiTrap™ Q FF and XL was found to be 32 % and 53 %, respectively, from the previous purification step (Table 12).

Since the HiTrap™ XL (strong anion) and HiTrap™ DEAE FF (weak anion) columns resulted in the highest virus recovery, they were further assessed for their rVSV binding capacity by loading them with 35 mL and 45 mL of feed (TFF retentate), respectively. The flow-through was collected every 5 mL and analyzed by spot blot analysis for VSV-N proteins and TCID50 test for the count of infectious viruses.

As presented in Fig. 12 E, the VSV-N leaking in the flow-through from the HiTrap™ DEAE FF column started after 15 mL of elution buffer feeding. However, the total number of infectious particles in the flow-through at that point was less than 1 % of the virus titer in the feed. The 5 % virus breakthrough for the HiTrap™ DEAE FF column was detected when 20 mL of elution buffer was fed, equivalent to 150 mL of supernatant and a total of 1.10E+10 infectious units passed through the column. A similar trend was observed for the HiTrap™ XL column, where the VSV leakage started after 30 mL of flow-through, but the number of viruses in the flow-through was less than 2 % of that in the feed. However, the 5 % VSV breakthrough in HiTrap™ XL occurred after the passage of 35 mL feed corresponding to 262 mL of supernatant and 1.93E+10 infectious particles.

Table 12. . Virus recovery and residual levels of HCP, total protein contents, and DNA for laboratory- and large-scale purification processes tested in the present work.

Purification step	Total protein contents		Residual DNA		Host cell protein		Recovery of infectious particles				
	Total protein (µg/mL)	Step RCV (%)	Host cell DNA (ng/mL)	Step RCV (%)	HCP contents (ng/mL)	Step RCV (%)	Titer (TCID50/mL)	Exit volume (mL)	Conc factor	Step RCV (%)	Global RCV (%)
Harvest	536	100	226	-	168,305	-	7.99E+07	2400	-	-	-
BZ treatment	-	-	48	21.2	169,713	101	9.77E+07	2400	-	122	122
LSP	473	88.2	43	89.6	130,864	77	9.77E+07	2400	-	100	122
MF (1.5 µm Miniprofile®)	421	89.4	39	91.1	83,906	64	7.99E+07	2410	-	82	100
MF (SartoScale 25)	436	92.2	36	83.7	76,339	58	8.70E+07	50	-	84	89
TFUF (Midikros®)	86	1.4	46	7.9	57,519	5	1.10E+09	160	15	91	92
UC (Pelleting)	216	37.7	192	80	61,648	12	1.09E+09	9	16	96	-
UC (6 layer gradient)	93	19.1	34	7.9	26,504	19	2.01E+09	4	2.25	81	-
HiTrap™ DEAE FF	23	13.4	6.7	7.3	9,359	8	1.69E+09	5	2	77	-
HiTrap™ ANX FF	-	-	-	-	-	-	-	-	-	18.69	-
HiTrap™ Q XL	34	30	31	51.2	6,181	8	2.67E+09	3.8	8	53	-
HiTrap™ Q FF	-	-	-		-	-	-	-	-	32.8	-

RCV: recovery, Step RCV: recovery from previous step, Conc: concentration, LSP: low-speed centrifugation, BZ: Benzonase® treatment, MF: microfiltration, TFUF: tangential flow ultrafiltration, UC: ultracentrifugation.

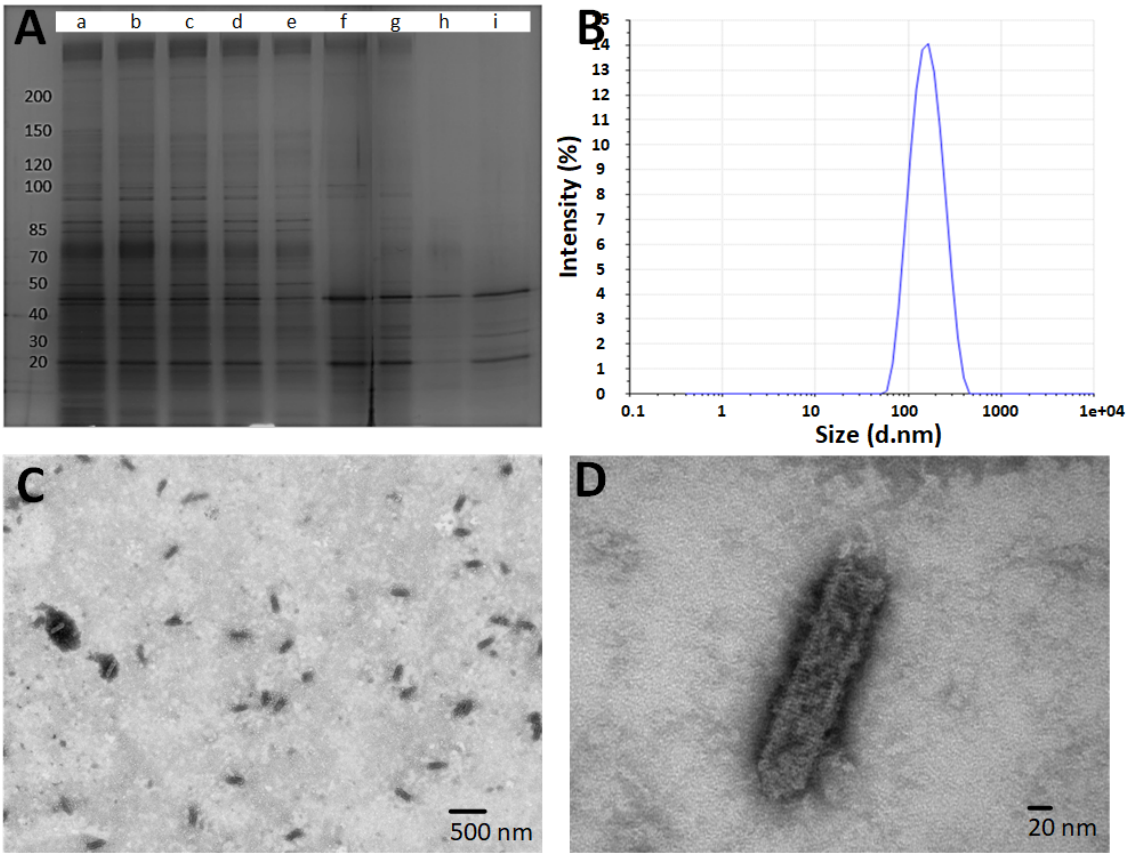

Fig 13. Purity, identity, and morphology of the purified virus. (A) Silver stained SDS-PAGE showing the protein profile of each purification step. a) Supernatant, b) Post Benzonase® treatment, c) Post centrifugation, d) Post microfiltration (miniprofile® II) , e) Post microfiltration (SartoScale 25), f) Post TFUF (1:10), g) Post density gradient ultracentrifugation (1:10), h) Eluate from HiTrap™ DEAE (1:5), i) Eluate from HiTrap™ Q XL (1:5). B) Measurement of a purified rVSV preparation particle size distribution by DLS. Visualization of purified rVSVs by transmission electron microscopy at 6800X (C) and 98000X (D).

Despite the higher rVSV binding capacity in HiTrap™ XL, the recovery of infectious rVSVs was less than that obtained from HiTrap™ DEAE FF. Overall, the HiTrap™ XL allowed a higher volume of feed processing but with a 50 % recovery of infective viruses, whereas HiTrap™ DEAE FF showed a lower binding capacity for rVSV but resulted in a higher recovery of infectious rVSVs (77 %). The amount of DNA in the eluates of HiTrap™ XL column was approximately 4 times higher than that measured in the eluates of HiTrap™ DEAE FF.

The main reason for such high DNA contents in the eluates of this strong anion-exchanger column is the use of high salt concentration for elution of tightly bound rVSVs at which DNA and other bound contaminants including host cell proteins elute too. Introduction of a diafiltration or a polishing chromatography step after HiTrap™ XL might help in lowering the high DNA contents in the eluates obtained from this column. Howerver, the DNA contents in the eluates of HiTrap™ DEAE FF column were lower than 10 ng which complies with FDA restrictions. However, both columns showed comparable efficacy in eliminating 92 % of the HCPs from the viruses with HCP concentrations lower than 10 ppm in the final preparations (Table 12). However, VSV as an enveloped virus carries several host cell proteins in its host-derived membrane, as previously reported by Schauwecker et al. [147]. That as such contributes to the HCP content measured.

The protein profile and the purity of the supernatant at each step of the purification were assessed through SDS-PAGE analysis followed by silver staining. As presented in Fig. 13 A., the intensity of the bands corresponding to VSV proteins, including VSV-M (26 kDa) and VSV-N (47 kDa) versus the background, is significantly different in purified virus preparations compared to the clarified supernatant. This indeed shows the strong removal of the HCPs through the purification process. Dynamic light scattering (DLS) verified the size of the purified rVSVs, and the presence of aggregates in the samples was verified using dynamic light scattering (DLS). Average size of 207.6 nm (Fig. 13 B) has been assigned to the purified rVSVs, which is following previous reports [151][168]. The morphology and the size of the virions were also observed by electron microscopy, further confirming the results from DLS analysis. The rVSV particles retained the classic morphology of wild-type VSV as a bullet-shaped virus (Fig. 13 C and D) [169].

3.5. Conclusion

The PP and PES-based membranes are the most suitable filtration media for clarifying rVSVs resulting in virus recoveries as high as 86.3 ± 7.4 %. The introduction of Benzonase® treatment in the early steps of the purification scheme resulted in the increased global recovery of infectious particles. Moreover, the

concentration of rVSV containing supernatant at a larger scale using mPES based TFUF modules resulted in up to 20 fold concentration, eliminating more than 90 % of the host residual DNA while retaining more than 90 % of the infective viruses. The concentration and purification of viruses using density gradient ultracentrifugation functioned effectively as TFUF on a large-scale by eliminating 92 % of the contaminant host DNA and proteins. The HiTrap™ Q XL and HiTrap™ DEAE FF columns revealed comparable results regarding rVSV binding capacity and virus recovery. While HiTrap™ Q XL exhibited higher dynamic binding capacity, HiTrap™ DEAE FF resulted in higher recovery of infective particles. Due to the use of high salt concentration, needed for elution of rVSVs from the HiTrap™ Q XL column, the eluates from this resin, still had high amounts of contaminant DNA, while the DNA contents of HiTrap™ DEAE FF were lower than 10 ng/mL. Overall, complete purification trains have been selected for either small- or large-scale purification of rVSV vaccines, based on the above results and providing recovery of 51% and 48% infective particles from the large-scale and small-scale schemes, respectively. These approaches resulted in eliminating more than 90% of contaminant DNA and HCPs from the virus preparation, bringing the level of these contaminants to the permitted quantity set by the regulatory authorities.

Declaration of competing interest

The authors declare that they have no known competing financial interests or personal relationships that could have influenced the work reported in this paper.

Acknowledgment

The authors thank the bio-imaging platform of the Infectious Disease Research Centre, CRCHU de Québec, for performing electron microscopy. We would also like to thank the Natural Sciences and Engineering Research Council (NSERC) and the Canadian Institute of Health Research (CIHR) for financing this project.

Chapter 4: Two-step chromatographic purification of an rVSV based HIV vaccine candidate expressing HIV and Ebola glycoproteins

Anahita Bakhshizadeh Gashti [a], Parminder S. Chahal [b], Bruno Gaillet [a], Alain Garnier [a*]

[a] Department of Chemical engineering, Faculty of Sciences and Engineering, Université Laval, Quebec, QC, Canada

[b] Human Health Therapeutics, National Research Council Canada, Montreal, QC, Canada

*Corresponding author: alain.garnier@gch.ulaval.ca

Manuscript

Résumé

Dans ce travail, nous proposons l'utilisation d'une nouvelle combinaison de méthodes chromatographiques pour le traitement en aval d'un vaccin candidat contre le VIH basé sur le virus de la stomatite vésiculeuse recombinant (rVSV) exprimant les glycoprotéines d'Ebola et du VIH à sa surface. Les rVSV sont produits dans des cellules Vero adhérentes en milieu de culture sans sérum. Le surnageant de culture cellulaire contenant le virus a été initialement traité avec de l'endonucléase pour réduire les teneurs en ADN. Le surnageant de culture cellulaire a ensuite été clarifié par centrifugation à basse vitesse et microfiltration avec un filtre 1,2 µm de taille de pore. Le surnageant clarifié a par la suite été traité avec une membrane échangeuse d'anions pour l'adsorption du virus. Cette étape a permis d'éliminer 91.5 % du contenu en ADN contaminant et 91.5 % des protéines de la cellule hôte (HCP). Cette étape de capture a été suivie d'une étape de polissage par l'intermédiaire d'une colonne multimodale pour compléter l'élimination des contaminants ADN et HCP. Le virus contenu dans l'écoulement non-retenu de cette colonne a alors été purifié par l'enlèvement supplémentaire de 77 % de l'ADN contaminant et de 42 % des HCP. La préparation virale purifiée a finalement été diafiltrée et dessalée à l'aide d'une unité d'ultrafiltration à flux tangentiel (TFUF), permettant d'atteindre une teneur finale en ADN inférieure à la limite maximale définie par les autorités réglementaires pour des préparations vaccinales (10 ng/dose).

Abstract

In the current work, we propose a combination of chromatographic methods for downstream processing (DSP) of a candidate HIV vaccine based on recombinant vesicular stomatitis virus (rVSV) expressing Ebola and HIV glycoproteins on its surface. The rVSVs are produced in serum-free media using adherent Vero cells. In this work, the virus-containing cell culture supernatant was initially treated with endonuclease to reduce the DNA contents. The cell culture supernatant was initially clarified using low-speed centrifugation and microfiltration through a 1.2 µm pore size filter. The clarified supernatant was passed through an anion exchange membrane adsorber for virus capture. This step removed 89 % of contaminant DNA contents, 91.5 % of host cell proteins (HCP) and 88.3 % of the total proteins. Since the DNA contents in the elution fractions of AEX were high (>10 ng/dose), the capture step was followed by a polishing step using a multimodal column to lower the DNA and HCPs level further. The flow-through from the second chromatography approach resulted in further elimination of 77 % of contaminant DNA, 42 % of HCPs and 20 % of total protein contents. The purified virus preparation was finally diafiltrated and desalted using a tangential flow ultrafiltration (TFUF) unit, ensuring a DNA content lower than the maximum limit defined by regulatory authorities (10 ng/dose) for vaccine preparations.

Keywords: recombinant vesicular stomatitis virus (rVSV), HIV glycoprotein, membrane chromatography, chromatographic purification, rVSV-ZEBOV

4.1. Introduction

The use of membrane adsorbers has become a method of choice for the purification and clearance of viruses and virus-like particles (VLP) in the pharmaceutical industries [170]. The advantages of membrane adsorbers for chromatographic separation of biomolecules over the traditional resin columns include the possibility of running the process at higher flow rates, the disposable nature of the columns, lower maintenance cost, the scalability of the approach, higher binding capacity, and elimination of difficulties associated with the packing step when working with the resin columns [171,172]. Moreover, these macroporous membranes have shown a higher dynamic binding capacity for large particles such as viruses [173] and DNA [174] compared to resin-based columns in practice.

Based on the latest UNAIDS report, there is 37.7 million human immunodeficiency virus (HIV) infected individuals globally, with 1.5 million new HIV infections in 2020 [175]. Despite the availability of anti-retroviral treatments and promising suppression of viral load in more than half of the infected people, there were still 680,000 lives lost due to the acquired immunodeficiency syndrome (AIDS) related diseases in year 2020. It is well-understood that the complete elimination of the occurrence of new HIV infections is only feasible through an efficient vaccine [176]. Even with the high number of ongoing research on vaccine development, none of the candidate vaccines has passed the trials successfully [177]. However, with possible chances of HIV-positive individuals infected with severe acute respiratory syndrome coronavirus-2 (SARS-CoV-2) developing infection [178] calls for an immediate HIV vaccine development.

Anion exchange (AEX) membranes are commercially available and offered by multiple companies, including Sartorius laboratory separations, Pall laboratories, and Millipore. AEX membrane adsorbers have primarily been used to eliminate host cell proteins and DNA in biopharmaceutical production of antibodies and virus clearance [179,180]. However, their application has been extended to the purification of viruses and VLPs, including recombinant baculoviruses [170], human

and equine influenza A virus [181], minute virus of mice [182], retroviruses [183], adeno-associated viruses [184], pseudorabies virus [183], lentiviruses [173] and densonucleosis virus [185]. Grein et al. [186] reported recovery of 90 % infective recombinant baculoviruses and DNA contents of lower than 10 ng/mL after purification using the Sartobind® Q membrane. Moreover, an average recovery of 72 % (based on HA assay) was found for influenza A virus when using the Sartobind® Q column by Kalbfuss *et al.* [181]. The same adsorber column was used by Wolff et al. [187] to purify vaccinia Ankara virus and resulted in the recovery of 77 % viruses, removal of 92 % protein contents, and 16 % residual DNA from the crude supernatant.

In the current work, we propose a purification scheme for DSP of an HIV vaccine candidate based on recombinant vesicular stomatitis virus (rVSV). VSV (*Rhabdoviridae* family) is a livestock pathogen, and its infection in humans is very rare and will only cause flu-like symptoms [3,188]. Due to the low occurrence of VSV infection in humans, it is a suitable platform for gene therapy and vaccine development. In addition, VSV offers other advantages that are: its ability to grow in many mammalian cell lines and a very low chance of viral RNA integration into the host DNA [189]. The rVSV used in this project is constituted based on the Ebola virus vaccine (FDA-approved and marketed under the name Ervebo) backbone (rVSV-ZEBOV) that, in the 2018 Ebola epidemic, was shown to have an efficacy of 97.5% [22]. The rVSV used in this study expresses the HIV glycoprotein and the Ebola (EBOV-gp) glycoprotein on its surface. The addition of Ebola-gp to this VSV variant was done to enhance the cell tropism of the virus.

We have previously proposed purification schemes for rVSV using strong (HiTrap™ Q XL) and weak anion exchanger (HiTrap™ DEAE FF) columns. These columns presented the high binding capacity for rVSV, including 1.10E+10 infectious unit (IU)/mL of DEAE FF and 1.93E+10 IU/mL of Q XL resins. However, it should be noted that the chromatography load used in these experiments had been partially concentrated and purified using tangential flow ultrafiltration. Due to the scalable capacity of the membrane adsorbers and elimination of the need for a concentration

step before chromatography, we sought to test this technology for purification of rVSV based HIV vaccine candidate. For this purpose, the rVSVs were produced in serum-free media using serum-free Vero cells with a low multiplicity of infection (MOI) to minimize the quantity of virus stock. Previous studies on VSV stability have shown low resistance of this virus to temperature (significant titer loss at or above 40 °C), low BSA concentration, and an acidic environment compared to alkaline media [25,190]. Therefore, due to the possible exposure of viruses to high concentrations of NaCl during the chromatographic experiments, their stability at high concentrations of NaCl was tested at different temperatures before the purification process.

The proposed membrane-based purification process begins with a nuclease treatment followed by clarification using low-speed centrifugation and microfiltration. The clarified supernatant was purified using the anion exchange membrane adsorber (Sartobind® Q) for virus capture. The virus elution was followed by polishing chromatography to further remove the contaminant DNA and proteins using Capto™ Core 700, a multi-modal column. The Capto™ Core 700 resin is composed of an inactive shell while being porous (700 kDa cut off) and charged in the core. This, in return, allows the larger molecules such as viruses to pass through the column while the smaller proteins and DNA are trapped in the charged resin core. The flow-through from the polishing step was diafiltrated and desalted using a Microkros® TFUF module before storage at -80 °C.

4.2. Material and methods

4.2.1. Cell lines and chemicals

All chemicals were of analytical grade, if not otherwise stated: sodium chloride (NaCl) (ACROS Organics, Canada), Tris buffer powder (Invitrogen, Canada), Tween-20 (Fisher Bioreagents, Canada), sodium hydroxide (NaOH) (Millipore Sigma, Canada), 1 M $MgCl_2$ (ThermoFisher Scientific, Canada), sucrose (Bioshop, Canada).

VP-SFM medium (ThermoFisher Scientific, Canada), 200 mM L-glutamine (Wisent Bio Products, Canada), Dulbecco′s Modified Eagle′s Medium (DMEM, Corning,

Canada), 1X TrypLE™ Select enzyme (Thermo Fisher Scientific, Canada), Fetal Bovine Serum (FBS, Wisent, St-Bruno, QC, Canada), Benzonase® (Millipore Sigma, Canada), 1 M $MgCl_2$ (ThermoFisher Scientific, Canada), sucrose (Bioshop, Canada). Serum-free adherent Vero cell line (CCL-81.5) was a generous gift from Dr. A. Kamen laboratory (McGill, Montreal), and HEK 293A cells were obtained from Dr. R. Gilbert laboratory (NRC-Montréal).

4.2.2. Cell culture and rVSV production

Vero cells used for virus production were maintained in serum-free VP-SFM medium, supplemented with 4mM L-glutamine, without antibiotics at 37 °C and 5 % CO_2 in a humidified incubator, and passaged twice weekly. Cells were detached using 1X TrypLE™ Select enzyme, centrifuged at 400 g, 5 min, resuspended in fresh medium, and seeded at 1.5 × 10^5 cells/mL in 100 mm cell culture dish holding 12 mL of medium.

HEK 293A cells used for virus titration were maintained in Dulbecco′s Modified Eagle′s Media supplemented with 2 mM L-glutamine and 5 % FBS, without antibiotics at 5 % CO_2 and 37 °C in a humidified incubator. The cells were passaged twice a week using the 1X TrypLE™ Select enzyme. They were pelleted at 400 g, 5 min, resuspended in fresh medium, and seeded at 1.5 × 10^5 cells/mL in a 100 mm cell culture dish holding 12 mL of medium.

Recombinant VSVs were produced following the protocol described previously [159]. Briefly, to produce 1 L of virus-containing supernatant, the cells were seeded in 175 cm^2 culture plates (35 plates) at the initial density of 3 × 10^6 cells per plate in 25 ml of medium, incubated at 37 °C, and 5 % CO_2. When 80 % confluent, the cells were infected with the rVSV stock at a multiplicity of infection (MOI) of 0.001, and incubated at 34 °C, 5 % CO_2 for 72 h.

4.2.3. Nucleic acid removal

The culture supernatant was harvested 72 hours post-infection (hpi), and was treated with Benzonase® (Millipore, Canada) at a concentration of 10 units per mL for 2 h, 37 °C in the presence of 2 mM $MgCl_2$ with a few seconds of gentle shaking every 30 min.

4.2.4. Clarification of supernatant

The Benzonase® treated supernatant was clarified by centrifugation at 3500 g, 4 °C for the removal of cellular debris, followed by microfiltration using a 1.2 µm Miniprofile™ filter (Pall Corporation, Canada). The filtration was performed at 400 Liter/m^2/h (LMH).

4.2.5. Virus stability assay

The clarified supernatant (2 x 30 mL) was loaded on 5 mL of 20 % sucrose solution in 20 mM Tris, 150 mM NaCl and centrifuged at 156,359 g for 3 h, 4 °C in a Sorvall legend XFR ultracentrifuge (Fisher Scientific, Canada) using SureSpin™ 630 (36 mL) swinging bucket rotor (Thermo Fisher Scientific, Canada). The supernatant was removed, and the pellet was re-suspended in 6 mL of 10 mM Tris, 4 % sucrose, pH 7.4. The purified viruses were aliquoted in different centrifuge tubes and stored in a thermocycler for 23 °C or in a refrigerator at 4 °C. The salt concentration in the samples was adjusted using a stock of NaCl (4 M NaCl, 10 mM Tris, 4 % sucrose, pH 7.4) and 10 mM Tris, 4 % sucrose, pH 7.4 was added to the control samples. The virus titer was measured using TCID50 assay after each incubation time. The TCID50 plates were read 5 days hpi.

4.2.6. Chromatographic purification

The ÄKTA Start chromatography system (Cytiva, Canada) operating with UNICORN start 1.0 software was used for the chromatographic experiments, monitoring the conductivity and UV absorbance at 280 nm. The fractions were collected in 1 mL aliquots, and the flow rate was maintained at 5 mL/min for anion exchange columns. Equilibration buffer (Buffer A) for AEX consisted of 20 mM Tris, 4% sucrose, pH 7.4, and elution buffer (Buffer B) was made up of 2 M NaCl, 20 mM Tris, 4% sucrose, pH 7.4.

4.2.6.1. Virus capture using Sartobind® Q membrane

The Sartobind® Q nano 3 mL membrane (Sartorius, Germany) was used for the virus capture step. The membrane was prepared following the manual of the manufacturer. The flow rate was maintained at 5 mL/min unless otherwise described. The membrane was flushed with 15 CV buffer A to remove the storage buffer (20 %

ethanol in A) to restore the pH to 7.4, followed by 10 CV of 1 M NaCl solution and 10 CV of A. The membrane was equilibrated with 10 CV of VP-SFM media mixed with A in a 1:1 ratio. The clarified supernatant was passed through the, and the flow-through was collected in 5 mL fractions.

Initially, a purification experiment with a linear gradient elution was performed to find the efficacy of the Sartobind® Q membrane in the elution of rVSVs and other contaminants in different peaks. For this purpose, 25 mL of the clarified supernatant was injected into the membrane. The membrane was washed with 2 % B, and the elution was performed by a linear gradient of B from 5 to 100 % in 15 mL. The chromatography feed always consisted of clarified supernatant mixed with A in a 1:1 ratio except for the purification with a linear gradient of NaCl.

To find the proper salt concentration for the elution of rVSVs from the membrane, 50 mL of the load was injected into the membrane adsorber. The membrane was washed with 2 % B, and the elution was carried out using a multistep gradient consisting of 5, 10, 20, 30, 40, 50, 60, 70, 80, 90, and 100 % B. Once the optimal salt concentration for elution was determined, the recovery of rVSVs from the membrane was measured. Therefore, a volume of 50 mL of the load was passed through the membrane, the column was washed in two steps, using 2 % and 10 % B, and the viruses were desorbed from the membrane adsorber using 50 % B (1M NaCl). The column was regenerated using a 2 M NaCl solution.

4.2.6.2. Polishing using Capto™ Core 700

A 1 mL Capto™ Core 700 (Cytiva, USA) column was used to extend virus purification, removal of impurities and improve the quality of final product. The column was washed with 20 CV A and equilibrated with 15 CV 50 % B. All steps, excluding the sample injection, were performed at 1 mL/min. All of what had been collected from the elution of the Sartobind® Q column was injected into the column at 0.7 mL/min, and the flow-through was collected in 2 mL fractions. The column was then washed with A and regenerated using 1 M NaOH, 30 % isopropanol.

4.2.7. Diafiltration and buffer exchange

The salt contained in fractions collected out of the polishing column was diluted to 200 mM using buffer A. The sample was diafiltrated (10 X) against 20 mM Tris, 150 mM NaCl, 4 % sucrose, pH 7.4, using Microkros® TFUF module maintaining a shear rate of 2000 s^{-1} was maintained throughout the experiment.

4.2.8. Determination of dynamic binding capacity

To measure the dynamic binding capacity of the Sartobind® Q membrane for rVSVs, the virus-containing clarified supernatant was conditioned with 20 mM Tris buffer pH 7.4 with 4 % sucrose and passed through the membrane. The flow-through was collected in 10 mL fractions. The flow-through fractions were analyzed for the presence of VSV-N protein using a spot blot test.

4.2.9. Titration of infectious particles

Quantification of infectious particles was measured following the method reported in Gélinas et al., using the TCID50 assay [160,191] with HEK 293A cells. Briefly, 100 µL/well of HEK293 A cells were seeded in 96 well plates at 5E04 cells/mL density. Once the cells were 80% confluent, a serial dilution of virus samples was performed in another 96 well plate (round/U bottom). For this purpose, the plate was first filled with DMEM medium (200 µL/well), then, 50 µL/well of the sample were added to the first column of the plate and mixed with the medium. From this mixture, 50 µL was pipetted and emptied in the next column, mixed, and the process was repeated for all the following columns of the plate. A total volume of 20 µL of each row, using a multichannel pipette, was transferred to the HEK293A containing plate. Samples of every experiment were titrated the same day, having undergone the same number of freeze-thaw cycles (N = 8). The virus titer, expressed in FFU/mL (FFU: Focus-forming units), was calculated following the Spearman & Kärber algorithm using the excel sheet provided by the University of Heidelberg.

4.2.10. Quantification of total protein

The total protein concentration was determined using the Bradford method with the BioRad protein assay kit II (BioRad, Canada). The assay was performed following the manual's instructions in a 96 well plate. Briefly, a standard curve was generated

using the BSA standards supplied in the kit. A volume of 150 µL of each sample was added to the plate (N=3). To the sample, 150 µL of the dye reagent was added. The mixture was incubated for 30 min at room temperature. The absorbance was measured at 595 nm.

4.2.11. Host cell proteins

HCP quantification in the samples was carried out using the Vero Cell HCP ELISA kit (Cygnus Technologies, Southport, NC, USA), following the manufacturer's instructions. A volume of 50 µL of diluted samples (1:250) was added to the microtiter strips coated with goat anti-Vero polyclonal antibodies, supplied by the company,. An amount of 100 µL of the HRP conjugated affinity-purified goat anti-Vero antibody was added to the existing mixture in the wells. The mixture was incubated for 2 h at 580 rpm, 25 °C. The wells were rinsed with wash buffer 4 X. The tetramethylbenzidine (TMB) solution (100 µL) was added to the wells and incubated for 30 min, 25 °C. To stop the reaction, 100 mL of stop solution was added, and the absorbance was measured at 450/650 nm using Synergy HTX multi-mode reader (BioTek, Winooski, VT, USA). The Vero cell lysates were used as a positive control (supplied in the kit).

4.2.12. Measurement of DNA contents

The residual double-stranded DNA was quantified using Quant-iT™ Picogreen™ ds DNA assay kit (Life Technologies, Canada) following the manual's instructions. Briefly, the samples were diluted at 1:2, 1:10, and 1:20 in 20mM DNase-free Tris buffer (N=3). A volume of 100 µL of the Quant-iT™ Picogreen™ reagent was added to the samples. The mixture was incubated for 5 min. The fluorescence was measured at 520 nm. The calibration curve was obtained using Lambda DNA (supplemented in the kit) in concentrations ranging from 1 to 1000 ng/mL.

4.2.13. Electrophoresis and immunoblot

The samples were denatured using 2x Laemmli buffer (BioRad, Canada) and 5% 2-mercaptoethanol (ACROS Organics™, Canada), followed by heating, 95 °C, 5 min.

The protein profile of the sample was assessed by SDS-PAGE. For this purpose, 15 µL/lane of each sample was loaded into a Novex™ 4-12% Tris-Glycine Mini Gel

(Invitrogen™, Canada) and ran at 120 volts in 1x Tris/Glycine/SDS buffer for approximately 1 h. PageRuler™ unstained protein ladder (Thermofisher Scientific, Canada) was used as the molecular weight marker. The gel was stained using Thermo Scientific™ Pierce™ Color Silver Stain Kit (Thermo Scientific, Canada) following the manufacturer's instructions and imaged with ImageQuant LAS 4000 imager (Cytiva, Canada).

Western blot analysis was performed following the same protocol as the SDS-PAGE. The protein bands were transferred to Amersham™ Protran® Western blotting membranes (Cytiva, Canada) using a wet blotting system (BioRad, Canada) at 300 mA for 1 h at 4 °C. The membrane was blocked using 5 % milk, PBS, 0.1 % Tween (PBST) for 1 h at room temperature. The membrane was incubated with the VSV-M/VSV-N (Kerafast, USA) antibody diluted with the blocking buffer (1:1000) overnight at 4 °C. The next day, the membrane was washed 3 times for 5 min with PBST on a shaker. The horse radish peroxidase (HRP) bound rabbit anti-mouse (Abcam) in PBST (1:10000) was added to the membrane and incubated for 1 h at room temperature. The membrane was washed 3 times for 5 min with blocking buffer with shaking. The membrane was semi-dried and covered with 2 mL of Pierce™ ECL western blotting substrate (Thermo Scientific, Canada) and incubated for 1 min and revealed using ImageQuant™ LAS 4000 unit.

Spot blot analysis was performed using 2 µL of the sample placed on a nitrocellulose membrane. The membrane was air-dried for 30 min, blocked with PBST containing 5% milk for 1 h, hybridized with VSV-N/VSV-M antibody, incubated 1 h with rabbit anti-mouse HRP bound antibody in the blocking buffer, and incubated with Pierce™ ECL western blotting substrate for 1 min. Gels were observed using an ImageQuant™ LAS 4000 imager.

4.2.14. Particle size distribution

The size distribution of particles was examined using a Zetasizer Nano ZS, Malvern. Prior, the samples were diluted at 1:2 or 1:4 using 20 mM Tris, 4% sucrose.

4.2.15. Negative staining of rVSVs

The virus-containing suspension was fixed with 4% paraformaldehyde for 1 h at room temperature. They were adsorbed on 400 mesh nickel grids coated with formvar and carbon for 20 minutes. The grids were blotted with bibulous paper and stained with 2% PTA (phosphotungstic acid) for 30 seconds, blotted, and let dry for at least 2 hours. They were then observed with a Tecnai Spirit G2 (FEI, Netherlands) at 80 kV. 10-20 images were taken per sample. Before TEM pretreatment and analysis, the samples were desalted using Amicon 15 (Millipore, Canada).

4.3. Results and discussion

4.3.1. Production and clarification of supernatant prior to chromatography

In this work, we propose a two-step chromatographic process to purify rVSVs expressing HIV and Ebola glycoproteins. The rVSVs used in this work were produced in serum-free adherent Vero cells that were maintained in VP-SFM serum-free media. The cells were seeded at the density of 3.5×10^6 cells in 175 cm^2 T-flasks in 30 mL of culture media. Once the cells reached 80 % or more confluency, they were infected with the rVSV stock with the multiplicity of infection (MOI) by 0.001 and incubated at 34 °C until a CPE of higher than 80 % was observed in about 72 hpi. The cell culture supernatant was collected and treated with Benzonase® immediately after harvest for two hours to eliminate contaminant nucleic acids. This step had no negative effect on the recovery of infectious particles. However, in a few experiments it resulted in a minor increase in the total number of infective viruses, which could be due to the release of virus-DNA aggregates after DNA digestion and the release of entrapped viruses from the aggregates. This nuclease treatment resulted in removing 73% of the contaminant DNA as measured by picogreen™ dsDNA assay (Data not shown), giving a final concentration of 380 ng/mL.

The supernatant was then clarified in a two-step, firstly, with low-speed centrifugation at 3500 g to remove cellular debris, then microfiltration using a 1.2 µm polypropylene filter. At the end of the clarification step, 78 ± 6 % of infective particles were recovered at 1.95E+08 TCID50/mL. The clarified supernatant was aliquoted and stored at -80 °C until further.

4.3.2. Stability of rVSV

The stability of rVSVs in high salt concentrations was tested before chromatography purifications. As presented in Fig. 14. rVSVs showed acceptable stability at 4 °C (18 % infectivity loss over 30 h) without salt. However, in the presence of 1 M NaCl, at 4 °C, the reduction in the number of infective particles starts from 6 hours of incubation (hpi) with a loss of 12 % and extends to 41 % at 30 hpi. Storage of rVSVs in no salt at room temperature caused a 12 % reduction in the number of the infective particles followed by a more distinctive effect after 14 hpi resulting in the 27 % loss of infective particles. However, in the presence of 1 M NaCl, at 23 °C, the viruses were stable for up to 2 hours. Incubation of viruses in 1 M NaCl at 23 °C for more than 6 hours reduced the number of infective particles by more than 70 %. These results confirm the stability of rVSV at 10 mM Tris, 150 mM NaCl, pH 7.4, 0 M NaCl up to 30 hours at 4 °C with the recovery of 82 % infective particles, and 6 hours at 23 °C with 88 % of infective particles at the end of incubation. However, longer incubations at room temperature can negatively impact the concentration of infective viruses. The stability of rVSVs in 1 M NaCl for incubating longer than 6 hours was better at 4 °C. Given the critical loss of infectivity of rVSVs in 1 M NaCl, both at 4 °C and at room temperature, the dialysis of chromatography products must be performed rapidly to lower the concentration of salt in preparations before storage (at 4 °C) or further purification steps.

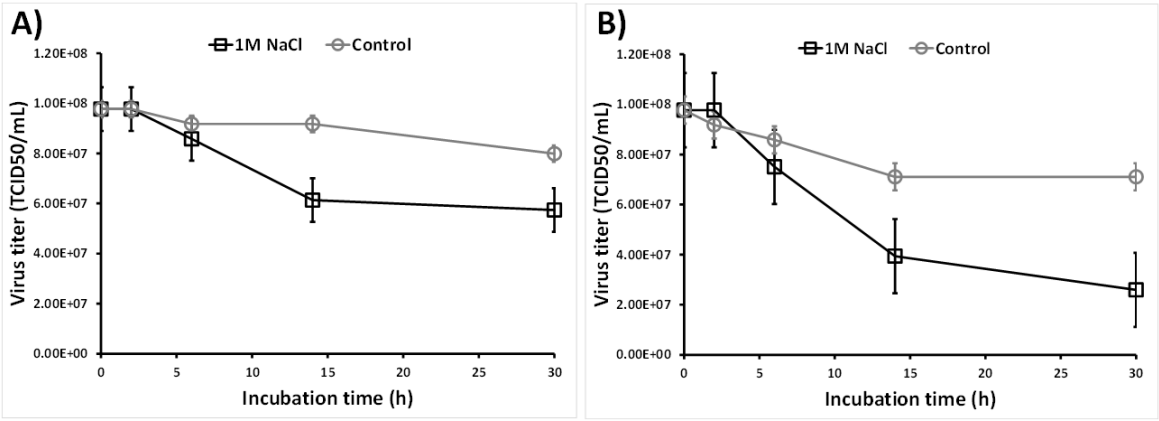

Fig 14. Recovery of infective rVSV particles after incubation with buffer A/no NaCl and 1 M NaCl in buffer A at A) 4 °C and B) 23 °C over 30 hours. The virus titer was measured by TCID50 assay (N = 3).

4.3.3. Chromatographic purification

The purification of rVSVs was performed in a two-step chromatographic process comprising a bind and elute step using an anion exchange membrane (Sartobind® Q) and a multimodal column (Capto™core 700). At first, to see the column's ability in the separation of rVSVs from cell culture contaminants, a total volume of 25 mL clarified supernatant was passed through the column. The column was washed, and the elution was performed using a linear gradient from 5 % to 100% B (100 mM to 2 M NaCl) (Fig. 15). The elution using a gradient of NaCl did not result in any distinct separation of rVSVs and HCPs, and they were all eluted in a single peak where the elution of rVSVs was detected in fractions 7 to 12. Therefore, to better separate the HCPs from rVSVs, a purification using a step gradient was performed.

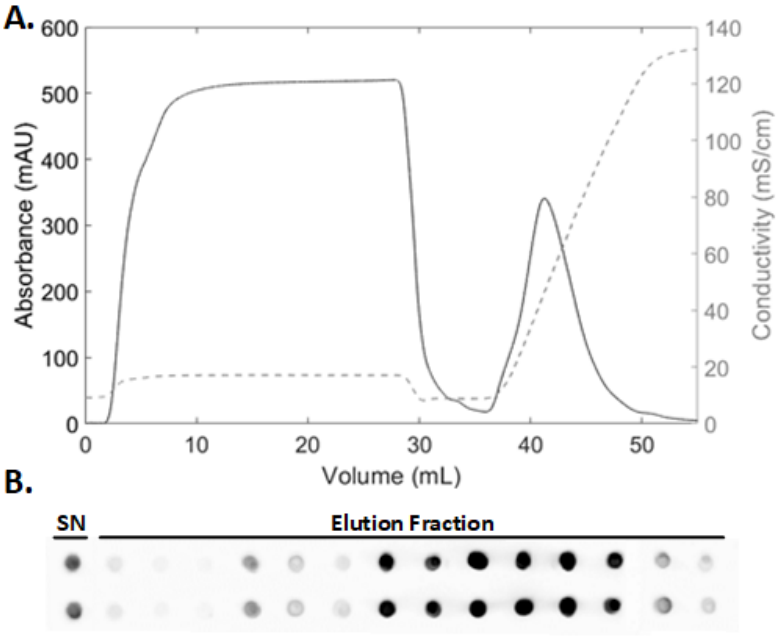

Fig 15. Purification of rVSV using Sartobind® Q column. A) Chromatogram of rVSV purification using a linear gradient of NaCl from 5 to 100 % corresponding to 100 to 2000 mM of NaCl. B) Spot blot analysis of the elution fractions. Anti VSV-N antibody was used for immunoblot analysis.

It was also found (data not shown) that mixing the chromatography feed with Buffer A in 1:1 results in more rVSV binding to the column. Therefore, the clarified supernatant was conditioned with 20 mM Tris buffer, pH 7.4 in 1:1 ratio. To find the proper salt concentration for elution of rVSVs from the Sartobind® Q column, 50 mL

of the conditioned supernatant was passed through the column. The elution was carried by step gradient using 5, 10, 20, 30, 40, 50, 60, 70, 80, 90, and 100 % B (Fig. 16 panel A). The fractions were analyzed using spot blot for detection of VSV-N protein.

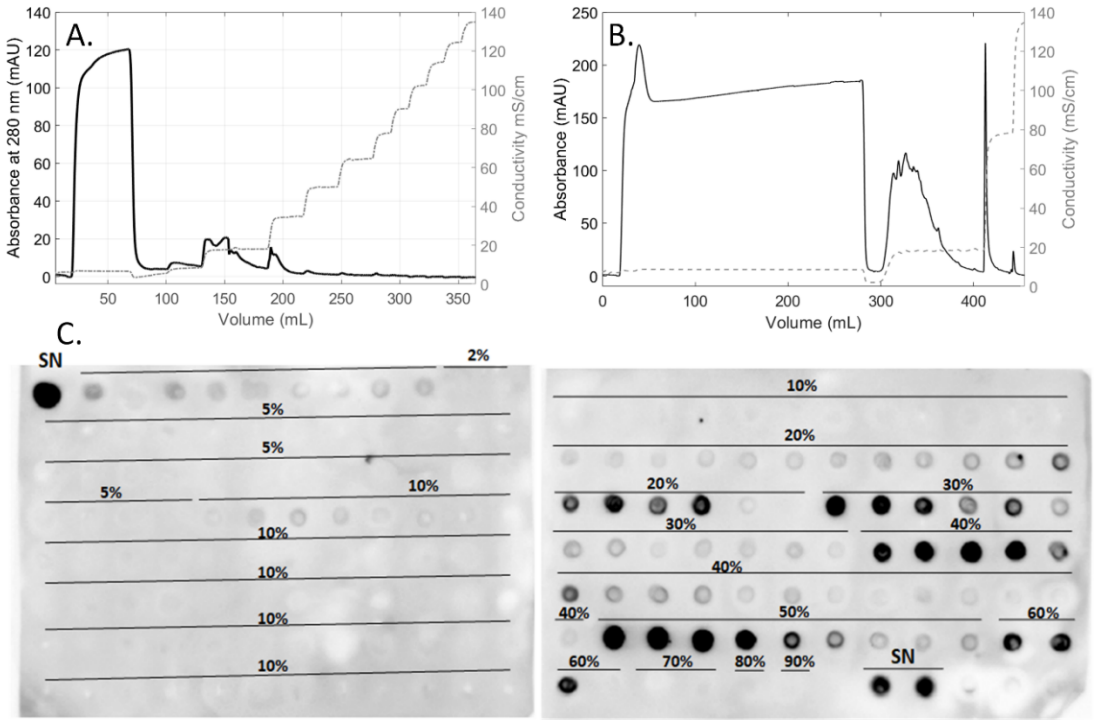

Fig 16. Determination of A) optimal salt concentration for elution of rVSVs from Sartobind® Q column using a step gradient from 5 to 100 % B (2 M NaCl), B) dynamic binding capacity of Sartobind® Q membrane for rVSVs. C) Spot blot analysis of fractions collected during experiment A using anti-VSV-N antibody.

As shown in Fig. 16 panel C, the dissociation of viruses from the Sartobind® Q membrane started from 20 % B corresponding to 400 mM NaCl and continued until 60 % B equivalent to 1.2 M NaCl. The results from titration of the virus-containing fractions from each salt concentration are presented in Table 13. The highest concentration of infective particles was eluted at 30 % B (600 mM NaCl) followed by 50 % B (1 M NaCl), 40 % B (800 mM NaCl), 20 % B (400 mM NaCl) and 60 % B (1.2 M NaCl). Despite the strong signals in spot blot analysis of 60 % B fractions, the number of infective particles in these fractions was very low, and hence they were

excluded from future experiments. The Overall recovery of infectious particles was found as 63 % as measured by TCID50.

Furthermore, to assess the dynamic binding capacity of Sartobind® Q membrane for rVSVs, we aimed to pass 300 mL of supernatant conditioned with buffer A in 1:1 dilution (corresponding to 150 mL of supernatant) through the Sartobind® Q column (fig. 16 panel B). The flow-through was collected every 10 mL for further analysis by spot blot for the presence of VSV-N protein. However, due to the column's high backpressure (≥ 0.4 Mpa) at about 260 mL of the load, no more supernatant was passed through, and therefore 260 mL of the feed corresponding to 130 mL of the supernatant was set as the column capacity due to the limit of operation.

Table 13. Recovery of rVSVs from Sartobind® Q membrane (step elution using 2 M NaCl).

	Sample	VSV-N positive fractions (mL)	Titer (TCID50/mL)	Total virus (TCID50)
	Load	50	4.37E+07	2.18E+09
	5	0	-	-
	10	0	-	-
	20	5	5.33E+07	2.66E+08
	30	5	7.99E+07	3.99E+08
	40	6	5.34E+07	3.20E+08
Elution	50	6	6.53E+07	3.92E+08
	60	3	6.92E+04	2.08E+05
	70	0	-	-
	80	0	-	-
	90	0	-	-
	100	0	-	-
	Recovery (%)		63%	

Previous reports on the capacity of the Sartobind® Q column for large- and small-scale purification of non-enveloped viruses highlight the impact of DNA concentration of the feed on the column DBC and pressure rise throughout the

process [194]. However, the feed used in this experiment was previously treated with endonuclease. The spot blot analysis of these flow-through fractions showed no VSV-N proteins, confirming a dynamic binding capacity of 5.68E+09 TCID50 per 3 mL or 110 cm^2 of Sartobind® Q membrane for rVSVs produced in VP-SFM media (With 4.37E+07 TCID50/mL rVSVs in the load). The DBC of the Q membrane for rVSVs used in this experiment was higher than the DBC of 9.30E+08 TCID50 of modified vaccinia Ankara Virus for 75 cm^2 or 2.1 mL of Sartobind® Q [187]. The binding capacity determined in this work was based on the column limitation in the continuation of the process due to pressure build-up and not based on the column capacity for rVSV binding. This could justify the lower DBC of the membrane for rVSV compared to the value of 6.9E+09 PFU of VSV/mL reported by Kang *et al*. [195].

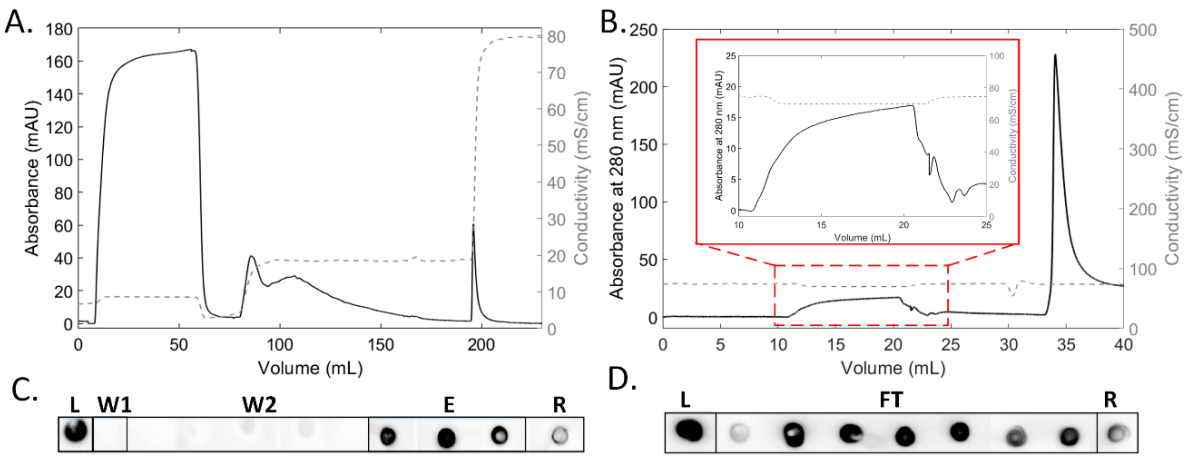

Fig 17. Chromatograms of rVSV purification using A) Sartobind® Q column with a single step elution by 1M NaCl (50% B) followed by a flow-through chromatography using B) Capto™ Core 700 column for further removal of DNA contents. C) and D) The chromatography fractions were analyzed by dot blot using an Anti-VSV-M antibody. (L) Chromatography load, (W1) first wash using 2% B, (W2) second column wash using 10 % B, (E) Elution using 50 % B, (R) column regeneration using 100 % B/ 2M NaCl for Sartobind® Q and 1M NaOH, 30 % isopropanol for Capto™ Core 700 , (FT) Flow-through.

Then, to find the recovery of infectious units eluted in a single step from Sartobind® Q 3 mL membrane, 50 mL of the load was passed through the column (Fig. 17 panel A and C). The column was washed in two steps using 1 % B followed by 10 % B corresponding to 200 mM NaCl to eliminate the HCPs from the column. The bound

rVSVs were then desorbed using 50 % B (1 M NaCl). Table 14. Presents the quality control assays of the fractions obtained at this step. This purification step resulted in the recovery of 66 ± 12 % infective particles from the feed and elimination of 88 % total proteins and 92% HCPs. The protein profile of the eluate versus the load is presented in Fig. 17 panel A. The DNA contents were reduced by 89 % in the elution peak; however, the quantity of dsDNA in the virus-containing fraction was beyond the recommendations of FDA (10 ng/dose), as presented in Table 14. The recovery of rVSVs from the Sartobind® Q column was close to the value of 68 % for Flavivirus VLP with 99.8 to 99.9 % elimination of DNA contents [196].

Therefore, the capture step was followed by a multi-modal column, Capto™ Core 700, to be used in the flow-through mode (Fig. 17 panel B and C). The Capto™ Core 700 column was equilibrated with 1 M NaCl before sample injection. The eluate from the Sartobind® Q purification was loaded into the column, followed by collection of the flow-through. The flow-through was collected in 2 mL fractions. The flow-through salt concentration was immediately adjusted to 200 mM NaCl using 20 mM Tris, pH 7.4, 4 % sucrose. The sample was diafiltrated (10 X) against 20 mM Tris, 150 mM NaCl, 4 % sucrose, pH 7.4, using Microkros® TFUF module maintaining a shear rate of 2000 s^{-1} throughout the experiment.

The application of the flow-through chromatography step resulted in the further elimination of 20 % of total proteins and 42 % of HCPs while recovering 78 ± 6 % of the infectious particles. The DNA contents were reduced notably to 14 ng/mL, slightly higher than the FDA limits but lowered by an additional 10 % from the AEX step. However, DNA concentration was lowered in the final preparations after diafiltration, measured as 8 ng/mL by Picogreen™ assay (Table 14). The final diafiltration step further removed proteins that were co-eluted with rVSVs in the capture step and were not removed through flow-through chromatography. The TFUF step did not influence the recovery of infective particles. However, we had previously found that achieving higher concentration factors affect the virus recovery negatively. The diafiltration brought down the level of HCPs from 12,726 ng/mL to 3,109 ng/mL (Table 14)

Table 14. The control assays for chromatography purified rVSVs.

Step	Vol (mL)	Virus titer			Total protein		HCP content		DNA content	
		TCID50/mL	Step RCV (%)	Global RCV (%)	Total protein (μg /mL)	Protein RMV (%)	HCP (ng/mL)	HCP RMV (%)	DNA (ng/mL)	DNA RMV (%)
AEX load	50	9.77E+07	100	100	281	-	72,515	0	164	0
AEX FT	50	8.36E+02	0	0	147	47.7	34,613	52	29	82
AEX Wash	85	1.02E+03	0	0	62	62.5	14,509	65.9	43	55
AEX Elution	12	2.68E+08	66 ± 12	66	137	88.3	25,614	91.5	72	89
Captocore700 FT	14	1.79E+08	78 ± 6	51	93	20.8	12,726	42	14	77
TFF Retentate	17	1.46E+08	99	51	42	54.8	3,109	70.3	8	30

Vol: Volume, HCP: host cell proteins, AEX: Anion-exchange chromatography, FT: flow-through, RMV: removal, RCV: recovery.

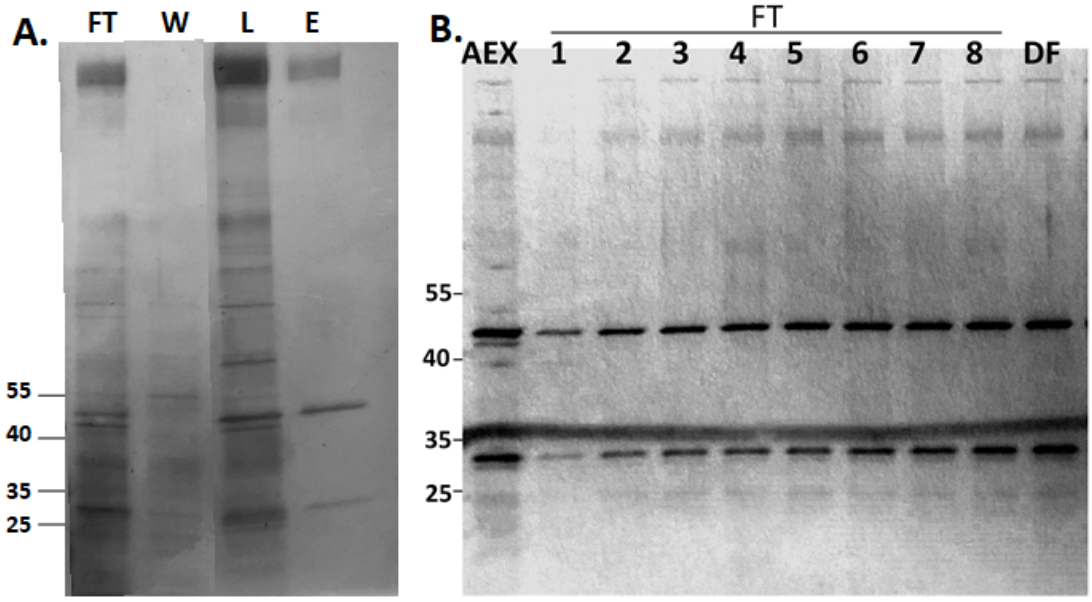

Fig 18. A) Silver stained SDS-PAGE analysis of the protein profile of the elution fraction from Sartobind® Q column versus the clarified supernatant (Load) in comparison to flow-through and column wash using 10 % B. (FT) Flow-through, (W) Wash using 10 % B/ 200 mM NaCl, (L) clarified supernatant/load, (E) elution using 50 % B/1 M NaCl from Sartobind® Q column. The staining was performed using Coomassie orange staining. B) The protein profile of the elution peak from Sartobind® Q (AEX) besides the flow-through fractions obtained from Capto™ Core 700 and final diafiltration (DF) using Microkros® TFUF cartridge.

The application of the flow-through chromatography step resulted in the further elimination of 20 % of total proteins and 42 % of HCPs while recovering 78 ± 6 % of the infectious particles. The DNA contents were reduced notably to 14 ng/mL, slightly higher than the FDA limits but lowered by an additional 10 % from the AEX step. However, DNA concentration was lowered in the final preparations after diafiltration, measured as 8 ng/mL by Picogreen™ assay (Table 14). The final diafiltration step further removed proteins that were co-eluted with rVSVs in the capture step and were not removed through flow-through chromatography. The TFUF step did not influence the recovery of infective particles. However, we had previously found that achieving higher concentration factors affect the virus recovery negatively. The

diafiltration brought down the level of HCPs from 12,726 ng/mL to 3,109 ng/mL (Table 14).

The protein profile of the fractions from AEX, Capto™ Core 700, and diafiltration steps is presented in Fig. 18. The visualization of the intensity of rVSV protein bands, including the VSV-N protein with MW of 47 kDa and VSV-N protein of 47 kDa in the elution fraction versus the background, is an indication of the purification efficacy in the eluate fraction of AEX compared to the clarified supernatant (Fig. 18 panel A). Further elimination of proteins and sharpening of the VSV protein bands can also be seen in the flow-through fractions obtained from Capto™ Core 700 column and diafiltration step (Fig. 18 panel B), indicating elimination of more contaminant proteins in this step.

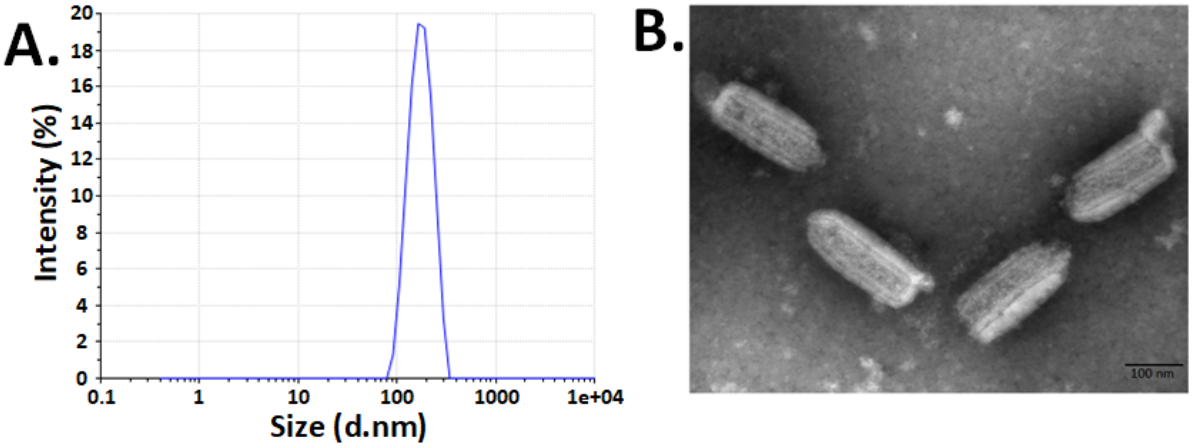

Fig 19. Confirmation of purified rVSV size and shape through A) dynamic light scattering (DLS) and B) transmission electron microscopy (TEM).

Furthermore, the final rVSV preparations' quality was confirmed by characterization of the size and shape of the virus (Fig. 19). The DLS analysis of the purified rVSV preparations showed an average particle diameter of 219.7 nm (Fig. 19 panel A) that was on par with the VSV size previously reported [197,198]. Moreover, the TEM analysis (Fig. 19 panel B) confirmed the bullet shape of the VSVs and their dimension in accordance with the results of Howatson & Whitmore [199]. Overall, the proposed purification scheme removed more than 95 % of contaminant DNA and 95 % of the HCP with the recovery of 51 % infective rVSVs.

4.4. Conclusion

In the current work, a two-step chromatographic purification scheme has been proposed for an rVSV based HIV vaccine candidate. In this approach, the rVSV containing clarified supernatant is passed through an initial AEX membrane chromatography using Sartobind® Q to capture and separate the viruses from the other contaminants. Introduction of AEX resulted in removing 89 % DNA contents and 91.5 % of the HCPs with the recovery of 66 ± 12 % of the rVSVs. A flow-through chromatographic purification was added to reduce the DNA contents further using the Capto™ Core 700 column. This step effectively lowered the quantity of residual DNA from 72 ng/mL to 14 ng/mL while recovering 78 ± 6% of infective particles. The virus-containing flow-through was immediately diluted to minimize high salt concentration's adverse effects on virus infectivity. The final buffer exchange and diafiltration were performed using Microkros® TFUF cartridge, leading to more DNA reduction and bringing the contents to a value accepted by regulatory authorities (< 10 ng/dose).

The proposed purification scheme can be used both for laboratory-scale purification of rVSVs and at pilot scale based on the size of the Sartobind® Q column selected. The possibility of running the process at a higher flow rate when using membrane chromatography makes it suitable for processing larger volumes at a lower process time. The current protocol results in highly pure rVSVs by removing 95 % of DNA contents and 85 % of total proteins. This highly pure preparation of rVSV can also be used in studies where the biochemical or physical properties of VSV are investigated.

Declaration of competing interest

The authors declare that they have no known competing financial interests or personal relationships that could have influenced the work reported in this paper.

Acknowledgment

The authors thank the bio-imaging platform of the Infectious Disease Research Centre, CRCHU de Québec, for performing electron microscopy. We would also like

to thank the Natural Sciences and Engineering Research Council (NSERC) and the Canadian Institute of Health Research (CIHR) for financing this project.

Chapter 5: Purification of recombinant vesicular stomatitis virus based HIV vaccine candidates using ceramic hydroxyapatite

Anahita Bakhshizadeh Gashti [a], Parminder S. Chahal [b], Bruno Gaillet [a], Alain Garnier [a*]

[a] Department of Chemical engineering, Faculty of Sciences and Engineering, Université Laval, Quebec, QC, Canada

[b] Human Health Therapeutics, National Research Council Canada, Montreal, QC, Canada

*Corresponding author: alain.garnier@gch.ulaval.ca

Manuscript

Résumé

Ce travail décrit la purification du virus de la stomatite vésiculeuse recombinant (rVSV), exprimant les glycoprotéines d'Ebola et du VIH à sa surface, par le biais d'une chromatographie à mode mixte d'échange anionique/cationique basé sur l'utilisation de l'hydroxyapatite. Par ailleurs, une amélioration de l'étape de clarification a également été testée en remplaçant la centrifugation à basse vitesse par un module de microfiltration séquentielle, mieux adaptée aux procédés à grande échelle. Cette approche a abouti à la récupération de 83,5% de particules infectieuses, inférieure à celle obtenue à partir d'une méthode de clarification en deux étapes (centrifugation basse vitesse suivie d'une microfiltration) mais plus adaptée aux procédés à plus grande échelle. Deux résines céramiques d'hydroxyapatite (CHT) ont été criblées pour leur capacité à récupérer les particules infectieuses. Les rVSV purifiés élués des colonnes CHT ont été analysés pour leur pureté en termes de teneur en ADN et en protéines contaminants et leur morphologie en utilisant la microscopie électronique à transmission (MET). L'analyse des fractions d'éluat contenant le rVSV de la colonne CHT II a révélé une quantité inférieure à 10 ng/dose qui représentait 2,8 % du contenu d'ADN résiduel de l'alimentation. Les teneurs en protéines ont été considérablement réduites de 28,5 fois par rapport à l'alimentation. De plus, l'observation par MET des préparations virales purifiées avec la colonne CHT II a montré un nombre inférieur de vésicules extracellulaires contaminantes par rapport à l'alimentation.

Abstract

This work describes a purification process for the recombinant vesicular stomatitis virus (rVSV) expressing Ebola and HIV glycoproteins based on weak anion/cation exchange mixed-mode chromatography using hydroxyapatite. Moreover, an improvement for the clarification step was tested by replacing low-speed centrifugation with sequential microfiltration that is scalable and better suited for large-scale processes. This approach resulted in the recovery of 83.5 % of infectious particles, lower than that obtained from the two-step clarification method but more suitable for larger-scale processes. Two ceramic hydroxyapatite (CHT) resins were screened for their ability to recover the infectious particles. The purified rVSVs eluted from the CHT columns were analyzed for their purity in terms of contaminant DNA and protein contents and their morphology using transmission electron microscopy (TEM). The analysis of DNA contents in the rVSV containing eluate fractions from the CHT II column revealed an amount lower than 10 ng/dose that accounted for 2.8 % of residual DNA contents in the column feed. The protein contents were reduced substantially by 28.5 folds compared to the feed. Moreover, the visual observation of the purified virus preparations and comparing it to the feed, showed a lower number of contaminant extracellular vesicles in the rVSV containing CHT II eluate fractions.

Keywords: VSV, Ceramic hydroxyapatite, chromatographic purification, HIV vaccine

5.1. Introduction

Ceramic hydroxyapatite (CHT) is formed by the hardening of the hydroxyapatite (HA) crystals, an inorganic mineral from phosphate and calcium, at high temperatures to a ceramic form. In general, the HA crystals carry both the positively charged calcium ions and the negatively charged phosphate groups along with hydroxyl groups on their surface. The interaction mechanism of HA with external molecules is not yet clear. However, it is believed to interact with them either through 1) Ca+ ions, either due to an affinity to calcium or weak anion exchange, 2) negatively charged phosphate groups by cation exchange, and less likely, due to 3) the hydrogen bonding with hydroxyl groups or 4) a combination of these bindings.

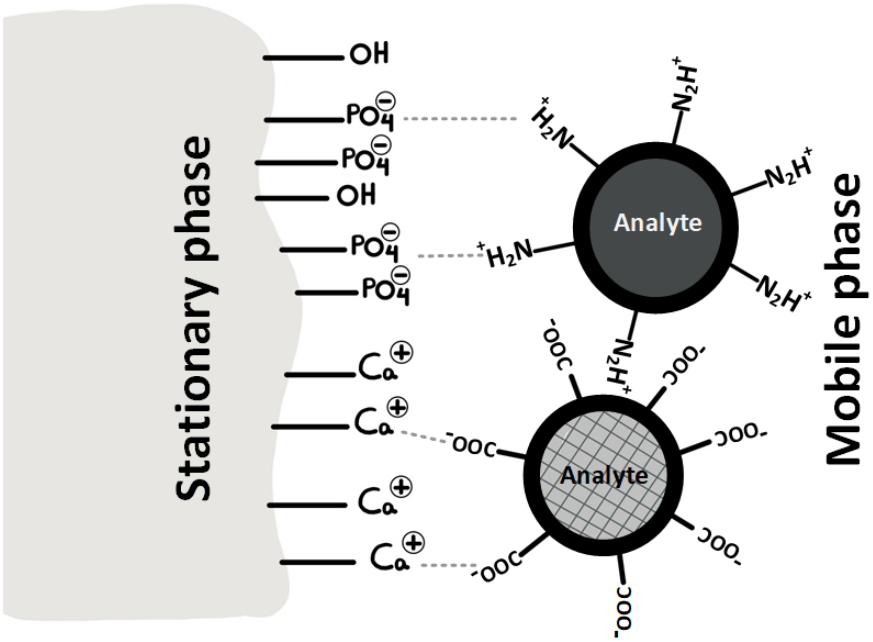

Fig 20. The working principle of the ceramic hydroxyapatite resin.

Once in contact with a charged molecule, the carboxyl groups (COOH) carrying the negative charges on the acidic proteins are attracted to the calcium ions on the HA resin through electrostatic interactions (Fig. 20). It has also been explained by Kawasaki [200] that the phosphoryl groups of the proteins have a stronger interaction with the calcium ions on HA in comparison to the carboxyl groups. However, the positively charged amino groups (NH_2) on the surface of the proteins are attracted to the phosphate groups on the HA [121,201–203]. This interaction is initiated

through electrostatic interactions that later result in the formation of solid coordination bonds.

HA resins are proposed by several manufacturers, including Bio-Rad laboratories (CHT I, CHT II, Bio-Gel HT, Bio-Gel HTP), Sartorius (HA Ultrogel), Pall Corporation (HA Ultrogel), Sigma Aldrich (Hydroxyapatite type I), Repligen (Calcium hydroxyapatite) and Clarkson chromatography (hydroxyapatite). However, the most commonly used CHT resin for the purification of biomolecules is manufactured by Bio-Rad and offered in two types: CHT type I (CHT I) and CHT type II (CHT II). Based on the Bio-Rad claims, the CHT I resin generally shows a higher binding capacity for proteins than CHT II, while CHT II offers a higher resolution for nucleic acids.

The use of HA to purify biomolecules was first introduced by Tiselius et al. [204] in 1956. Since then, there have been several reports on the purification of proteins [205], antibodies [206,207], enzymes [208–211], bacteriophages [212], nucleic acids [213,214], viruses [31,215–217], and virus-like particles (VLPs) [218–221] using HA. Moreover, Aizawa et al. [222] reported the capability of HA chromatography to distinguish the native and denatured forms of human lysozymes. In addition to this feature, HA chromatography has been remarked to separate protein aggregates from monomers [223,224].

Extracellular vesicles (EV) and exosomes are the main contaminants in the production of enveloped viruses and yet,their separation from viruses remains a challenge, as they share many physicochemical properties. In this work, we compare the CHT type I and CHT type II resins from Bio-Rad for their capabilities to purify a human immunodeficiency virus (HIV) vaccine candidate based on the recombinant vesicular stomatitis virus (rVSV) from the cell culture contaminants. The rVSV used here carries the whole VSV genome except for the gene encoding for the VSV glycoprotein being replaced by the genes encoding for HIV glycoprotein (HIV-gp) and Ebola glycoprotein (Ebola-gp). This rVSV variant is produced in serum-free adherent Vero cells. We have previously developed laboratory-scale and large-scale purification schemes for DSP of the rVSV using ultracentrifugation and anion exchange chromatography with resin or membrane-based columns. However, when

observed under transmission electron microscopy (TEM), the purified virus preparations were still contaminated by microvesicles that morphologically resembled EVs and exosomes. Therefore, we will initially test the CHT column's ability to recover infectious particles and then assess their ability to remove the EVs or exosomes through TEM analysis.

5.2. Materials and Methods

5.2.1. Cell line and chemicals

All chemicals were of analytical grade, if not otherwise stated: sodium chloride (NaCl) (ACROS Organics, Canada), Tris buffer powder (Invitrogen, Canada), Tween-20 (Fisher Bioreagents, Canada), sodium hydroxide (NaOH) (Millipore Sigma, Canada), 1 M $MgCl_2$ (ThermoFisher Scientific, Canada), sucrose (Bioshop, Canada).

VP-SFM medium (ThermoFisher Scientific, Canada), 200 mM L-glutamine (Wisent Bio Products, Canada), Dulbecco′s Modified Eagle′s Medium (DMEM, Corning, Canada), 1X TrypLE™ Select enzyme (Thermo Fisher Scientific, Canada), Fetal Bovine Serum (FBS, Wisent, St-Bruno, QC, Canada), Benzonase® (Millipore Sigma, Canada), 1 M $MgCl_2$ (ThermoFisher Scientific, Canada), sucrose (Bioshop, Canada). Serum-free adherent Vero cell line (CCL-81.5) was a generous gift from Dr. A. Kamen laboratory (McGill, Montreal), and HEK 293A cells were obtained from Dr. R. Gilbert laboratory (NRC-Montréal).

5.2.2. Cell maintenance and virus production

Vero cells used for virus production were maintained in serum-free VP-SFM medium, supplemented with 4mM L-glutamine, without antibiotics at 37 °C and 5 % CO_2 in a humidified incubator, and passaged twice weekly. Cells were detached using 1X TrypLE™ Select enzyme, centrifuged at 400 g, 5 min, resuspended in fresh medium, and seeded at 1.5 × 10^5 cells/mL in 100 mm cell culture dish holding 12 mL of medium.

HEK 293A cells used for virus titration were maintained in Dulbecco′s Modified Eagle′s Media supplemented with 2 mM L-glutamine and 5 % FBS, without antibiotics at 5 % CO_2 and 37 °C in a humidified incubator. The cells were passaged

twice a week using the 1X TrypLE™ Select enzyme. They were pelleted at 400 g, 5 min, resuspended in fresh medium, and seeded at 1.5 × 10^5 cells/mL in a 100 mm cell culture dish holding 12 mL of medium.

Recombinant VSVs were produced following the protocol described previously [159]. Briefly, to produce 1 L of virus-containing supernatant, the cells were seeded in 175 cm^2 culture plates (35 plates) at the initial density of 3 × 10^6 cells per plate in 25 ml of medium, incubated at 37 °C, and 5 % CO_2. When 80 % confluent, the cells were infected with the rVSV stock at a multiplicity of infection (MOI) of 0.001, and incubated at 34 °C, 5 % CO_2 for 72 h.

5.2.3. Chromatography feed preparation

The supernatant was primarily treated with 10 units/mL of Benzonase® (Millipore Sigma, Canada) and 2 mM $MgCl_2$, 2 h, 37 °C. The bottle was gently shaken every 30 minutes to ensure the uniform distribution of the endonuclease. The supernatant was clarified by sequential filtration using Sartopure PP3 filters (Sartorius, Canada) with decreasing pore sizes of 20 µm, 1.2 µm, and 0.6 µm, respectively. The filters were pre-equilibrated with 20 mM Tris pH 7.4 and cell culture medium. The filtration steps were performed at 200 L/m^2/h (LMH).

The clarified supernatant was then concentrated and partially purified by tangential flow ultrafiltration (TFUF) using a Midikros® 750 kDa hollow fiber TFUF system (Spectrum Laboratories, Rancho Domingez, CA, USA). All the virus concentrates except the one used to optimize the elution were diafiltrated using the same TFUF unit against 100 mL of 20 mM Tris, 4 % sucrose, pH 7.4. The cartridge was sanitized with 0.5 M NaOH for 2 h at room temperature, washed with distilled water (0.2 µm filtered), PBS, and pre-equilibrated with the culture medium. Throughout the process, the flow rate was maintained at 53 mL/min with a transmembrane flux rate of 25 LMH and a transmembrane pressure difference (TMP) of 0.1 bar (shear rate of 2000 s^{-1}). The concentrated virus preparation was aliquoted and preserved at -80 °C until further use.

5.2.4. Chromatography purification

Chromatography purifications were performed using an ÄKTA start chromatography system (GE Healthcare, Canada) operated with the UNICORN start 1.0 software and equipped with 280 nm absorbance and conductivity sensors. The buffers consisted of 20 mM Tris with 5 mM $NaPO_4$, 4 % sucrose, pH 7.5 (Buffer A), and 1 M $NaPO_4$, 4 % sucrose, pH 7.5 (Buffer B). A flow rate of 2.0 mL/min was maintained throughout the process unless otherwise stated. The column was equilibrated with 15 column volume (CV) of 50:50 A: B buffers, followed by 15 CV of 100 % A.
The 5 mL Bio-scale™ mini CHT type I cartridge and Bio-scale™ mini CHT Type II cartridge (Bio-Rad, Canada) with a particle size of 40 µm were tested for their ability in purification of rVSVs. The batch mode purification was first carried out using free resins. Different quantities of diluted virus preparation (1:1 in buffer A, thereafter named "feed"), including 1, 2, and 5 mL were added to microcentrifuge tubes containing 750 µg of either CHT I or CHT II resins (mixed in 1:1 with A). The mixture was incubated at room temperature for two hours, centrifuged to separate the unbound material. It was then followed by a wash step using 5 mM $NaPO_4$ and elution using 50:50 buffers A: B.

For the column chromatography, the concentrated and equilibrated virus preparation (1:1, virus preparation: buffer A) was passed through the column at 1 mL/min (contact time of 5 min). The column was washed with 5 CV of 0.5 % buffer B in A. The elution phase consisted in a series of step increase of B to find the suitable concentration of $NaPO_4$ for the elution of rVSVs, including 50, 100, 200, 300, 400, 500, 600, 700, 800, 900, and 1000 mM $NaPO_4$ (Buffer B). The column was regenerated using 10 mL of 1 M NaOH and stored in 0.1 M NaOH. The virus-containing fractions were titrated using the TCID50 method to measure the virus infectivity and recovery.

The dynamic binding capacity (DBC) was determined by passing the 350 mL of the feed through the column. The flow-through was collected in 15 mL fractions and analyzed for the presence of VSV-N or VSV-M protein using a spot blot test.

5.2.5. Infective viral particle titer

Quantification of infectious particles was measured following the method reported in Gélinas et al., using the TCID50 assay [160,191] with HEK 293A cells. Briefly, 100 µL/well of HEK293 A cells were seeded in 96 well plates at 5E04 cells/mL density. Once the cells were 80% confluent, a serial dilution of virus samples was performed in another 96 well plate (round/U bottom). For this purpose, the plate was first filled with DMEM medium (200 µL/well), then, 50 µL/well of the sample were added to the first column of the plate and mixed with the medium. From this mixture, 50 µL was pipetted and emptied in the next column, mixed, and the process was repeated for all the following columns of the plate. A total volume of 20 µL of each row, using a multichannel pipette, was transferred to the HEK293A containing plate. Samples of every experiment were titrated the same day, having undergone the same number of freeze-thaw cycles (N = 8). The virus titer, expressed in FFU/mL (FFU: Focus-forming units), was calculated following the Spearman & Kärber algorithm using the excel sheet provided by the University of Heidelberg.

5.2.6. Total protein

The total protein concentration was determined using the Bradford method with the BioRad protein assay kit II (BioRad, Canada). The assay was performed following the manual's instructions in a 96 well plate. Briefly, a standard curve was generated using the BSA standards supplied in the kit. A volume of 150 µL of each sample was added to the plate (N=3). To the sample, 150 µL of the dye reagent was added. The mixture was incubated for 30 min at room temperature. The absorbance was measured at 595 nm.

5.2.7. DNA content

The residual double-stranded DNA was quantified using Quant-iT™ Picogreen™ ds DNA assay kit (Life Technologies, Canada) following the manual's instructions. Briefly, the samples were diluted at 1:2, 1:10, and 1:20 in 20mM DNase-free Tris buffer (N=3). A volume of 100 µL of the Quant-iT™ Picogreen™ reagent was added to the samples. The mixture was incubated for 5 min. The fluorescence was

measured at 520 nm. The calibration curve was obtained using Lambda DNA (supplemented in the kit) in concentrations ranging from 1 to 1000 ng/mL.

5.2.8. Dynamic light scattering (DLS)

The size distribution of particles was examined using a Zetasizer Nano ZS, Malvern. Prior, the samples were diluted at 1:2 or 1:4 using 20 mM Tris, 4% sucrose.

5.2.9. Electrophoresis and immunoblot assays

The samples were denatured using 2x Laemmli buffer (BioRad, Canada) and 5% 2-mercaptoethanol (ACROS Organics™, Canada), followed by heating, 95 °C, 5 min.

The protein profile of the sample was assessed by SDS-PAGE. For this purpose, 15 µL/lane of each sample was loaded into a Novex™ 4-12% Tris-Glycine Mini Gel (Invitrogen™, Canada) and ran at 120 volts in 1x Tris/Glycine/SDS buffer for approximately 1 h. PageRuler™ unstained protein ladder (Thermofisher Scientific, Canada) was used as the molecular weight marker. The gel was stained using Thermo Scientific™ Pierce™ Color Silver Stain Kit (Thermo Scientific, Canada) following the manufacturer's instructions and imaged with ImageQuant LAS 4000 imager (Cytiva, Canada).

Western blot analysis was performed following the same protocol as the SDS-PAGE. The protein bands were transferred to Amersham™ Protran® Western blotting membranes (Cytiva, Canada) using a wet blotting system (BioRad, Canada) at 300 mA for 1 h at 4 °C. The membrane was blocked using 5 % milk, PBS, 0.1 % Tween (PBST) for 1 h at room temperature. The membrane was incubated with the VSV-M/VSV-N (Kerafast, USA) antibody diluted with the blocking buffer (1:1000) overnight at 4 °C. The next day, the membrane was washed 3 times for 5 min with PBST on a shaker. The horse radish peroxidase (HRP) bound rabbit anti-mouse (Abcam) in PBST (1:10000) was added to the membrane and incubated for 1 h at room temperature. The membrane was washed 3 times for 5 min with blocking buffer with shaking. The membrane was semi-dried and covered with 2 mL of Pierce™ ECL western blotting substrate (Thermo Scientific, Canada) and incubated for 1 min and revealed using ImageQuant™ LAS 4000 unit.

Spot blot analysis was performed using 2 µL of the sample placed on a nitrocellulose membrane. The membrane was air-dried for 30 min, blocked with PBST containing 5% milk for 1 h, hybridized with VSV-N/VSV-M antibody, incubated 1 h with rabbit anti-mouse HRP bound antibody in the blocking buffer, and incubated with Pierce™ ECL western blotting substrate for 1 min. Gels were observed using an ImageQuant™ LAS 4000 imager.

5.2.10. Transmission electron microscopy (TEM)

The virus-containing suspension was fixed with 4% paraformaldehyde for 1 h at room temperature. They were adsorbed on 400 mesh nickel grids coated with formvar and carbon for 20 minutes. The grids were blotted with bibulous paper and stained with 2% PTA (phosphotungstic acid) for 30 seconds, blotted, and let dry for at least 2 hours. They were then observed with a Tecnai Spirit G2 (FEI, Netherlands) at 80 kV. 10-20 images were taken per sample. Before TEM pretreatment and analysis, the samples were desalted using Amicon 15 (Millipore, Canada).

5.3. Results and discussion

In this work, we tested the efficacy of CHT resins in the purification of rVSV produced using serum-free adherent Vero cells. We have previously (Chapters 3 and 4 of this thesis) proposed purification schemes for small-scale and large purification of rVSVs. The virus-containing supernatant was harvested 72 hours post-infection (hpi) and treated with Benzonase® for the reduction of contaminant DNA contents. Afterward, the supernatant underwent a clarification step using a series of 3 filters with decreasing pore sizes of 20, 1.2, and 0.6 µm, using Sartopure® PP3 filters, (Sartorius, Canada).

The serial microfiltration was employed to eliminate the low-speed centrifugation step that was previously used to improve the scalability of the overall process. The recovery of infectious particles from each filter is listed in Table 15. Overall, this clarification process resulted in the recovery of 68.8 % of the infective VSVs with specific virus recoveries of 82, 98, and 69 % from the 20, 1.2, and 0. 6 µm filters, respectively (Table 15).

The highest loss of viral particles was observed when using the 0.6 µm filter. The overall recovery of infectious particles at the clarification step was lower compared to that obtained from our previous purification schemes (Chapter 3 of the thesis) using a combination of low-speed centrifugation and microfiltration. However, the current method is more applicable for pilot- and large-scale purification processes. Moreover, the serial microfiltration step eliminated 18 % of total proteins from the crude supernatant, bringing the protein concentration in the 0.6 µm filtrate to 574 µg/mL. The clarified supernatant was then concentrated 16 X by TFUF, aliquoted, and stored at -80 °C until further use. The TFUF concentration reduced the protein contents by 96 % without any loss of infective viruses (Table 15).

Table 15. Recovery of infectious particles and total protein contents throughout the clarification step using Sartopure® PP3 filters and tangential flow ultrafiltration (TFF).

	Infectious particles				**Protein content**		
Step	Titer (FFU/mL)	Volume (mL)	Step RCV (%)	Global RCV (%)	Protein conc (µg/mL)	Step RCV (%)	Global RCV (%)
Virus preparation*	8.24E+07	1176	100	-	703	100	100.0
20 µm MF	6.74E+07	1184	82	82	641	92	91.8
1.2 µm MF	6.55E+07	1191	98	80.4	622	98	89.6
0.6 µm MF	4.51E+07	1200	69	67.6	574	93	83.3
TFF	7.57E+08	75	100	69	370	4	3.4

MF: microfiltration, FFU: Focus-forming units, TFF: tangential flow ultrafiltration, RCV: recovery, Conc: concentration. * The Benzonase® treated cell culture supernatant.

The chromatographic purification of rVSV based HIV vaccine produced in Vero-SF cells by CHT I and II was initiated by performing a batch test of these resins and analyzing their eluate using SDS-Page and western blot methods (Fig. 21). The TFUF retentate was mixed with Buffer A (1:1) prior to chromatographic experiments

(referred to as "feed" hereafter) and mixed with 750 µg of unpacked CHT I or CHT II resins. Different quantities of feed were incubated with each of the resins for 2 h. The resin was washed with buffer A of low salt concentration to remove the loosely bound materials followed by elution of the bound material using 500 mM $NaPO_4$.

As it is shown in Fig 21. Panel A, the major VSV protein, including the VSV-N (47 kDa), can be spotted in the eluate of both resins. Moreover, the purity of these eluates can be observed visually by comparing the intensity of the viral proteins against the background in both eluates and non-purified samples. The presence of rVSVs in these eluates was further confirmed by western blot using VSV-N antibody (Fig. 21. B). These preliminary results confirmed that the rVSV HIV vaccine binds to both CHT I and CHT II resins.

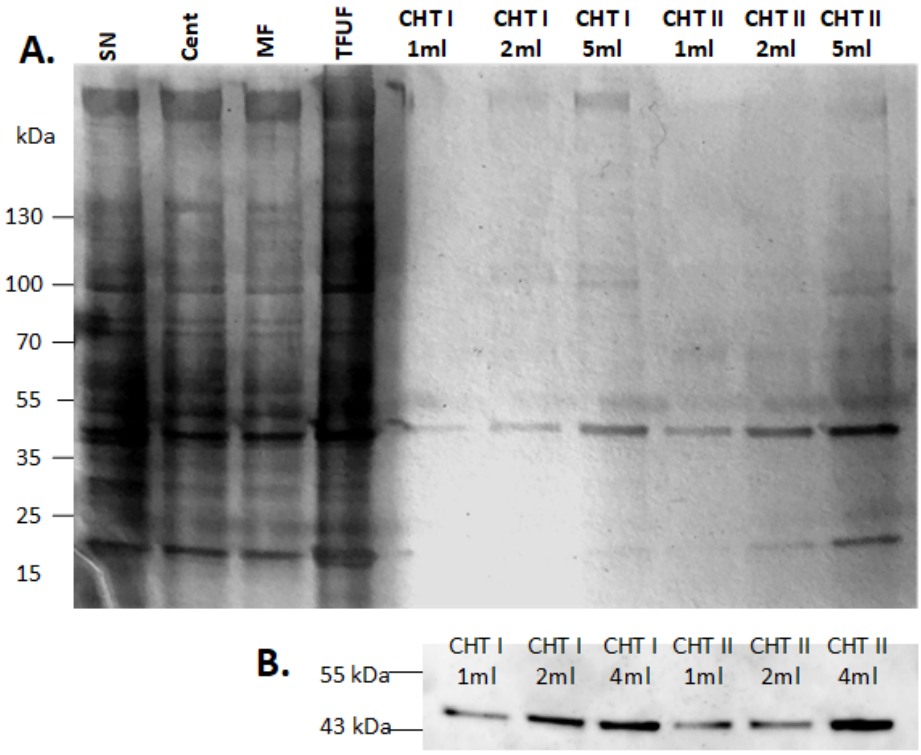

Fig 21. A) Silver staining SDS PAGE analysis of the batch mode chromatography using CHT I and CHT II resins. SN: Supernatant, Cent: Low-speed centrifugation, MF: microfiltration, TFUF: tangential flow ultrafiltration. The quantity of the feed added to the resin is mentioned on the top of each lane. B) Western blot analysis of the eluates using an anti-VSV-N antibody. A pre-stained Page ruler molecular weight ladder was used.

Therefore, to find the best candidate for the recovery of these infective particles, the two resins in 5-ml prepacked column forms were used. For this purpose, a certain volume of the feed was passed through the column. The virus load step was followed by two wash steps with 0.5 and 5 % buffer B (in buffer A), to remove the host cell or other loosely bound proteins and DNA. The bound material was then eluted using 500 mM $NaPO_4$ (50 % B in A).

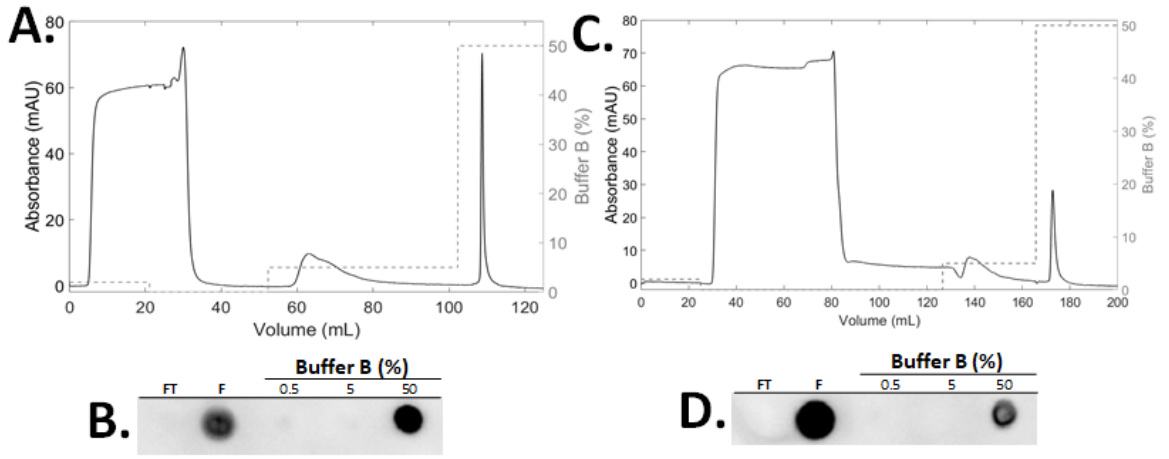

Fig 22. Chromatograms of rVSV purification using A) CHT II and C) CHT I columns. Dot blot analysis of the fractions obtained from the chromatographic purification using B) CHT II and D) CHT I columns. FT: Flow-through, F: Feed, 0.5%: column wash using 0.5 % B, 5%: Column wash using 5 % B, 50 %: elution using 50 % B.

The spot blot analysis of the fractions obtained throughout the process confirmed the absence of rVSV in the flow-through when passing 25 mL and 50 mL of the feed through the CHT II (Fig. 22.B) and CHT I (Fig. 22.D) columns, respectively. As presented in Table 16 the recovery of infectious particles from the CHT II column was higher than the CHT I column. The TCID50 reads from the elution peak of the CHT II column showed the presence of 6.92E+09 FFU of rVSVs, which corresponds to the recovery of 72.2 % infectious particles. This recovery is higher than the one reported for the same resin used to purify human papillomavirus type 33 L1 virus-like particles (58.7 %) [221]. Considering these points, the CHT II column was found superior for purification of rVSVs compared to CHT I column based on the recovery of virus particles.

Table 16. Infective virus titers of the chromatography feed and the elution fractions obtained from CHT I and CHT II columns. The titers were determined using the TCID50 assay.

Column	Feed			Elution			
	Titer (FFU/mL)	Volume (mL)	Total virus (FFU)	Titer (FFU/mL)	Volume (mL)	Total virus (FFU)	Virus RCV (%)
CHT I	3.79E+08	50	1.89E+10	6.18E+08	8.4	5.19E+09	27.5
CHT II	3.79E+08	25	9.46E+09	1.38E+09	5.2	7.18E+09	75.9

RCV: recovery.

To find the right salt concentration for elution of rVSVs, a total volume of 100 mL feed was passed through the column, followed by two wash steps comprising of 0.5 % and 5 % B. The 0.5 % B was carried out to wash away the unbound materials in the column while the 5 % B wash targets the loosely bound compounds that elute at a very low concentration of salt. The elution was carried out using an increasing step-gradient of B from 10 % B corresponding to 100 mM $NaPO_4$ to 100 % B, matching 1 M $NaPO_4$ (Fig. 23. A). The fractions were collected based on the 280 nm absorbances between 5 mAU to 2000 mAU. The spot blot analysis of the fractions using VSV-N antibody showed the release of VSV-N protein into the elution fractions from 10 % B (100 mM $NaPO_4$) and last until 50 % B (500 mM $NaPO_4$) (Fig. 23. B).

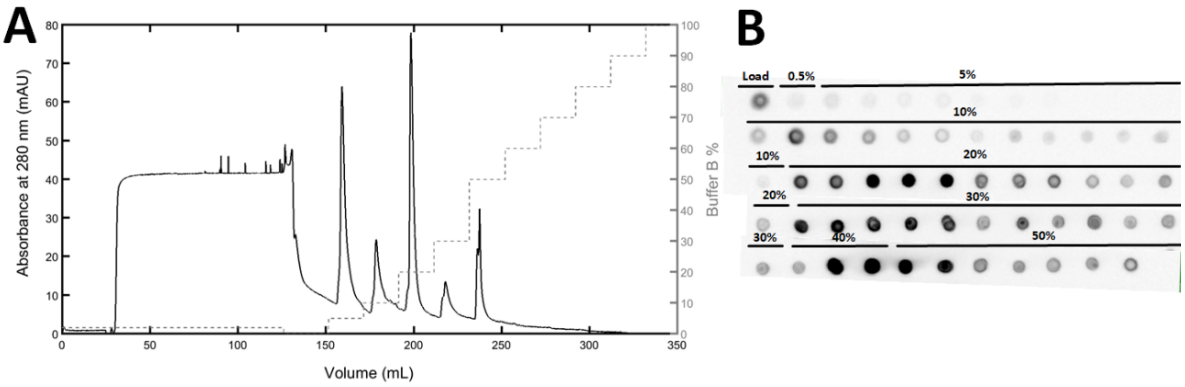

Fig 23. A) Chromatogram of rVSV elution from the CHT type II column using a step salt concentration gradient. B) Dot blot analysis of the fractions obtained from the rVSV elution using a step gradient of buffer B using VSV-N antibody. Load: Column feed, 5%/10%/20%/30%/40%/50%: the percentages of buffer B used for elution.

Compared to other chromatograms of the CHT II column, the amount of impurities washed from the column using 5 % B was higher in this experiment. The addition of these impurities is speculated to be due to the exclusion of the diafiltration step after the TFF concentration of the supernatant serving as the feed for this experiment. This indeed shows the role of diafiltration in addition to the TFF concentration step in the removal of contaminants that will compete with the viral particles in binding to the chromatography separation media. As it can be observed in Fig. 23. A, diafiltration of the supernatant at the TFF step has a positive impact on the elimination of impurities that were loosely bound to the column and eluted at 5 % B.

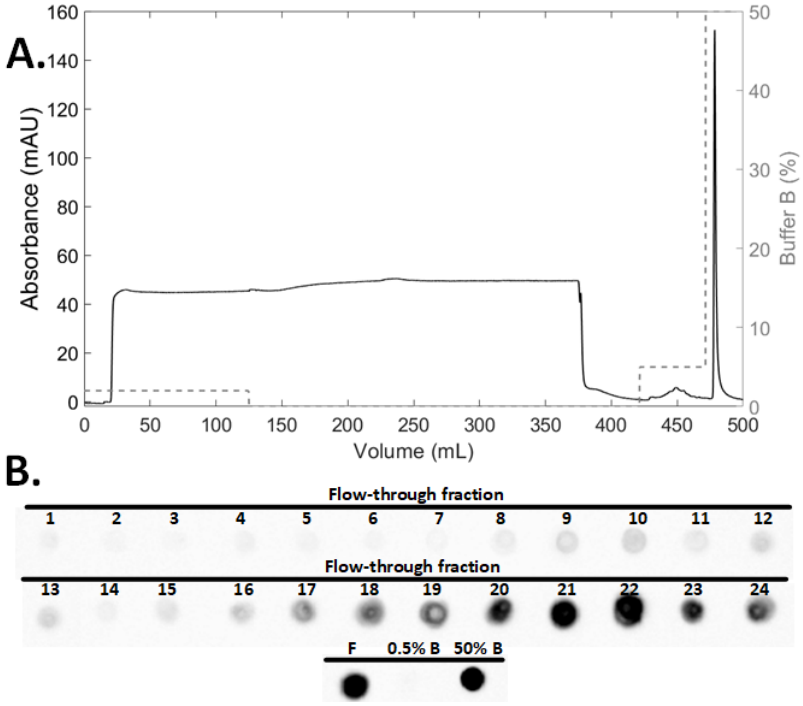

Fig 24. Determination of dynamic binding capacity of the CHT II resin for rVSV presenting the Ebola and HIV glycoproteins and produced using serum-free Vero cells. A) Chromatogram showing the absorbance at 280 nm and the conductivity. B) Spot-blot analysis of the 15 ml fractions obtained from purification using CHT II resin. VSV-N antibody was used.

Next, in order to determine the dynamic binding capacity (DBC) of the CHT II resin for rVSVs, a total volume of 350 mL of the feed was passed through the column while the flow-through was collected in 15 mL fractions (Fig. 24). The column was washed with 0.5 % B followed by elution of bound virus particles with 50 % B corresponding to 500 mM $NaPO_4$ (Fig. 24. A). The spot blot analysis of the flow-

through fractions using VSV-N antibody showed the presence of VSV-N protein, starting from fraction 17 of the flow-through (Fig. 24. B).

However, the TCID50 assay confirmed the presence of 6.55E+05 FFU in fraction 17 that only corresponds to 0.17 % of infectious particles in the feed, while the number of viruses in fractions 18 and 19 was quantified to be 1.10E+07 FFU matching 2.9 % of the virus content of the feed (Table 17). The titer of the rVSV determined in the consecutive 15 fractions corresponded to 14.5 % (Fraction 20), 26.6 % (Fraction 21), 48.7 % (Fraction 22), 72.9 % (Fraction 23) and 89.1 % (Fraction 24) of the infective virus content of the feed (Table 17). Therefore, the DBC of the CHT II resin for rVSV was selected as 2.27E+10 FFU per mL of the resin, corresponding to the volume of 270 mL of the feed (1:1 virus preparation: buffer A).

Table 17. Infective virus titers were obtained from VSV-N positive fractions of the flow-through from the dynamic binding capacity assay.

Sample		Titer (FFU/mL)	RCV from the feed (%)
Feed		3.79E+08	
Flow-through fraction number	17	6.55E+05	0.17
	18	1.10E+07	2.90
	19	1.10E+07	2.90
	20	5.51E+07	14.54
	21	1.01E+08	26.59
	22	1.85E+08	48.74
	23	2.76E+08	72.88
	24	3.38E+08	89.12

RCV: recovery.

As presented in the SDS-PAGE performed on fractions of the step-gradient chromatography, Fig. 25. A, one of the major rVSV proteins, including VSV-N, can be observed in the eluates. Comparing the intensity of these major rVSV bands to the background in the eluates and the feed can show the level of purity of these

fractions. The identity of these protein bands was further confirmed by western blot using VSV-M antibody (Fig. 25. B). Based on the eluates' western blot analysis and protein profile, the highest amount of VSV-M antibody is found in 40 % B followed by 30 % B, 20 % B, and 10 % B eluates. However, the titers derived from the TCID50 analysis showed the highest number of infectious particles in the 20 % B eluate, followed by 30 % B, 50 % B, and 40 % B (Table 17). The titer of the fractions obtained from 40 % B and 50 % B were higher per milliliter of the sample than that measured in other fractions; however, the total number of the viruses eluted using 20 % B was higher than the rest of the elution steps.

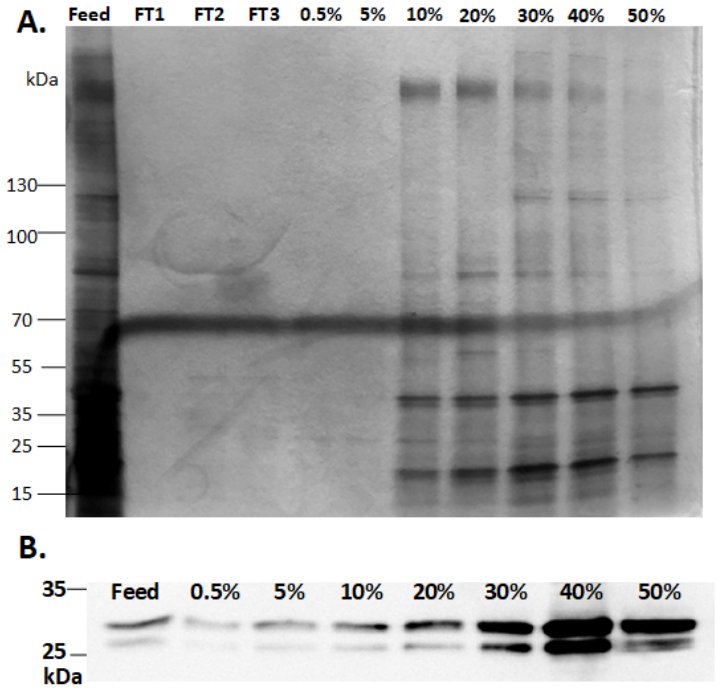

Fig 25. A) Silver-stained SDS-PAGE of the chromatography fractions obtained from the purification of rVSV using CHT type II column. Unstained Page ruler molecular weight marker was used as a ladder. Feed: chromatography feed, FT1-FT3: Flow-through fractions, wash steps including 0.5 % and 5 % B, elution fractions from 10 % B, 20 % B, 30 % B, 40 %, 50 % B. B) Western blot analysis of the chromatography fractions using VSV-M antibody.

To ensure that higher concentrations of $NaPO_4$ do not affect the integrity of rVSV, the virus-containing peaks from 40 % B and 50 % B elution were analyzed by DLS and TEM. Multiple factors have been linked to the formation of virus aggregates in a suspension, including the fibers or lipids present in virus structure, the presence of

cellular debris released into the medium after cell lysis, the addition of organic matters and disinfectants, medium pH, and salt concentration. More precisely, different types and concentrations of salts can change the repulsive electrostatic charges on the surface of viruses and therefore affecting the surface charge of the viral particles [225–227]. The absence of virus aggregates in these samples was confirmed by TEM analysis (Fig. 25. C, D, E). The DLS analysis of the peaks obtained at different salt concentrations showed a homogenous size distribution with an average size of 210 nm (Fig. 26. A).

An additional TFUF and diafiltration applied prior to chromatography purification is another key step that was as well shown to further lower the residual DNA contents by an additional 94 %. After all, the DNA contents found in the 20 % to 50 % elution fractions accounted for 2.8 % (Table 19) of the DNA in the feed, which indicates 38.5 folds lower quantities in the eluates compared to that in the feed. The rest of the DNA contents, which were bound to the column, started eluting at low salt concentrations, including 5 % B and 10 % B. The DNA contents in the other eluate fractions were found, varying between 3.2 to 11.1 ng/mL (Table 19). All the fractions except the 50 % B eluate had DNA contents lower than the limit defined by FDA (10 ng/dose). However, when pooling all the eluates together, the sample's total DNA contents per milliliter was lower than 10 ng, which falls in the expected range.

Electron micrographs of the feed and the peaks obtained from CHT II chromatography are shown in Fig. 26. The feed (fig. 26. A) shows a heterogeneous distribution of rVSVs and spherical structures round dimple-shaped structures that resemble extracellular vesicles and have been described as the typical morphology of exosomes [228]. The size of these round-shaped particles was found around 100 nm, which is within the range reported for exosomes [229]. As it can be seen from Fig. 26. B, the 10 % B fraction seems to selectively elute most of these vesicles, as this micrograph shows the largest number of these round-shaped particles. This could partially explain why the number of spherical particles decreases in the following fractions (Fig. 26. C, D, E, and F) and why the 10 % B fraction shows a

very low infective virus titer while still exhibiting a significant level of viral proteins (Fig. 26).

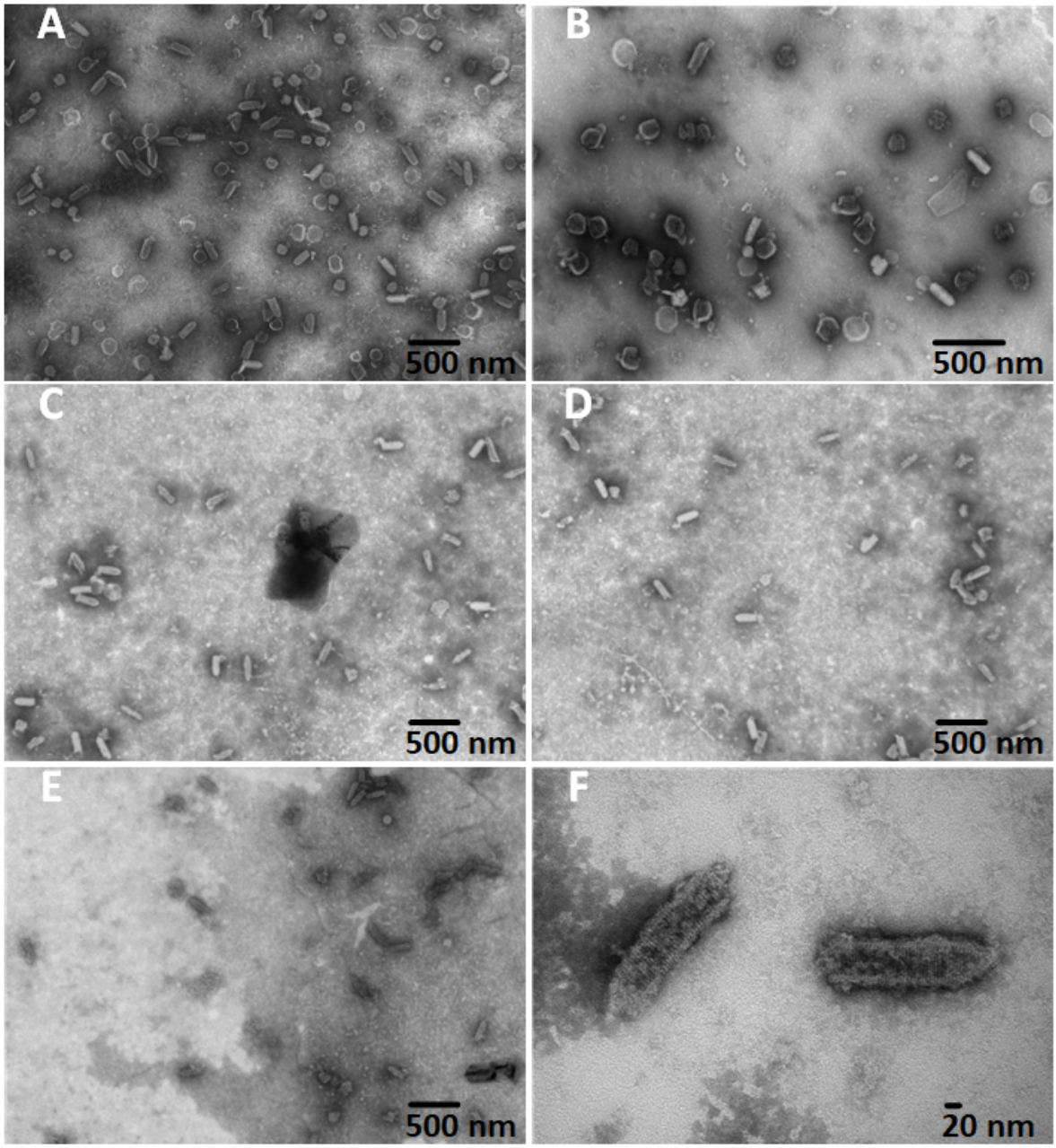

Fig 26. Electron micrographs of the CHT II chromatography fractions. A) Feed, B) peak from the elution with 10 % B, C) 20 % B, D) 30 % B, and E) 40 % B, F) Higher magnification of the purified rVSVs.

Table 18. Incorporation of virus-containing fractions collected from elution with 10 % B into the final compiled virus-containing fractions obtained from the eluates of the CHT II column and its effect on the protein, dsDNA concentration, virus titer, and the recovery of infectious particles.

condition	Total protein contents		Residual DNA		Infectious particles		
	Protein mass (µg)	RCV from feed (%)	DNA mass (ng)	RMV from feed (%)	Volume (mL)	Total virus (FFU)	RCV from feed (%)
Compile W/O 10%B	647	3.5	87.4	87.9%	15	2.62E+10	69.2
Compile W/ 10%B	982	5.3	272.4	60.7%	20	2.74E+10	72.2

RCV: Recovery, RMV: removal, W/O: without, W/: With, 10%B: elution fractions from 10 % buffer B.

These observations highlight the possible potential of the CHT II resin for separation of rVSVs from extracellular vesicles. This is an important application for purification of enveloped viruses since the extracellular vesicles share morphological as well as chemical characteristics with budding viruses, as they are both decorated with very similar membrane proteins. However, it has been previously demonstrated that hydroxyapatite, in other instances, had the capability of separating proteins with only slight structural dissimilarities such as monomers, dimers, aggregates or the native and denatured forms of the same protein [207,222–224].

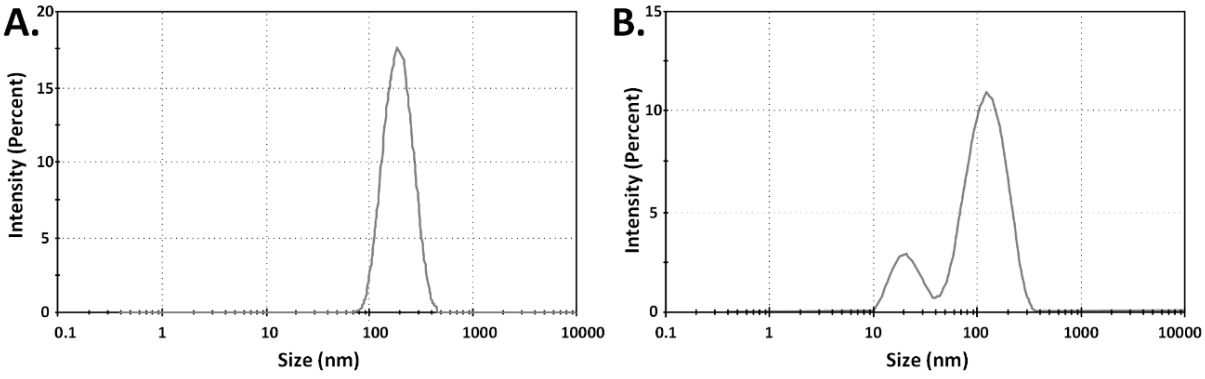

Fig 27. A) Size distribution diagram obtained by DLS for A) the pool of fractions obtained from elution at 20, 30, 40, and 50 % B, and B) the fraction obtained from elution with 10 % B.

The identity, purity, and size of the purified particles were confirmed using TEM and DLS. As shown in Fig. 26. Panel F, the purified rVSVs present the typical bullet-shaped structure of VSV [169]. The purity of the fractions obtained from the elution of rVSVs from the CHT II column and their comparison to the TFF concentrate (Feed) was also observed through TEM. The average size of the rVSVs captured by TEM was found to be approximately 200 nm which is in concordance with the previous reports [151][168]. The size distribution of the particles in different samples was measured using DLS (Fig. 27). An average size of 210 nm was measured for the purified fractions (20 – 50% B, Fig. 27. A). However, the DLS analysis of the fraction obtained at 10 % B showed two peaks representing two major populations of 130 nm and 21 nm mean sizes (Fig. 27. B), which differs significantly from the size distribution of the purified sample (Fig. 27. A).

Table 19. Analysis of virus titer, total protein content, and residual DNA in the fractions obtained from the purification of rVSV HIV vaccine with the CHT II column.

Step	Total protein		Residual DNA		Infectious particles		
	Protein conc * (µg/ml)	RCV from feed (%)	ds DNA conc (ng/ml)	RCV from feed (%)	Titer (FFU/mL)	Volume (mL)	RCV (%)
Feed	185	-	32	-	3.79E+08	100	-
FT	157	84.9%	21.8	68.1%	1.95E+03	100	0.00%
0.5%B w	12	1.6%	1.4	1.1%	4.78E+04	25	0.00%
5%B w	38	5.1%	12.8	10.0%	2.39E+05	25	0.02%
E 10%B	67	1.8%	37	5.8%	2.26E+08	5	2.98%
E 20%B	35	1.1%	3.2	0.6%	1.69E+09	6	26.9%
E 30%B	59	1.6%	7.6	1.2%	1.38E+09	5	18.3%
E40%B	46	0.5%	4	0.3%	2.07E+09	2	10.9%
E50%B	25	0.3%	11.1	0.7%	2.53E+09	2	13.4%

RCV: Recovery, w: wash, FT: flow-through, Conc: Concentration.

5.4. Conclusion

The current work focuses on the purification of rVSVs carrying Ebola and HIV glycoproteins using a multimodal chromatographic approach. The current purification process replaces an existing low-speed centrifugation with sequential microfiltration at the clarification stage to more easily meet GMP requirements. The new clarification process results in a slightly lower recovery compared to the two-step clarification process using low-speed centrifugation and microfiltration. Moreover, two ceramic hydroxyapatite resins were screened, and among them, the CHT II resin (Biorad) showed promising results in terms of infectious virus recovery.

Further analysis of the purified rVSV containing fractions showed the recovery of 2.8 % residual DNA from the feed in the elution fractions, if the 10 % B fractions were excluded. Also, the total protein contents in the CHT II column eluates, after 28.5 fold reduction, accounted for 0.3 % to 1.8 % of the total proteins present in the feed. The TEM images of the purified rVSVs showed a promising reduction in the number of structures that resemble extracellular vesicles and exosomes. These findings highlight the advantage of the CHT II resin, particularly for the elimination of microvesicles that have closely related physical and biochemical characteristics to the budding viruses, thus making them difficult to separate by other means. However, the identity of these vesicles needs to be further investigated using exosome and extracellular vesicle hallmarks.

Declaration of competing interest

The authors declare that they have no known competing financial interests or personal relationships that could have appeared to influence the work reported in this paper.

Acknowledgment

The authors thank the bio-imaging platform of the Infectious Disease Research Centre, CRCHU de Québec, for performing electron microscopy. We would also like to thank the Natural Sciences and Engineering Research Council (NSERC) and the Canadian Institute of Health Research (CIHR) for financing this project.

General conclusion

In this work, multiple technologies and a few purification schemes have been tested to treat a candidate HIV vaccine. The candidate HIV vaccine used in this work is made using rVSV backbone, carrying HIV and Ebola glycoproteins, and it was produced in the serum-free cultured Vero cell line. Two main schemes were proposed that can be used for laboratory- and large-scale purification of rVSV based HIV vaccine candidate. The small-scale protocol uses the density gradient ultracentrifugation as the main purification step, and the highly pure material produced from this step served as the standard for evaluating virus purity in other samples. A series of strong and weak anion-exchange columns, strong anion-exchange membrane, and multi-modal ceramic hydroxyapatite column were tested for their efficacy in purification and recovery of rVSVs and removal of contaminants including proteins, DNA, and microvesicles.

The clarification step initially consisted of the low-speed centrifugation at 3500 g, 20 min, to remove the larger contaminants including the cellular debris, followed by a 0.45 µm pore size microfiltration. This clarification step was optimized, in a first pass, by testing different filter materials and pore sizes. To that end, different membrane materials, including SFCA, CA, PVDF, PP, PES, and RC, with pore sizes varying from 0.45 to 30 µm, were tested for their potential as an improved and scalable alternative. Titration of the filtrates from the tested candidates showed more promising virus recovery from the PP–based filters for processing 400 to 2000 mL of LSC supernatant with the recovery of 86.3 ± 7.4 % using Mini Profile® II filter (Pall, PP, 1.5 µm pore size). The Miniprofile® filter was used at 200 LMH for the microfiltration step of supernatant volume larger than 400 mL, and it resulted in the elimination of 64 % of the host cell proteins and 8.9 % of the contaminant DNA in the filtrate. Additionally, the SartoScale 25 filter (Sartorius, PES, 1.2 µm pore size) with the recovery of 84 ± 6 % was selected to clarify smaller sample volumes (less than 200 mL). The SartoScale 25, when employed for filtration of 50 mL of supernatant, eliminated 58 % of the host cell proteins and 16.3 % of the contaminant DNA. On the other hand, the cellulose-based membranes (RC, CA, and SFCA)

resulted in higher virus loss with the recovery of 38.3 ± 7.1 % infectious particles in the best conditions, in accordance with previous reports.

Clarifying the supernatant using low-speed centrifugation is not the method of choice at larger scales, and it is usually replaced by microfiltration that will also minimize the number of purification steps. In this study, sequential microfiltration using the Sartopure® PP3 3-filter units (Sartorius) with decreasing pore sizes of 20 µm, 1.2 µm, and 0.6 µm were tested. The final virus recovery from the clarification using these filters was 68.8 % which was lower than that obtained from the combination of low-speed centrifugation and microfiltration (82 %). However, this latter approach is more scalable, robust, and easier to use at the large-scale.

One of the critical steps in DSP of cell culture harvest at the large-scale is volume reduction. Indeed, reducing the volume to be treated impacts the purification equipment scale and, therefore, its cost. Also, the use of concentration approaches such as when large-scale approaches, such as ultrafiltration can have the added benefit of contributing to the elimination of contaminants. The most commonly used approach for the concentration of small entities (molecules and viruses) at laboratory-scale is ultracentrifugation, either by virus pelleting using a homogeneous medium or the use of a step or continuous gradient of different densities. In this work, the clarified supernatant was initially UC pelleted using a cushion of 20 % sucrose. After resuspension in the buffer, the pellet from this step was later purified using a discontinuous gradient of iodixanol.

Virus pelleting resulted in 16 x concentrations and the elimination of 62.3 % proteins and 20 % DNA while recovering 96 % of the infective particles. However, it was found that loosening the virus pellet by its overnight incubation in the buffer before re-suspension plays a critical role in the virus recovery compared to when the pellet is re-suspended immediately. Moreover, the rVSV band after density gradient ultracentrifugation using 18 layers of iodixanol was found between 18 % and 28 % of iodixanol concentration, corresponding to densities between 1.100 and 1.153 g/mL, respectively, that was consistent with previous reports [230]. The purification of rVSV using a discontinuous iodixanol gradient allowed the recovery of 81 % of the

infectious viral particles while eliminating 80.9 % of proteins and 92.7 % of residual DNA.

Moreover, a gradient consisting of 6 layers of iodixanol was tested for separation of rVSVs that simplified the process and allowed an increase in the volume of virus preparation that could be charged on top of the centrifugation tube from 9 ml, when using the previous protocol, to 14 mL with this 6-layer gradient. Purification of rVSVs using this gradient resulted in eliminating 81 % of proteins and 86 % of the dsDNA contents while recovering 81 % of infective particles. The virus preparations purified through a gradient of iodixanol showed a noticeable difference in the number of structures that morphologically resemble the extracellular vesicles compared to the concentrate obtained from virus pelleting. This finding suggest that density gradient ultracentrifugation might have the potential to partially eliminate some of the microvesicles from the purified viruses. Such level of purification at small-scale can be useful for studies dealing with the biochemical and physical properties of VSV.

For concentration at a larger scale, a number of TFUF units were tested while maintaining the shear rate below or at 2000 s^{-1} throughout the process. Amongst the tested TFUF units, Midikros® TFUF module, mPES, 700 kDa MWCO showed the most promising rVSV recovery. It resulted in the recovery of 94.6 ± 1.5 % particles and removal of 92.1 % residual DNA and 98.6 % of the total proteins while concentrating the supernatant 15 times. However, the DNA contents after this step were still 46 ng/mL, which was higher than the FDA recommendation and needed further purification steps to reduce it. Concentration at a scale of 120 mL was carried out by pelleting using UC, which resulted in a similar concentration factor to that obtained from TFUF (≈ 15 x). Both concentrations approaches resulted in virus recovery of higher than 90 % with slightly higher (5 %) recoveries from UC. Moreover, comparable results were obtained regarding eliminating proteins (96 % and 99 %) from TFUF and UC usage. However, TFUF outperformed pelleting by UC in the removal of contaminating dsDNA.

First, in order to find the right candidate for the final purification step of rVSVs at a larger scale, anion-exchange resins including two weak anion exchangers, namely,

HiTrap™ DEAE FF and HiTrap™ ANX FF, and two strong anion exchangers comprising of HiTrap™ Q XL, HiTrap™ Q FF columns, were tested. The feed used for these columns was the virus concentrate obtained from TFUF that was equilibrated with the chromatography buffer A (0 mM NaCl) prior to injection. The highest recovery of rVSVs (77 % and 53 %) was found when using HiTrap™ DEAE FF followed by HiTrap™ Q XL, therefore one weak and one strong exchanging resins. However, the HiTrap™ Q XL showed higher DBC (1.93E+10 FFU) for viral particles compared to HiTrap™ DEAE FF (1.10E+10 FFU). However, the weak anion-exchanger column (HiTrap™ DEAE FF) resulted in the elimination of 92.7 % of DNA while the strong anion exchanger column (HiTrap™ Q XL) lowered the DNA contents by 48 %. Therefore, the DNA contents in the eluates of HiTrap™ Q XL were higher than the amount recommended by FDA (≤10 ng/dose). The performance of HiTrap™ DEAE FF column for removal of total proteins was also superior to HiTrap™ Q XL column by lowering the level of the total proteins by 86.6 % while the HiTrap™ Q XL column resulted in 70 % lower protein contents in the eluates.

Membrane chromatography allows a higher flow rate and has a higher binding capacity for viral particles than traditional resin-based column chromatography [172,173]. Therefore, to further explore the available technologies for large-scale purification of these candidate vaccines, an anion-exchange membrane (Sartobind® Q, Sartorius) was tested. The membrane-based purification scheme was initiated with a nuclease treatment, followed by a clarification step using a combination of low-speed centrifugation and microfiltration. The clarified supernatant was then passed through the Sartobind® Q membrane. The eluate from the anion-exchange membrane showed 88.3 % reduction in the total protein contents and 92 % lower concentration of HCPs while recovering 66 % of infective rVSVs. However, due to the usage of high salt concentration for the stripping of viruses that favors elution of DNA from the membrane, the DNA content in the eluates was relatively high (70 ng/mL), even though it was lowered by 89 %. Therefore, a second chromatography step using Capto™ Core 700, a multimodal column, was added that was carried out in flow-through mode. The addition of this step lowered the concentration of DNA in the rVSV preparation by 30 % by bringing it to 14 ng/mL and recovering 78 ± 6 % of

the infectious particles. The overall recovery of viruses after the two chromatography steps was 51 %. A TFUF followed the two-step chromatographic purification for buffer exchange and desalting that had no effect on the virus titer but reduced the DNA contents further to 8 ng/mL.

Finally, since the electron micrographs of the purified viruses using anion-exchange resins and membrane showed high quantities of microvesicles, we sought to test hydroxyapatite columns for their ability in separation of rVSVs from these components. Hydroxyapatite has been previously reported to be able to separate proteins with slight structural dissimilarities such as monomers, dimers, and aggregates or the native and denatured forms of the same protein [222–224]. Among the two columns tested (CHT type I and CHT type II, Bio-Rad), CHTII was a better candidate in terms of virus recovery. Purification of rVSV using the CHT II column eliminated 87.9 % residual DNA and 96.5 % total protein contents while recovering 69.2 % of infectious particles. The electron micrograph of the CHTII elution fractions showed a noticeably lower amount of structures that morphologically resemble extracellular vesicles and exosomes than those from other column-type eluates. The biophysical similarity of these structures to enveloped viruses makes their separation challenging. These findings suggest CHTII resin as an interesting candidate for a better separation of rVSVs from microvesicles, as well as contaminant DNA and proteins. However, to better understand the identity of these entities, detection of EV or exosome hallmarks including heat shock proteins, acetylcholinesterase enzyme activity assay, CD81 and CD63 need to be measured and compared in the purified and non-purified samples from this chromatography column in future studies.

The overall purification schemes proposed for small-scale as depicted in Fig. 9 (Chapter 3), comprise a nuclease treatment, low-speed centrifugation, microfiltration, and pelleting by ultracentrifugation, purification by density gradient UC and diafiltration by ultrafiltration. The use of this protocol resulted in a global recovery of 47.6 % of the infectious particles. On the other hand, the large-scale purification scheme, based on the AEX column selected, resulted in an overall recovery of 51.3 % and 35.1 % when using HiTrap™ DEAE FF and HiTrap™ Q XL

columns, respectively. These results show comparable virus recovery values at best conditions from small-scale, and large-scale purification approaches. In the purification scheme for large-scale, concentration by pelleting was replaced by TFUF that is proven as a more scalable approach. Application of TFUF prior to chromatography helps in the removal of the proteins and DNA that, if not removed, can interfere with the DBC of the column and compete with viruses for binding to the column.

Table 20. Comparison of different chromatography approaches in terms of virus recovery and rVSV purification.

Purification step	Total protein		Residual DNA		Infectious particles		
	Protein (µg/mL)	Step RMV (%)	DNA (ng/mL)	Step RMV (%)	Titer (FFU/mL)	Volume (mL)	RCV (%)
HiTrap™ DEAE FF	23	93	6.7	92.72	1.69E+09	5	77
HiTrap™ Q XL	34	95	31	85.37	2.67E+09	3.8	53
CHTII	165	87	25.9	87.9	7.67E+09	15	69.2
Sartobind® Q	137	88.3	72	89	2.68E+08	12	66
Capto™ core 700	93	54.8	14	30	1.79E+08	14	78

RCV: recovery, RMV: removal

Amongst the tested chromatographic approaches (Table 20), the highest DBC for rVSVs was observed in CHTII column, being able to hold 2.27E+10 FFU of rVSV per mL of the resin, followed by HiTrap™ Q XL, HiTrap™ DEAE FF and Sartobind® Q. Despite higher DBC, the recovery of rVSVs from the HiTrap™ Q XL column was lower than that of HiTrap™ DEAE FF, which could be due to the loss of the rVSV population that was strongly bound to the column and needed a higher concentration of salt for elution. It could also be justified by the trapping of viruses or virus aggregates in the column prefilter that did not allow the viruses to enter the column. Although the effectiveness of the membrane-based Sartobind® Q chromatography was a little lower than the resin-based ones, an advantage of the former is the lack of need for virus concentration before chromatography and the possibility of running the experiment at a higher flow rate. However, the rapid pressure rise that occurred with Sartobind® Q would need to be considered if making this choice of technology,

by, for instance, having a 2-column swing system that would allow recycling one adsorber while using the other in a cycle fashion. The strong anion exchanger resin-based column (HiTrap™ Q XL) and membrane (Sartobind® Q) resulted in rVSV recoveries lower than that obtained from CHTII and the weak anion exchanger column (HiTrap™ DEAE FF). Overall, CHTII resin, despite slightly lower virus recoveries compared to two of the anion exchangers, showed higher DBC for rVSVs and presented promising results in terms of eliminating exosomes and extracellular particles. To further improve the recovery of infectious particles from the CHTII column, modifications of parameters such as pH of the column equilibration buffer and the type of the equilibration and storage buffer could be useful.

The virus count in this study was measured using a TCID50 assay that estimates the number of infective viruses. This value does not therefore represents the total number of viral particles, which includes both infective and non-infedtive particles, such as those that could have lost their infectivity upon DSP treatment. These non-infective viral particles, if injected to a host, could interfere both positively or negatively upon vaccination. They most likely exhibit HIV proteins on their surfaces and hence could contribute to the increase in immune response of the host. But since the infective viruses penetrate the host cells and replicate, contributing in this fashion to the greater part of the immune response, non-infective particles could also, especially if they are in great quantities, adsorb on the host cell receptors and hinder the entry of infective particles. It would be therefore important to know what is the concentration of the total viral particles, to be able to calculate the non-infective ones by subtracting the total by the infective viruses. Such viral count could be obtained using assays that quantify the viral RNA including RT-PCR. The analysis of the total particles using flow cytometry that counts the particles based on their size could also provide useful information. However, detection of the VSV particles (200 nm approximately) that are not fluorescently labelled using flow cytometer is challenging since contaminants of similar size including microvesicles cannot be differentiated from the viruses by the instrument and could therefore contribute to the total virus count. However, if the instrument is designed for detection of nanoparticles, such as CytoFLEX flow cytometer (Beckman), it might detect the

particles of 200 nm but still might not be able to differentiate the other entities from the virus particles unless it is labelled.

Although this work focused principally on the purification of a rVSV carrying HIV and Ebola glycoproteins, we hypothesized that the purification schemes proposed in this work should also be able to purify other rVSV based vaccine candidates. However, this promising generalization remains to be demonstrated by future investigations. Therefore, applying the purification schemes identified in this study to rVSV expressing antigens other than HIV and Ebola gp would allow to know if resins and membranes characterized in this project would also interact with other rVSV constructs and also clarify the mechanism for such an interaction. This would allow generalizing the applicability of the approaches selected in this study to all VSV based vaccines.

References

[1] UNAIDS. Gobal AIDS update 2020 n.d.

[2] Liang B, Li H, Li L, Omange RW, Hai Y, Luo M. Current advances in HIV vaccine preclinical studies using Macaque models. Vaccine 2019;37:3388–99. https://doi.org/10.1016/j.vaccine.2019.04.094.

[3] Clarke DK, Cooper D, Egan MA, Hendry RM, Parks CL, Udem SA. Recombinant vesicular stomatitis virus as an HIV-1 vaccine vector. Springer Semin Immun 2006;28:239–53. https://doi.org/10.1007/s00281-006-0042-3.

[4] Furuyama W, Reynolds P, Haddock E, Meade-White K, Quynh Le M, Kawaoka Y, et al. A single dose of a vesicular stomatitis virus-based influenza vaccine confers rapid protection against H5 viruses from different clades. Npj Vaccines 2020;5:1–10. https://doi.org/10.1038/s41541-019-0155-z.

[5] Pavlovic J, Zürcher T, Haller O, Staeheli P. Resistance to influenza virus and vesicular stomatitis virus conferred by expression of human MxA protein. J Virol 1990;64:3370–5. https://doi.org/10.1128/JVI.64.7.3370-3375.1990.

[6] Reif JS, Webb PA, Monath TP, Emerson JK, Poland JD, Kemp GE, et al. Epizootic vesicular stomatitis in Colorado, 1982: infection in occupational risk groups. Am J Trop Med Hyg 1987;36:177–82. https://doi.org/10.4269/ajtmh.1987.36.177.

[7] Letchworth GJ, Rodriguez LL, Del cbarrera J. Vesicular stomatitis. Vet J 1999;157:239–60. https://doi.org/10.1053/tvjl.1998.0303.

[8] Flanagan EB, Zamparo JM, Ball LA, Rodriguez LL, Wertz GW. Rearrangement of the Genes of Vesicular Stomatitis Virus Eliminates Clinical Disease in the Natural Host: New Strategy for Vaccine Development. J Virol 2001;75:6107–14. https://doi.org/10.1128/JVI.75.13.6107-6114.2001.

[9] Knipe DM, Baltimore D, Lodish HF. Separate pathways of maturation of the major structural proteins of vesicular stomatitis virus. J Virol 1977;21:1128–39. https://doi.org/10.1128/JVI.21.3.1128-1139.1977.

[10] Bishnoi S, Tiwari R, Gupta S, Byrareddy SN, Nayak D. Oncotargeting by Vesicular Stomatitis Virus (VSV): Advances in Cancer Therapy. Viruses 2018;10:E90. https://doi.org/10.3390/v10020090.

[11] Lichty BD, Power AT, Stojdl DF, Bell JC. Vesicular stomatitis virus: re-inventing the bullet. Trends Mol Med 2004;10:210–6. https://doi.org/10.1016/j.molmed.2004.03.003.

[12] Haglund K, Leiner I, Kerksiek K, Buonocore L, Pamer E, Rose JK. High-Level Primary CD8+ T-Cell Response to Human Immunodeficiency Virus Type 1 Gag and Env Generated by Vaccination with Recombinant Vesicular Stomatitis Viruses. J Virol 2002;76:2730–8. https://doi.org/10.1128/JVI.76.6.2730-2738.2002.

[13] Geisbert TW, Feldmann H. Recombinant vesicular stomatitis virus-based vaccines against Ebola and Marburg virus infections. J Infect Dis 2011;204 Suppl 3:S1075-1081. https://doi.org/10.1093/infdis/jir349.

[14] Munis AM, Bentley EM, Takeuchi Y. A tool with many applications: vesicular stomatitis virus in research and medicine. Expert Opinion on Biological Therapy 2020;20:1187–201. https://doi.org/10.1080/14712598.2020.1787981.

[15] Roberts A, Kretzschmar E, Perkins AS, Forman J, Price R, Buonocore L, et al. Vaccination with a Recombinant Vesicular Stomatitis Virus Expressing an Influenza Virus Hemagglutinin Provides Complete Protection from Influenza Virus Challenge. J Virol 1998;72:4704–11. https://doi.org/10.1128/JVI.72.6.4704-4711.1998.

[16] Schlereth B, Rose JK, Buonocore L, ter Meulen V, Niewiesk S. Successful vaccine-induced seroconversion by single-dose immunization in the presence of measles

virus-specific maternal antibodies. J Virol 2000;74:4652–7. https://doi.org/10.1128/jvi.74.10.4652-4657.2000.
[17] Emanuel J, Callison J, Dowd KA, Pierson TC, Feldmann H, Marzi A. A VSV-based Zika virus vaccine protects mice from lethal challenge. Sci Rep 2018;8:11043. https://doi.org/10.1038/s41598-018-29401-x.
[18] Rose NF, Marx PA, Luckay A, Nixon DF, Moretto WJ, Donahoe SM, et al. An effective AIDS vaccine based on live attenuated vesicular stomatitis virus recombinants. Cell 2001;106:539–49. https://doi.org/10.1016/s0092-8674(01)00482-2.
[19] Marzi A, Feldmann F, Geisbert TW, Feldmann H, Safronetz D. Vesicular Stomatitis Virus–Based Vaccines against Lassa and Ebola Viruses. Emerg Infect Dis 2015;21:305–7. https://doi.org/10.3201/eid2102.141649.
[20] Monath TP, Fast PE, Modjarrad K, Clarke DK, Martin BK, Fusco J, et al. rVSVΔG-ZEBOV-GP (also designated V920) recombinant vesicular stomatitis virus pseudotyped with Ebola Zaire Glycoprotein: Standardized template with key considerations for a risk/benefit assessment. Vaccine: X 2019;1:100009. https://doi.org/10.1016/j.jvacx.2019.100009.
[21] Haug CJ. Keeping Your Cool - Doing Ebola Research during an Emergency. N Engl J Med 2018;378:2353–5. https://doi.org/10.1056/NEJMp1806978.
[22] World Health Organisation. Preliminary results on the efficacy of rVSV-ZEBOVGP Ebola vaccine using the ring vaccination strategy in the control of an Ebola outbreak in the Democratic Republic of the Congo. 2019.
[23] Firquet S, Beaujard S, Lobert P-E, Sané F, Caloone D, Izard D, et al. Survival of Enveloped and Non-Enveloped Viruses on Inanimate Surfaces. Microbes Environ 2015;30:140–4. https://doi.org/10.1264/jsme2.ME14145.
[24] Alcock R, Cottingham MG, Rollier CS, Furze J, De Costa SD, Hanlon M, et al. Long-Term Thermostabilization of Live Poxviral and Adenoviral Vaccine Vectors at Supraphysiological Temperatures in Carbohydrate Glass. Science Translational Medicine 2010;2:19ra12-19ra12. https://doi.org/10.1126/scitranslmed.3000490.
[25] Zimmer B, Summermatter K, Zimmer G. Stability and inactivation of vesicular stomatitis virus, a prototype rhabdovirus. Veterinary Microbiology 2013;162:78–84. https://doi.org/10.1016/j.vetmic.2012.08.023.
[26] Segura M de LM, Kamen A, Garnier A. Downstream processing of oncoretroviral and lentiviral gene therapy vectors. Biotechnol Adv 2006;24:321–37. https://doi.org/10.1016/j.biotechadv.2005.12.001.
[27] McCarron A, Donnelley M, McIntyre C, Parsons D. Challenges of up-scaling lentivirus production and processing. J Biotechnol 2016;240:23–30. https://doi.org/10.1016/j.jbiotec.2016.10.016.
[28] Schweizer M, Merten O-W. Large-scale production means for the manufacturing of lentiviral vectors. Curr Gene Ther 2010;10:474–86. https://doi.org/10.2174/156652310793797748.
[29] Yamada K, McCarty DM, Madden VJ, Walsh CE. Lentivirus vector purification using anion exchange HPLC leads to improved gene transfer. Biotechniques 2003;34:1074–8, 1080. https://doi.org/10.2144/03345dd04.
[30] Baekelandt V, Eggermont K, Michiels M, Nuttin B, Debyser Z. Optimized lentiviral vector production and purification procedure prevents immune response after transduction of mouse brain. Gene Ther 2003;10:1933–40. https://doi.org/10.1038/sj.gt.3302094.
[31] Rodrigues T, Carvalho A, Roldão A, Carrondo MJT, Alves PM, Cruz PE. Screening anion-exchange chromatographic matrices for isolation of onco-retroviral vectors.

Journal of Chromatography B 2006;837:59–68. https://doi.org/10.1016/j.jchromb.2006.03.061.
[32] Josefsberg JO, Buckland B. Vaccine process technology. Biotechnology and Bioengineering 2012;109:1443–60. https://doi.org/10.1002/bit.24493.
[33] Wolf MW, Reichl U. Downstream processing of cell culture-derived virus particles. Expert Review of Vaccines 2011:10:1451-75. https://doi.org/10.1586/erv.11.111.
[34] de las Mercedes Segura M, Kamen A, Lavoie M-C, Garnier A. Exploiting heparin-binding properties of MoMLV-based retroviral vectors for affinity chromatography. Journal of Chromatography B 2007;846:124–31. https://doi.org/10.1016/j.jchromb.2006.08.032.
[35] de las Mercedes Segura M, Kamen A, Garnier A. Downstream processing of oncoretroviral and lentiviral gene therapy vectors. Biotechnology Advances 2006;24:321–37. https://doi.org/10.1016/j.biotechadv.2005.12.001.
[36] McCarron A, Donnelley M, McIntyre C, Parsons D. Challenges of up-scaling lentivirus production and processing. Journal of Biotechnology 2016;240:23–30. https://doi.org/10.1016/j.jbiotec.2016.10.016.
[37] Schweizer M, Merten O-W. Large-scale production means for the manufacturing of lentiviral vectors. Current Gene Therapy 2010;10:474–86. https://doi.org/10.2174/156652310793797748.
[38] Yamada K, McCarty DM, Madden VJ, Walsh CE. Lentivirus vector purification using anion exchange HPLC leads to improved gene transfer. Biotechniques 2003;34:1074–81. https://doi.org/10.2144/03345dd04.
[39] Baekelandt V, Eggermont K, Michiels M, Nuttin B, Debyser Z. Optimized lentiviral vector production and purification procedure prevents immune response after transduction of mouse brain. Gene Therapy 2003;10:1933. https://doi.org/10.1038/sj.gt.3302094.
[40] Scherr M, Battmer K, Eder M, Schüle S, Hohenberg H, Ganser A, et al. Efficient gene transfer into the CNS by lentiviral vectors purified by anion exchange chromatography. Gene Therapy 2002;9:1708. https://doi.org/10.1038/sj.gt.3301848.
[41] Merten O-W, Schweizer M, Chahal P, Kamen A. Manufacturing of viral vectors: part II. Downstream processing and safety aspects. Pharmaceutical Bioprocessing 2014;2:237–51.
[42] Morenweiser R. Downstream processing of viral vectors and vaccines. Gene Therapy 2005;12:S103. https://doi.org/10.1038/sj.gt.3302624.
[43] Rodrigues T, Carrondo MJT, Alves PM, Cruz PE. Purification of retroviral vectors for clinical application: biological implications and technological challenges. Journal of Biotechnology 2007;127:520–41. https://doi.org/10.1016/j.jbiotec.2006.07.028.
[44] Bandeira V, Peixoto C, Rodrigues AF, Cruz PE, Alves PM, Coroadinha AS, et al. Downstream processing of lentiviral vectors: releasing bottlenecks. Human Gene Therapy, Part B: Methods 2012;23:255–63. https://doi.org/10.1089/hgtb.2012.059.
[45] Josefsberg JO, Buckland B. Vaccine process technology. Biotechnology and Bioengineering 2012;109:1443–60. https://doi.org/10.1002/bit.24493
[46] Cureton DK, Massol RH, Whelan SPJ, Kirchhausen T. The length of vesicular stomatitis virus particles dictates a need for actin assembly during clathrin-dependent endocytosis. PLoS Pathogens 2010;6:e1001127.https://doi-org/10.1371/journal.ppat.1001127
[47] Emanuel J, Callison J, Dowd KA, Pierson TC, Feldmann H, Marzi A. A VSV-based Zika virus vaccine protects mice from lethal challenge. Scientific Reports 2018;8:11043. https://doi.org/10.1038/s41598-018-29401-x.
[48] Strauss EG, Strauss JH. Viruses and human disease. Elsevier; 2007.

[49] Jones SM, Feldmann H, Ströher U, Geisbert JB, Fernando L, Grolla A, et al. Live attenuated recombinant vaccine protects nonhuman primates against Ebola and Marburg viruses. Nature Medicine 2005;11:786. https://doi.org/10.1038/nm1258.
[50] Rose NF, Marx PA, Luckay A, Nixon DF, Moretto WJ, Donahoe SM, et al. An effective AIDS vaccine based on live attenuated vesicular stomatitis virus recombinants. Cell 2001;106:539–49. https://doi.org/10.1016/S0092-8674(01)00482-2.
[51] Lauretti F, Chattopadhyay A, de Oliveira França RF, Castro-Jorge L, Rose J, Fonseca BAL da. Recombinant vesicular stomatitis virus-based dengue-2 vaccine candidate induces humoral response and protects mice against lethal infection. Human Vaccines & Immunotherapeutics 2016;12:2327–33. https://doi.org/10.1080/21645515.2016.1183857.
[52] Lovalenti PM, Anderl J, Yee L, Nguyen V, Ghavami B, Ohtake S, et al. Stabilization of Live Attenuated Influenza Vaccines by Freeze Drying, Spray Drying, and Foam Drying. Pharm Res 2016;33:1144–60. https://doi.org/10.1007/s11095-016-1860-1.
[53] Zimmer B, Summermatter K, Zimmer G. Stability and inactivation of vesicular stomatitis virus, a prototype rhabdovirus. Veterinary Microbiology 2013;162:78–84. https://doi.org/10.1016/j.vetmic.2012.08.023.
[54] Wiggan O, Livengood JA, Silengo SJ, Kinney RM, Osorio JE, Huang CY-H, et al. Novel formulations enhance the thermal stability of live-attenuated flavivirus vaccines. Vaccine 2011;29:7456–62. https://doi.org/10.1016/j.vaccine.2011.07.054.
[55] Wan Y, Gupta V, Bird C, Pullagurla SR, Fahey P, Forster A, et al. Formulation Development and Improved Stability of a Combination Measles and Rubella Live-Viral Vaccine Dried for Use in the NanopatchTM Microneedle Delivery System. Human Vaccines & Immunotherapeutics 2021;0:1–16. https://doi.org/10.1080/21645515.2021.1887692.
[56] Kumru OS, Saleh-Birdjandi S, Antunez LR, Sayeed E, Robinson D, van den Worm S, et al. Stabilization and formulation of a recombinant Human Cytomegalovirus vector for use as a candidate HIV-1 vaccine. Vaccine 2019;37:6696–706. https://doi.org/10.1016/j.vaccine.2019.09.027.
[57] Nicola A V., Aguilar HC, Mercer J, Ryckman B, Wiethoff CM. Virus entry by endocytosis. Advances in Virology 2013. https://doi.org/10.1155/2013/469538.
[58] Arnemo M, Viksmoen Watle SS, Schoultz KM, Vainio K, Norheim G, Moorthy V, et al. Stability of a Vesicular Stomatitis Virus–Vectored Ebola Vaccine. The Journal of Infectious Diseases 2015;213:930–3. https://doi.org/10.1093/infdis/jiv532.
[59] Racine T, Kobinger GP, Arts EJ. Development of an HIV vaccine using a vesicular stomatitis virus vector expressing designer HIV-1 envelope glycoproteins to enhance humoral responses. AIDS Res Ther 2017;14:55. https://doi.org/10.1186/s12981-017-0179-2.
[60] Segura MM, Mangion M, Gaillet B, Garnier A. New developments in lentiviral vector design, production and purification. Expert Opinion on Biological Therapy 2013;13:987–1011. https://doi.org/10.1517/14712598.2013.779249.
[61] Chen J, Reeves L, Sanburn N, Croop J, Williams DA, Cornetta K. Packaging cell line DNA contamination of vector supernatants: implication for laboratory and clinical research. Virology 2001;282:186–97. https://doi.org/10.1006/viro.2001.0826.
[62] Kang Y, Cutler MW, Ouattara AA, et al. Purification processes for isolating purified vesicular stomatitis virus from cell culture. WO patent 2011/123961 A2.
[63] Bandeira V, Peixoto C, Rodrigues AF, Cruz PE, Alves PM, Coroadinha AS, et al. Downstream Processing of Lentiviral Vectors: Releasing Bottlenecks. Human Gene Therapy Methods 2012:23: 255-63. https://doi.org/10.1089/hgtb.2012.059.

[64] Nestola P, Peixoto C, Silva RRJS, Alves PM, Mota JPB, Carrondo MJT. Improved virus purification processes for vaccines and gene therapy. Biotechnology and Bioengineering 2015;112:843–57. https://doi.org/10.1002/bit.25545
[65] Singh N, Pizzelli K, Romero JK, Chrostowski J, Evangelist G, Hamzik J, et al. Clarification of recombinant proteins from high cell density mammalian cell culture systems using new improved depth filters. Biotechnology and Bioengineering 2013;110:1964–72. https://doi.org/10.1002/bit.24848
[66] Reeves L, Cornetta K. Clinical retroviral vector production: step filtration using clinically approved filters improves titers. Gene Therapy 2000;7:1993-98. https://doi.org/10.1038/sj.gt.3301328.
[67] de las Mercedes Segura M, Kamen A, Trudel P, Garnier A. A novel purification strategy for retrovirus gene therapy vectors using heparin affinity chromatography. Biotechnology and Bioengineering 2005;90:391–404. https://doi.org/10.1002/bit.20301.
[68] Vogt VM. Retroviral virions and genomes 1997.
[69] Reiser J. Production and concentration of pseudotyped HIV-1-based gene transfer vectors. Gene Therapy 2000;7:910. https://doi.org/10.1038/sj.gt.3301188.
[70] Geraerts M, Michiels M, Baekelandt V, Debyser Z, Gijsbers R. Upscaling of lentiviral vector production by tangential flow filtration. The Journal of Gene Medicine: A Cross-disciplinary Journal for Research on the Science of Gene Transfer and Its Clinical Applications 2005;7:1299–310. https://doi.org/10.1002/jgm.778.
[71] Sena-Esteves M, Tebbets JC, Steffens S, Crombleholme T, Flake AW. Optimized large-scale production of high titer lentivirus vector pseudotypes. Journal of Virological Methods 2004;122:131–9. https://doi.org/10.1016/j.jviromet.2004.08.017.
[72] Livshits MA, Khomyakova E, Evtushenko EG, Lazarev VN, Kulemin NA, Semina SE, et al. Isolation of exosomes by differential centrifugation: Theoretical analysis of a commonly used protocol. Sci Rep 2015;5:17319. https://doi.org/10.1038/srep17319.
[73] Burdon RH, Knippenberg PH van, Sharpe PT, editors. Chapter 3: Centrifugation. Laboratory Techniques in Biochemistry and Molecular Biology, vol. 18, Elsevier; 1988, p. 18–69. https://doi.org/10.1016/S0075-7535(08)70628-4.
[74] Chattopadhyay SK, Hartley JW, Lander MR, Kramer BS, Rowe WP. Biochemical characterization of the amphotropic group of murine leukemia viruses. Journal of Virology 1978;26:29–39. https://doi.org/10.1128/jvi.26.1.29-39.1978.
[75] Okuda K, Ito K, Miyake K, Morita M, Ogonuki M. Purification of Japanese encephalitis virus vaccine by zonal centrifugation. Journal of Clinical Microbiology 1975;1:96–101. https://doi.org/10.1128/jcm.1.1.96-101.1975.
[76] Hilfenhaus J, Köhler R, Gruschkau H. Large-scale purification of animal viruses in the RK-model zonal ultracentrifuge: III. Semliki Forest virus and vaccinia virus. Journal of Biological Standardization 1976;4:285–93. https://doi.org/10.1586/erv.11.111.
[77] Prem Kumar AA, Mani KR, Palaniappan C, Bhau LNR, Swaminathan K. Purification, potency and immunogenicity analysis of Vero cell culture-derived rabies vaccine: a comparative study of single-step column chromatography and zonal centrifuge purification. Microbes Infect 2005;7:1110–6. https://doi.org/10.1016/j.micinf.2005.03.034.
[78] Dettenhofer M, Yu X-F. Highly purified human immunodeficiency virus type 1 reveals a virtual absence of Vif in virions. Journal of Virology 1999;73:1460–7. https://doi.org/10.1128/JVI.73.2.1460-1467.1999.
[79] Møller-Larsen A, Christensen T. Isolation of a retrovirus from multiple sclerosis patients in self-generated Iodixanol gradients. Journal of Virological Methods 1998;73:151–61. https://doi.org/10.1016/S0166-0934(98)00052-4.

[80] Liu HF, Ma J, Winter C, Bayer R. Recovery and purification process development for monoclonal antibody production. MAbs, vol. 2, Taylor & Francis; 2010, p. 480–99. https://doi.org/10.4161/mabs.2.5.12645.

[81] Zydney AL. Membrane technology for purification of therapeutic proteins. Biotechnology and Bioengineering 2009;103:227–30. https://doi.org/10.1002/bit.22308.

[82] Bellintani F, Piacenza L, Birolo RS, Martelli A, Massa S, Vallanti G, et al. Large scale process for the production and purification of lentiviral vectors for clinical applications. Human gene therapy, vol. 19, Mary ann libert Inc 140 huguenot street, 3rd floor, New Rochelle, NY 10801 USA; 2008, p. 1089.

[83] Marino MP, Luce MJ, Reiser J. Small-to large-scale production of lentivirus vectors. Lentivirus Gene Engineering Protocols, Springer; 2003; p. 43–55. https://doi.org/10.1385/1-59259-393-3:43.

[84] Merten O-W, Charrier S, Laroudie N, Fauchille S, Dugué C, Jenny C, et al. Large-scale manufacture and characterization of a lentiviral vector produced for clinical ex vivo gene therapy application. Human Gene Therapy 2010;22:343–56. https://doi.org/10.1089/hum.2010.060.

[85] Merten O-W, Charrier S, Laroudie N, Fauchille S, Dugué C, Jenny C, et al. Large-Scale Manufacture and Characterization of a Lentiviral Vector Produced for Clinical *Ex Vivo* Gene Therapy Application. Human Gene Therapy 2011;22: 343-56. https://doi.org/10.1089/hum.2010.060.

[86] Slepushkin, Vladimir, Chang N, Gan Y, Jiang B, Andre K, Humeau L. Large-scale Purification of a Lentiviral Vector by Size Exclusion Chromatography or Mustang Q Ion Exchange Chromatography. Bioprocessing Journal 2003;2:89-95.

[87] Subramanian S, Altaras GM, Chen J, Hughes BS, Zhou W, Altaras NE. Pilot-scale adenovirus seed production through concurrent virus release and concentration by hollow fiber filtration. Biotechnology Progress 2005;21: 851-9. https://doi.org/10.1021/bp049561a.

[88] Rodriques T, Carvalho A, Carmo M, Carrondo MJT, Alves PM, Cruz PE. Scaleable purification process for gene therapy retroviral vectors. Journal of Gene Medicine 2007;9:233-243. https://doi.org/10.1002/jgm.1021.

[89] Kotani H, Newton Iii,' PB, Zhang S, Chiang,' YL, Otto E, Weaver L, et al. Improved Methods of Retroviral Vector Transduction and Production for Gene Therapy. Human Gene Therapy 1994;5:19-28. https://doi.org/10.1089/hum.1994.5.1-19.

[90] Kalbfuss B, Genzel Y, Wolff M, Zimmermann A, Morenweiser R, Reichl U. Harvesting and concentration of human influenza a virus produced in serum-free mammalian cell culture for the production of vaccines. Biotechnology and Bioengineering 2007;97:73-85. https://doi.org/10.1002/bit.21139.

[91] Nayak DP, Lehmann S, Reichl U. Downstream processing of MDCK cell-derived equine influenza virus. Journal of Chromatography B: Analytical Technologies in the Biomedical and Life Sciences 2005;823:75-81. https://doi.org/10.1016/j.jchromb.2005.05.022.

[92] Wickramasinghe SR, Kalbfuß B, Zimmermann A, Thorn V, Reichl U. Tangential flow microfiltration and ultrafiltration for human influenza A virus concentration and purification. Biotechnology and Bioengineering 2005;92: 199-208. https://doi.org/10.1002/bit.20599.

[93] Kuiper M, Sanches RM, Walford JA, Slater NKH. Purification of a functional gene therapy vector derived from moloney murine leukaemia virus using membrane filtration and ceramic hydroxyapatite chromatography. Biotechnology and Bioengineering 2002;80:445-53. https://doi.org/10.1002/bit.10388.

[94] Transfiguracion J, Jaalouk DE, Ghani K, Galipeau J, Kamen A. Size-Exclusion Chromatography Purification of High-Titer Vesicular Stomatitis Virus G Glycoprotein-Pseudotyped Retrovectors for Cell and Gene Therapy Applications. Human Gene Therapy 2003;14:1139-53. https://doi.org/10.1089/104303403322167984.
[95] Bowles NE, Eisensmith RC, Mohuiddin R, Pyron M, Woo SL. A simple and efficient method for the concentration and purification of recombinant retrovirus for increased hepatocyte transduction in vivo. Hum Gene Ther 1996;7:1735-42.. https://doi.org/10.1089/hum.1996.7.14-1735.
[96] Koldej R, Cmielewski P, Stocker A, Parsons DW, Anson DS. Optimisation of a multipartite human immunodeficiency virus based vector system; control of virus infectivity and large-scale production. Journal of Gene Medicine 2005; 7, 1390-9. https://doi.org/10.1002/jgm.803.
[97] Lyddiatt A. Process chromatography: Current constraints and future options for the adsorptive recovery of bioproducts. Current Opinion in Biotechnology 2002;13:95-103. https://doi.org/10.1016/S0958-1669(02)00293-8.
[98] Jungbauer A, Hahn R. Polymethacrylate monoliths for preparative and industrial separation of biomolecular assemblies. Journal of Chromatography A 2008;1184:62-79. https://doi.org/10.1016/j.chroma.2007.12.087.
[99] Jungbauer A. Chromatographic media for bioseparation. Journal of Chromatography A 2005;1065:3-12. https://doi.org/10.1016/j.chroma.2004.08.162.
[100] Rodrigues T, Carvalho A, Roldão A, Carrondo MJT, Alves PM, Cruz PE. Screening anion-exchange chromatographic matrices for isolation of onco-retroviral vectors. Journal of Chromatography B: Analytical Technologies in the Biomedical and Life Sciences 2006;837:59-68. https://doi.org/10.1016/j.jchromb.2006.03.061.
[101] Arora DJS, Tremblay P, Bourgault R, Boileau S. Concentration and purification of influenza virus from allantoic fluid. Analytical Biochemistry 1985;144:189-192. https://doi.org/10.1016/0003-2697(85)90103-4.
[102] Chen Z, Hsu FC, Battigelli D, Chang HC. Capture and release of viruses using amino-functionalized silica particles. Analytica Chimica Acta 2006;569:76-82. https://doi.org/10.1016/j.aca.2006.03.103.
[103] Chahal PS, Aucoin MG, Kamen A. Primary recovery and chromatographic purification of adeno-associated virus type 2 produced by baculovirus/insect cell system. Journal of Virological Methods 2007;139:61-70. https://doi.org/10.1016/j.jviromet.2006.09.011.
[104] Podgornik A, Jančar J, Merhar M, Kozamernik S, Glover D, Čuček K, et al. Large-scale methacrylate monolithic columns: Design and properties. Journal of Biochemical and Biophysical Methods 2004;60:179-89. https://doi.org/10.1016/j.jbbm.2004.01.002.
[105] Banjac M, Roethl E, Gelhart F, Kramberger P, Jarc BL, Jarc M, et al. Purification of Vero cell derived live replication deficient influenza A and B virus by ion exchange monolith chromatography. Vaccine 2014; 32:2487-92. https://doi.org/10.1016/j.vaccine.2014.02.086.
[106] Forcic D, Brgles M, Ivancic-Jelecki J, Šantak M, Halassy B, Barut M, et al. Concentration and purification of rubella virus using monolithic chromatographic support. Journal of Chromatography B: Analytical Technologies in the Biomedical and Life Sciences 2011;87:981-6. https://doi.org/10.1016/j.jchromb.2011.03.012.
[107] Kovač K, Gutiérrez-Aguirre I, Banjac M, Peterka M, Poljšak-Prijatelj M, Ravnikar M, et al. A novel method for concentrating hepatitis A virus and caliciviruses from bottled water. Journal of Virological Methods 2009;162:272-5. https://doi.org/10.1016/j.jviromet.2009.07.013.

[108] Benčina K, Benčina M, Podgornik A, Štrancar A. Influence of the methacrylate monolith structure on genomic DNA mechanical degradation, enzymes activity and clogging. Journal of Chromatography A 2007;1160:176-83. https://doi.org/10.1016/j.chroma.2007.05.034.
[109] Charcosset C. Membrane processes in biotechnology: An overview. Biotechnology Advances 2006;24:482-92. https://doi.org/10.1016/j.biotechadv.2006.03.002.
[110] Vicente T, Fáber R, Alves PM, Carrondo MJT, Mota JPB. Impact of ligand density on the optimization of ion-exchange membrane chromatography for viral vector purification. Biotechnology and Bioengineering 2011;108,1347-59. https://doi.org/10.1002/bit.23058.
[111] Kramberger P, Urbas L, Štrancar A. Downstream processing and chromatography based analytical methods for production of vaccines, gene therapy vectors, and bacteriophages. Human Vaccines & Immunotherapeutics 2015;11:1010–21. https://doi.org/10.1080/21645515.2015.1009817.
[112] Richieri SP, Bartholomew R, Aloia RC, Savary J, Gore R, Holt J, et al. Characterization of highly purified, inactivated HIV-1 particles isolated by anion exchange chromatography. Vaccine 1998;16:119-129. https://doi.org/10.1016/S0264-410X(97)00196-5.
[113] Eriksson KO. Chapter 19 - Hydrophobic Interaction Chromatography. In: Jagschies G, Lindskog E, Łącki K, Galliher P, editors. Biopharmaceutical Processing, Elsevier; 2018, 401–8. https://doi.org/10.1016/B978-0-08-100623-8.00019-0.
[114] Simpson RJ. Purifying Proteins for Proteomics: A Laboratory Manual. I.K. International Publishing House Pvt. Limited; 2004.
[115] Li H, Yang Y, Zhang Y, Zhang S, Zhao Q, Zhu Y, et al. A hydrophobic interaction chromatography strategy for purification of inactivated foot-and-mouth disease virus. Protein Expression and Purification 2015;113:23–9. https://doi.org/10.1016/j.pep.2015.04.011.
[116] Wolff MW, Siewert C, Hansen SP, Faber R, Reichl U. Purification of cell culture-derived modified vaccinia ankara virus by pseudo-affinity membrane adsorbers and hydrophobic interaction chromatography. Biotechnology and Bioengineering 2010;107:312–20. https://doi.org/10.1002/bit.22797.
[117] Weigel T, Soliman R, Wolff MW, Reichl U. Hydrophobic-interaction chromatography for purification of influenza A and B virus. Journal of Chromatography B 2019;1117:103–17. https://doi.org/10.1016/j.jchromb.2019.03.037.
[118] Sviben D, Forcic D, Ivancic-Jelecki J, Halassy B, Brgles M. Recovery of infective virus particles in ion-exchange and hydrophobic interaction monolith chromatography is influenced by particle charge and total-to-infective particle ratio. Journal of Chromatography B 2017;1054:10–9. https://doi.org/10.1016/j.jchromb.2017.04.015.
[119] Zhang K, Liu X. Mixed-mode chromatography in pharmaceutical and biopharmaceutical applications. Journal of Pharmaceutical and Biomedical Analysis 2016;128:73–88. https://doi.org/10.1016/j.jpba.2016.05.007.
[120] Itoh D, Yoshimoto N, Yamamoto S. Retention Mechanism of Proteins in Hydroxyapatite Chromatography – Multimodal Interaction Based Protein Separations: A Model Study. Curr Protein Pept Sci 2018;20:75–81. https://doi.org/10.2174/1389203718666171024122106.
[121] Cummings LJ, Snyder MA, Brisack K. Chapter 24 Protein Chromatography on Hydroxyapatite Columns. In: Burgess RR, Deutscher MP, editors. Methods in Enzymology, vol. 463, Academic Press; 2009,387–404. https://doi.org/10.1016/S0076-6879(09)63024-X.

[122] Kurosawa Y, Saito M, Kobayashi S, Okuyama T. Purification of <i>Dengue Virus</i> Particles by One-Step Ceramic Hydroxyapatite Chromatography. WJV 2012;02:155–60. https://doi.org/10.4236/wjv.2012.23020.
[123] Kuiper M, Sanches RM, Walford JA, Slater NKH. Purification of a functional gene therapy vector derived from Moloney murine leukaemia virus using membrane filtration and ceramic hydroxyapatite chromatography. Biotechnology and Bioengineering 2002;80:445–53. https://doi.org/10.1002/bit.10388.
[124] Zhao M, Vandersluis M, Stout J, Haupts U, Sanders M, Jacquemart R. Affinity chromatography for vaccines manufacturing: Finally ready for prime time? Vaccine 2019;37:5491–503. https://doi.org/10.1016/j.vaccine.2018.02.090.
[125] Hughes C, Galea-Lauri J, Farzaneh F, Darling D. Streptavidin paramagnetic particles provide a choice of three affinity-based capture and magnetic concentration strategies for retroviral vectors. Molecular Therapy 2001;3:623-30. https://doi.org/10.1006/mthe.2001.0268.
[126] Williams SL, Nesbeth D, Darling DC, Farzaneh F, Slater NKH. Affinity recovery of Moloney Murine Leukaemia Virus. Journal of Chromatography B: Analytical Technologies in the Biomedical and Life Sciences 2005;820:111-9.. https://doi.org/10.1016/j.jchromb.2005.03.016.
[127] Williams SL, Eccleston ME, Slater NKH. Affinity capture of a biotinylated retrovirus on macroporous monolithic adsorbents: Towards a rapid single-step purification process. Biotechnology and Bioengineering 2005;89:783-7. https://doi.org/10.1002/bit.20382.
[128] Ye K, Jin S, Ataai MM, Schultz JS, Ibeh J. Tagging Retrovirus Vectors with a Metal Binding Peptide and One-Step Purification by Immobilized Metal Affinity Chromatography. Journal of Virology 2004;78:9820-7. https://doi.org/10.1128/JVI.78.18.9820-9827.2004.
[129] Elkana Y, Thornton A, Zuckerman AJ. Purification of hepatitis A virus by affinity chromatography. J Immunol Methods 1979;25:185–7. https://doi.org/10.1016/0022-1759(79)90054-1.
[130] Njayou M, Quash G. Purification of measles virus by affinity chromatography and by ultracentrifugation: a comparative study. Journal of Virological Methods 1991;32:67–77. https://doi.org/10.1016/0166-0934(91)90186-4.
[131] Hu J, Ni Y, Dryman BA, Meng XJ, Zhang C. Purification of porcine reproductive and respiratory syndrome virus from cell culture using ultrafiltration and heparin affinity chromatography. Journal of Chromatography A 2010;1217:3489–93. https://doi.org/10.1016/j.chroma.2010.03.023.
[132] Brown F, Underwood B O, Fantes K H. Purification of poliovirus by affinity chromatography. Journal of medical virology 1979;4:315-9. https://doi.org /10.1002/jmv.1890040409
[133] Kalbfuss B, Wolff M, Geisler L, Tappe A, Wickramasinghe R, Thom V, et al. Direct capture of influenza A virus from cell culture supernatant with Sartobind anion-exchange membrane adsorbers. Journal of Membrane Science 2007; 299:251-60. https://doi.org/10.1016/j.memsci.2007.04.048.
[134] Opitz L, Lehmann S, Reichl U, Wolff MW. Sulfated membrane adsorbers for economic pseudo-affinity capture of influenza virus particles. Biotechnology and Bioengineering 2009;103:1144-54. https://doi.org/10.1002/bit.22345.
[135] McTaggart S, Al-Rubeai M. Retroviral vectors for human gene delivery. Biotechnology Advances 2002;20:391-419. https://doi.org/10.1016/S0734-9750(01)00087-8.

[136] Shieh MT, WuDunn D, Montgomery RI, Esko JD, Spear PG. Cell surface receptors for herpes simplex virus are heparan sulfate proteoglycans. Journal of Cell Biology 1992;116:1273-81. https://doi.org/10.1083/jcb.116.5.1273.
[137] Chen Y, Maguire T, Hileman RE, Fromm JR, Esko JD, Linhardt RJ, et al. Dengue virus infectivity depends on envelope protein binding to target cell heparan sulfate. Nature Medicine 1997. https://doi.org/10.1038/nm0897-866.
[138] Vivès RR, Imberty A, Sattentau QJ, Lortat-Jacob H. Heparan sulfate targets the HIV-1 envelope glycoprotein gp120 coreceptor binding site. Journal of Biological Chemistry 2005. https://doi.org/10.1074/jbc.M500911200.
[139] Huyghe BG, Liu X, Sutjipto S, Sugarman BJ, Horn MT, Shepard HM, et al. Purification of a type 5 recombinant adenovirus encoding human p53 by column chromatography. Hum Gene Ther 1995;6:1403–16. https://doi.org/10.1089/hum.1995.6.11-1403.
[140] Segura MM, Kamen AA, Garnier A. Overview of current scalable methods for purification of viral vectors. Methods in Molecular Biology (Clifton, NJ) 2011. https://doi.org/10.1007/978-1-61779-095-9_4.
[141] Vajda J, Weber D, Brekel D, Hundt B, Müller E. Size distribution analysis of influenza virus particles using size exclusion chromatography. Journal of Chromatography A 2016;1465:117–25. https://doi.org/10.1016/j.chroma.2016.08.056.
[142] Zimmer B, Summermatter K, Zimmer G. Stability and inactivation of vesicular stomatitis virus, a prototype rhabdovirus. Veterinary Microbiology 2013. https://doi.org/10.1016/j.vetmic.2012.08.023.
[143] Gélinas J-F, Azizi H, Kiesslich S, Lanthier S, Perdersen J, Chahal PS, et al. Production of rVSV-ZEBOV in serum-free suspension culture of HEK 293SF cells. Vaccine 2019;37:6624–32. https://doi.org/10.1016/j.vaccine.2019.09.044.
[144] Hierholzer JC, Killington RA. Virology methods manual. In: Mahy BW, Kangro HO, editors. Virology Methods Manual, London: Academic Press; 1996, p. 374. https://doi.org/10.1016/B978-012465330-6/50003-8.
[145] The Binder Lab (@TheBinderLab) / Twitter. Twitter n.d. https://twitter.com/TheBinderLab (accessed September 11, 2021).
[146] Clarke DK, Cooper D, Egan MA, Hendry RM, Parks CL, Udem SA. Recombinant vesicular stomatitis virus as an HIV-1 vaccine vector. Springer Seminars in Immunopathology 2006;28:239–53. https://doi.org/10.1007/s00281-006-0042-3.
[147] Moerdyk-Schauwecker M, Hwang S Il, Grdzelishvili VZ. Cellular proteins associated with the interior and exterior of vesicular stomatitis virus virions. PLoS ONE 2014. https://doi.org/10.1371/journal.pone.0104688.
[148] Roberts A, Buonocore L, Price R, Forman J, Rose JK. Attenuated vesicular stomatitis viruses as vaccine vectors. Journal of Virology 1999;73:3723–32.
[149] Pavlovic J, Zürcher T, Haller O, Staeheli P. Resistance to influenza virus and vesicular stomatitis virus conferred by expression of human MxA protein. Journal of Virology 1990. https://doi.org/10.1128/jvi.64.7.3370-3375.1990.
[150] Furuyama W, Reynolds P, Haddock E, Meade-White K, Quynh Le M, Kawaoka Y, et al. A single dose of a vesicular stomatitis virus-based influenza vaccine confers rapid protection against H5 viruses from different clades. Npj Vaccines 2020. https://doi.org/10.1038/s41541-019-0155-z.
[151] Akpinar F, Yin J. Characterization of vesicular stomatitis virus populations by tunable resistive pulse sensing. Journal of Virological Methods 2015. https://doi.org/10.1016/j.jviromet.2015.02.006.
[152] Bishnoi S, Tiwari R, Gupta S, Byrareddy SN, Nayak D. Oncotargeting by Vesicular Stomatitis Virus (VSV): Advances in cancer therapy. Viruses 2018. https://doi.org/10.3390/v10020090.

[153] Lichty BD, Power AT, Stojdl DF, Bell JC. Vesicular stomatitis virus: Re-inventing the bullet. Trends in Molecular Medicine 2004. https://doi.org/10.1016/j.molmed.2004.03.003.
[154] Geisbert TW, Feldmann H. Recombinant vesicular stomatitis virus-based vaccines against Ebola and marburg virus infections. Journal of Infectious Diseases 2011. https://doi.org/10.1093/infdis/jir349.
[155] Fathi A, Dahlke C, Addo MM. Recombinant vesicular stomatitis virus vector vaccines for WHO blueprint priority pathogens. Human Vaccines and Immunotherapeutics 2019. https://doi.org/10.1080/21645515.2019.1649532.
[156] Monath TP, Fast PE, Modjarrad K, Clarke DK, Martin BK, Fusco J, et al. rVSVΔG-ZEBOV-GP (also designated V920) recombinant vesicular stomatitis virus pseudotyped with Ebola Zaire Glycoprotein: Standardized template with key considerations for a risk/benefit assessment. Vaccine: X 2019. https://doi.org/10.1016/j.jvacx.2019.100009.
[157] WHO WHO. 2018 Annual review of diseases prioritized under the Research and Development Blueprint Informal consultation. WHO Research and Development Blueprint 2018.
[158] World Health Organisation. Preliminary results on the efficacy of rVSV-ZEBOVGP Ebola vaccine using the ring vaccination strategy in the control of an Ebola outbreak in the Democratic Republic of the Congo. 2019.
[159] Mangion M, Gélinas J-F, Bakhshi Zadeh Gashti A, Azizi H, Kiesslich S, Nassoury N, et al. Evaluation of novel HIV vaccine candidates using recombinant vesicular stomatitis virus vector produced in serum-free Vero cell cultures. Vaccine 2020. https://doi.org/10.1016/j.vaccine.2020.10.058.
[160] Gélinas JF, Kiesslich S, Gilbert R, Kamen AA. Titration methods for rVSV-based vaccine manufacturing. MethodsX 2020;7:100806. https://doi.org/10.1016/j.mex.2020.100806.
[161] Bandeira V, Peixoto C, Rodrigues AF, Cruz PE, Alves PM, Coroadinha AS, et al. Downstream processing of lentiviral vectors: Releasing bottlenecks. Human Gene Therapy Methods 2012. https://doi.org/10.1089/hgtb.2012.059.
[162] Segura MM, Mangion M, Gaillet B, Garnier A. New developments in lentiviral vector design, production and purification. Expert Opinion on Biological Therapy 2013. https://doi.org/10.1517/14712598.2013.779249.
[163] Ma Y, Li J. Vesicular Stomatitis Virus as a Vector To Deliver Virus-Like Particles of Human Norovirus: a New Vaccine Candidate against an Important Noncultivable Virus. Journal of Virology 2011. https://doi.org/10.1128/jvi.02332-10.
[164] Rodriques T, Carvalho A, Carmo M, Carrondo MJT, Alves PM, Cruz PE. Scaleable purification process for gene therapy retroviral vectors. Journal of Gene Medicine 2007. https://doi.org/10.1002/jgm.1021.
[165] Sena-Esteves M, Tebbets JC, Steffens S, Crombleholme T, Flake AW. Optimized large-scale production of high titer lentivirus vector pseudotypes. Journal of Virological Methods 2004; 122:131-139. https://doi.org/10.1016/j.jviromet.2004.08.017.
[166] Gluschankof P, Mondor I, Gelderblom HR, Sattentau QJ. Cell membrane vesicles are a major contaminant of gradient-enriched human immunodeficiency virus type-1 preparations. Virology 1997; 125-33. https://doi.org/10.1006/viro.1997.8453.
[167] Knezevic I, Stacey G, Petricciani J, Sheets R. Evaluation of cell substrates for the production of biologicals: Revision of WHO recommendations. Report of the WHO Study Group on Cell Substrates for the Production of Biologicals, 22-23 April 2009, Bethesda, USA. Biologicals, 2010; 162-169. https://doi.org/10.1016/j.biologicals.2009.08.019.

[168] Thomas D, Newcomb WW, Brown JC, Wall JS, Hainfeld JF, Trus BL, et al. Mass and molecular composition of vesicular stomatitis virus: a scanning transmission electron microscopy analysis. Journal of Virology 1985; 54:598-607. https://doi.org/10.1128/jvi.54.2.598-607.1985.
[169] Howatson AF, Whitmore GF. The development and structure of vesicular stomatitis virus. Virology 1962;16:466–78. https://doi.org/10.1016/0042-6822(62)90228-3.
[170] Vicente T, Sousa MFQ, Peixoto C, Mota JPB, Alves PM, Carrondo MJT. Anion-exchange membrane chromatography for purification of rotavirus-like particles. Journal of Membrane Science 2008;311:270–83. https://doi.org/10.1016/j.memsci.2007.12.021.
[171] Woo M, Khan NZ, Royce J, Mehta U, Gagnon B, Ramaswamy S, et al. A novel primary amine-based anion exchange membrane adsorber. Journal of Chromatography A 2011;1218:5386–92. https://doi.org/10.1016/j.chroma.2011.03.068.
[172] Orr V, Zhong L, Moo-Young M, Chou CP. Recent advances in bioprocessing application of membrane chromatography. Biotechnology Advances 2013;31:450–65. https://doi.org/10.1016/j.biotechadv.2013.01.007.
[173] Kutner RH, Puthli S, Marino MP, Reiser J. Simplified production and concentration of HIV-1-based lentiviral vectors using HYPERFlask vessels and anion exchange membrane chromatography. BMC Biotechnology 2009;9:10. https://doi.org/10.1186/1472-6750-9-10.
[174] Teeters MA, Conrardy SE, Thomas BL, Root TW, Lightfoot EN. Adsorptive membrane chromatography for purification of plasmid DNA. Journal of Chromatography A 2003;989:165–73. https://doi.org/10.1016/S0021-9673(03)00027-X.
[175] Global AIDS update 2019 — Communities at the centre — Defending rights, breaking barriers, reaching people with HIV services n.d.:316.
[176] Burton DR. Advancing an HIV vaccine; advancing vaccinology. Nature Reviews Immunology 2019;19:77–8. https://doi.org/10.1038/s41577-018-0103-6.
[177] Haynes BF, Burton DR. Developing an HIV vaccine. Science 2017;355:1129–30. https://doi.org/10.1126/science.aan0662.
[178] Lesko CR, Bengtson AM. HIV and COVID-19: Intersecting Epidemics With Many Unknowns. Am J Epidemiol 2021;190:10–6. https://doi.org/10.1093/aje/kwaa158.
[179] Weaver J, Husson SM, Murphy L, Wickramasinghe SR. Anion exchange membrane adsorbers for flow-through polishing steps: Part I. clearance of minute virus of mice. Biotechnology and Bioengineering 2013;110:491–9. https://doi.org/10.1002/bit.24720.
[180] Zhou JX, Tressel T, Yang X, Seewoester T. Implementation of advanced technologies in commercial monoclonal antibody production. Biotechnol J 2008;3:1185–200. https://doi.org/10.1002/biot.200800117.
[181] Kalbfuss B, Wolff M, Geisler L, Tappe A, Wickramasinghe R, Thom V, et al. Direct capture of influenza A virus from cell culture supernatant with Sartobind anion-exchange membrane adsorbers. Journal of Membrane Science 2007;299:251–60. https://doi.org/10.1016/j.memsci.2007.04.048.
[182] Weaver J, Husson SM, Murphy L, Wickramasinghe SR. Anion exchange membrane adsorbers for flow-through polishing steps: Part II. Virus, host cell protein, DNA clearance, and antibody recovery. Biotechnol Bioeng 2013;110:500–10. https://doi.org/10.1002/bit.24724.
[183] Karger A, Schmidt J, Mettenleiter TC. Infectivity of a Pseudorabies Virus Mutant Lacking Attachment Glycoproteins C and D. Journal of Virology 1998;72:7341–8. https://doi.org/10.1128/JVI.72.9.7341-7348.1998.

[184] Okada T, Nonaka-Sarukawa M, Uchibori R, Kinoshita K, Hayashita-Kinoh H, Nitahara-Kasahara Y, et al. Scalable purification of adeno-associated virus serotype 1 (AAV1) and AAV8 vectors, using dual ion-exchange adsorptive membranes. Hum Gene Ther 2009;20:1013–21. https://doi.org/10.1089/hum.2009.006.
[185] Specht R, Han B, Wickramasinghe SR, Carlson JO, Czermak P, Wolf A, et al. Densonucleosis virus purification by ion exchange membranes. Biotechnol Bioeng 2004;88:465–73. https://doi.org/10.1002/bit.20270.
[186] Grein TA, Michalsky R, Vega López M, Czermak P. Purification of a recombinant baculovirus of Autographa californica M nucleopolyhedrovirus by ion exchange membrane chromatography. Journal of Virological Methods 2012;183:117–24. https://doi.org/10.1016/j.jviromet.2012.03.031.
[187] Wolff MW, Siewert C, Lehmann S, Hansen SP, Djurup R, Faber R, et al. Capturing of cell culture-derived modified Vaccinia Ankara virus by ion exchange and pseudo-affinity membrane adsorbers. Biotechnology and Bioengineering 2010;105:761–9. https://doi.org/10.1002/bit.22595.
[188] Moerdyk-Schauwecker M, Hwang S-I, Grdzelishvili VZ. Cellular Proteins Associated with the Interior and Exterior of Vesicular Stomatitis Virus Virions. PLOS ONE 2014;9:e104688. https://doi.org/10.1371/journal.pone.0104688.
[189] Fathi A, Dahlke C, Addo MM. Recombinant vesicular stomatitis virus vector vaccines for WHO blueprint priority pathogens. Hum Vaccin Immunother 2019;15:2269–85. https://doi.org/10.1080/21645515.2019.1649532.
[190] Arnemo M, Viksmoen Watle SS, Schoultz KM, Vainio K, Norheim G, Moorthy V, et al. Stability of a Vesicular Stomatitis Virus–Vectored Ebola Vaccine. The Journal of Infectious Diseases 2016;213:930–3. https://doi.org/10.1093/infdis/jiv532.
[191] Mangion M, Gélinas J-F, Bakhshi Zadeh Gashti A, Azizi H, Kiesslich S, Nassoury N, et al. Evaluation of novel HIV vaccine candidates using recombinant vesicular stomatitis virus vector produced in serum-free Vero cell cultures. Vaccine 2020;38:7949–55. https://doi.org/10.1016/j.vaccine.2020.10.058.
[192] Spearman C. The Method of 'Right and Wrong Cases' ('constant Stimuli') Without Gauss's Formulae. British Journal of Psychology, 1904-1920 1908;2:227–42. https://doi.org/10.1111/j.2044-8295.1908.tb00176.x.
[193] Kärber G. Beitrag zur kollektiven Behandlung pharmakologischer Reihenversuche. Archiv f experiment Pathol u Pharmakol 1931;162:480–3. https://doi.org/10.1007/BF01863914.
[194] O'Donnell K, Krishnathu S, Bhatia R, Huang Z, Kelly W. Evaluation of two-species binding model with anion-exchange membrane chromatography to predict pressure buildup during recovery of virus. Chemical Engineering Science 2021;237:116535. https://doi.org/10.1016/j.ces.2021.116535.
[195] Kang Y, Cutler MW, Ouattara AA, Syvertsen KE. Purification processes for isolating purified vesicular stomatitis virus from cell culture. US7875446B2, 2011.
[196] Lima TM, Souza MO, Castilho LR. Purification of flavivirus VLPs by a two-step chomatographic process. Vaccine 2019;37:7061–9. https://doi.org/10.1016/j.vaccine.2019.05.066.
[197] Thomas D, Newcomb WW, Brown JC, Wall JS, Hainfeld JF, Trus BL, et al. Mass and molecular composition of vesicular stomatitis virus: a scanning transmission electron microscopy analysis. Journal of Virology 1985;54:598–607. https://doi.org/10.1128/jvi.54.2.598-607.1985.
[198] Akpinar F, Yin J. Characterization of vesicular stomatitis virus populations by tunable resistive pulse sensing. J Virol Methods 2015;218:71–6. https://doi.org/10.1016/j.jviromet.2015.02.006.

[199] Howatson AF, Whitmore GF. The development and structure of vesicular stomatitis virus. Virology 1962;16:466–78. https://doi.org/10.1016/0042-6822(62)90228-3.
[200] Kawasaki T. Hydroxyapatite as a liquid chromatographic packing. Journal of Chromatography A 1991;544:147–84. https://doi.org/10.1016/S0021-9673(01)83984-4.
[201] Kandori K, Miyagawa K, Ishikawa T. Adsorption of immunogamma globulin onto various synthetic calcium hydroxyapatite particles. J Colloid Interface Sci 2004;273:406–13. https://doi.org/10.1016/j.jcis.2004.01.069.
[202] Kawasaki T, Ikeda K, Takahashi S, Kuboki Y. Further study of hydroxyapatite high-performance liquid chromatography using both proteins and nucleic acids, and a new technique to increase chromatographic efficiency. Eur J Biochem 1986;155:249–57. https://doi.org/10.1111/j.1432-1033.1986.tb09483.x.
[203] Gagnon P. Purification tools for monoclonal antibodies. Tucson, AZ: Validated Biosystems, Inc.; 1996.
[204] Tiselius A, Hjertén S, Levin Ö. Protein chromatography on calcium phosphate columns. Archives of Biochemistry and Biophysics 1956;65:132–55. https://doi.org/10.1016/0003-9861(56)90183-7.
[205] Cummings LJ, Snyder MA, Brisack K. Protein chromatography on hydroxyapatite columns. Methods Enzymol 2009;463:387–404. https://doi.org/10.1016/S0076-6879(09)63024-X.
[206] Mazzola GJ, Smith TM. Methods for purifying antibodies using ceramic hydroxyapatite. EP2069387A1, 2009.
[207] Gagnon P. Monoclonal antibody purification with hydroxyapatite. New Biotechnology 2009;25:287–93. https://doi.org/10.1016/j.nbt.2009.03.017.
[208] Thorson JS, Lo SF, Ploux O, He X, Liu HW. Studies of the biosynthesis of 3,6-dideoxyhexoses: molecular cloning and characterization of the asc (ascarylose) region from Yersinia pseudotuberculosis serogroup VA. J Bacteriol 1994;176:5483–93. https://doi.org/10.1128/jb.176.17.5483-5493.1994.
[209] Gajko A, Gałasiński W, Gindzieński A. Purification and characterization of the protein kinase eEF-2 isolated from rat liver cells. Acta Biochim Pol 1994;41:421–7. https://doi.org/10.18388/abp.1994_4687.
[210] Eis C, Griessler R, Maier M, Weinhäusel A, Bock B, Kulbe KD, et al. Efficient downstream processing of maltodextrin phosphorylase from Escherichia coli and stabilization of the enzyme by immobilization onto hydroxyapatite. J Biotechnol 1997;58:157–66. https://doi.org/10.1016/s0168-1656(97)00145-4.
[211] Sun S, Luo Y, Jennings P. Purification of acidic proteins using ceramic hydroxyapatite chromatography. US20100113751A1, 2010.
[212] Smith GP, Gingrich TR. Hydroxyapatite chromatography of phage-display virions. Biotechniques 2005;39:879–84. https://doi.org/10.2144/000112032.
[213] Andrews-Pfannkoch C, Fadrosh DW, Thorpe J, Williamson SJ. Hydroxyapatite-Mediated Separation of Double-Stranded DNA, Single-Stranded DNA, and RNA Genomes from Natural Viral Assemblages. Appl Environ Microbiol 2010;76:5039–45. https://doi.org/10.1128/AEM.00204-10.
[214] Purdy KJ, Embley TM, Takii S, Nedwell DB. Rapid Extraction of DNA and rRNA from Sediments by a Novel Hydroxyapatite Spin-Column Method. Applied and Environmental Microbiology 1996;62:3905–7. https://doi.org/10.1128/AEM.62.10.3905-3907.1996.
[215] Niimi M, Masuda T, Kaihatsu K, Kato N, Nakamura S, Nakaya T, et al. Virus purification and enrichment by hydroxyapatite chromatography on a chip. Sensors and Actuators B: Chemical 2014;201:185–90. https://doi.org/10.1016/j.snb.2014.04.011.

[216] Kurosawa Y, Sato S, Okuyama T, Taoka M. Sequential two-step chromatographic purification of infectious poliovirus using ceramic fluoroapatite and ceramic hydroxyapatite columns. PLOS ONE 2019;14:e0222199. https://doi.org/10.1371/journal.pone.0222199.
[217] Saito M, Kurosawa Y, Okuyama T. Scanning electron microscopy-based approach to understand the mechanism underlying the adhesion of dengue viruses on ceramic hydroxyapatite columns. PLoS One 2013;8:e53893. https://doi.org/10.1371/journal.pone.0053893.
[218] Lin S-Y, Chiu H-Y, Chiang B-L, Hu Y-C. Development of EV71 virus-like particle purification processes. Vaccine 2015;33:5966–73. https://doi.org/10.1016/j.vaccine.2015.04.077.
[219] Iii JCC. Process for purifying human papillomavirus virus-like particles. WO2000009671A1, 2000.
[220] Wenger MD, Dephillips P, Price CE, Bracewell DG. An automated microscale chromatographic purification of virus-like particles as a strategy for process development. Biotechnol Appl Biochem 2007;47:131–9. https://doi.org/10.1042/BA20060240.
[221] Baek J-O, Seo J-W, Kim I-H, Kim CH. Production and purification of human papillomavirus type 33 L1 virus-like particles from Spodoptera frugiperda 9 cells using two-step column chromatography. Protein Expression and Purification 2011;75:211–7. https://doi.org/10.1016/j.pep.2010.08.005.
[222] Aizawa T, Koganesawa N, Kamakura A, Masaki K, Matsuura A, Nagadome H, et al. Adsorption of human lysozyme onto hydroxyapatite. Identification of its adsorbing site using site-directed mutagenesis. FEBS Lett 1998;422:175–8. https://doi.org/10.1016/s0014-5793(97)01621-9.
[223] Cj M, P G, Sm C. Unique selectivity windows using selective displacers/eluents and mobile phase modifiers on hydroxyapatite. J Chromatogr A 2010;1217:6484–95. https://doi.org/10.1016/j.chroma.2010.08.038.
[224] Luellau E, von Stockar U, Vogt S, Freitag R. Development of a downstream process for the isolation and separation of monoclonal immunoglobulin A monomers, dimers and polymers from cell culture supernatant. J Chromatogr A 1998;796:165–75. https://doi.org/10.1016/s0021-9673(97)01046-7.
[225] Wong K, Mukherjee B, Kahler AM, Zepp R, Molina M. Influence of inorganic ions on aggregation and adsorption behaviors of human adenovirus. Environ Sci Technol 2012;46:11145–53. https://doi.org/10.1021/es3028764.
[226] Gerba CP. Applied and theoretical aspects of virus adsorption to surfaces. Adv Appl Microbiol 1984;30:133–68. https://doi.org/10.1016/s0065-2164(08)70054-6.
[227] Gerba CP, Betancourt WQ. Viral Aggregation: Impact on Virus Behavior in the Environment. Environ Sci Technol 2017;51:7318–25. https://doi.org/10.1021/acs.est.6b05835.
[228] Petersen KE, Manangon E, Hood JL, Wickline SA, Fernandez DP, Johnson WP, et al. A review of exosome separation techniques and characterization of B16-F10 mouse melanoma exosomes with AF4-UV-MALS-DLS-TEM. Anal Bioanal Chem 2014;406:7855–66. https://doi.org/10.1007/s00216-014-8040-0.
[229] Brennan K, Martin K, FitzGerald SP, O'Sullivan J, Wu Y, Blanco A, et al. A comparison of methods for the isolation and separation of extracellular vesicles from protein and lipid particles in human serum. Sci Rep 2020;10:1039. https://doi.org/10.1038/s41598-020-57497-7.
[230] Vogt VM. Retroviral Virions and Genomes. In: Coffin JM, Hughes SH, Varmus HE, editors. Retroviruses, Cold Spring Harbor (NY): Cold Spring Harbor Laboratory Press; 1997.